

# **Residual Stresses in Cast Iron**

Measurement and simulations of residual stresses in heat treated cast iron materials

by

ANTON MARBERG  
JOHAN PAL

**Diploma work No. 200/2017**

At Department of Materials and Manufacturing Technology  
CHALMERS UNIVERSITY OF TECHNOLOGY  
Gothenburg, Sweden

Diploma work in the Master program Materials engineering

Performed at: Volvo Materialteknik  
Gropegårdsgatan 417 15 Gothenburg

Supervisor(s): Pål Schmidt  
Volvo Powertrain AB  
Gropegårdsgatan 417 15 Gothenburg

**Examiner:** Johan Ahlström  
Department of Materials and Manufacturing Technology  
Chalmers University of Technology, SE - 412 96 Gothenburg

**Residual stresses in cast iron**

Measurements and simulations of residual stresses in heat treated cast iron materials

ANTON MARBERG

JOHAN PAL

© ANTON MARBERG, JOHAN PAL, 2017.

Diploma work no 200/2017

Department of Materials and Manufacturing Technology

Chalmers University of Technology

SE-412 96 Gothenburg

Sweden

Telephone + 46 (0)31-772 1000

Printed by Chalmers Reproservice

Gothenburg, Sweden 2017

**Residual stresses in cast iron**

Measurements and simulations of residual stresses in heat treated cast iron materials

ANTON MARBERG, JOHAN PAL, 2017.

Department of Materials and Manufacturing Technology

Chalmers University of Technology

# ACKNOWLEDGEMENT

First, we like to bring our gratitude to our supervisor, Doctor Pål Schmidt. He has provided us with an interesting topic of thesis work and has always guided us along the project work. We feel like we learned a lot more about theory behind cast iron materials and a friendlier supervisor would be hard to think of. Also, great thanks to our supervisor from Chalmers Johan Ahlström, who has supported the project and brought good ideas from an academic perspective.

Thanks to Volvo Materials Technology and Ulla Boman for the financial support and the kind treatment.

Thanks to the colleagues Mattias Widmark, Joachim Lindqvist, Markku Rausa and all the other team members that helped us along the way. They have explained the practical testing methods and all the equipment and we would like to bring our gratitude to them.

Jag, Anton skulle även vilja passa på att ägna ett stort tack till min Mamma Ann-Margret & Pappa Rustan för all uppmuntran till studierna genom åren, nu har vi fått en till ingenjör i familjen.

Jag, Johan vill gärna tacka min familj för att jag fick möjlighet att göra det jag själv ville och aldrig var pressad till att bli något, tack för all moralisk hjälp och omtanken ni har gett mig.

Anton Marberg, Johan Pal, Gothenburg, June 2017



# ABSTRACT

Unpredictable residual stresses are in most components considered to be a defect. The stresses are formed during the cooling process, caused by the temperature and viscoplastic strains. Performing a heat treatment (HT), the material starts to creep and residual stresses can be reduced with over 90% of the total initial stress. This study has been done in order to examine residual stress relieving in the HT for three cast iron materials, VIG-275/190, GJL-250 and GJS-500-7. The purpose is to find the effect of varying parameters and compare the result against simulation. A stress lattice component, designed to create residual stress are used to investigate the stress relieving. Through a sectioning method the stress is released and can be measured by strain gauges placed on the surface. The stresses are measured on each material both as cast and after HT and through empirical testing the effect of different parameters during the HT was established.

Comparing the practical test against simulations by Magma5 the cooling rate during solidification process is too quick in simulations. This fault is attributed to the non-included latent heat release during phase transformation at 723 °C (austenite to pearlite). By changing the specific heat capacity of sand and the cast iron this error can be corrected. The simulations also predict the stress to be fully relieved when reaching the hold temperature of 610 °C, this have been confirmed to be wrong shown by the significant effect of hold time in all investigated materials. The effects of varying cooling rates and drop temperatures are also difficult for the simulations to predict.

Heat treatment experiments on of VIG-275/190 shows that the alloying of Molybdenum and Chromium makes the material more resistant against creep at elevated temperatures. The hold time and time spent over 500 °C are the most significant parameters. The unalloyed GJL-250 creeps more easily which makes all the heat treatment parameters more important, i.e. heating rate, hold time and cooling rates. Lastly the ductile iron GJS-500-7 has the highest residual stress in as cast condition and shows the largest stress relief after the heat treatments.



# GLOSSARY

*	= Signifies foot note
, (comma)	=Notation Decimal symbol
E	= Young's modulus
$\epsilon$	= Elongation
R	= resistivity
°C	= Degrees Celsius
Chills	= Unwished cementite growth and carbide concentrations.
m	= meter
1 $\mu\text{m}$	= $10^{-6}$ meter
CGI	= Compacted Graphite Iron
SFI	= Spheroidal Graphite iron
Wt%	= Weight percent, the weight of a specific element a material consists of.
Mo	= Molybdenum
Cr	= Chromium
HT	= Heat treatment
MPa	= Mega Pascal
GPa	= Giga Pascal
Stress lattice	= A geometry designed to form residual stresses in purpose of measurements.
Strain gauge	=Measure the strain with resistance difference
$R_m$	=Ultimate tensile strength
HB	=Hardness Brinell



# TABLE OF CONTENT

1.1 Background .....	1
1.2 Purpose and goals .....	1
1.3 Limitations .....	2
2 THEORETICAL BACKGROUND .....	3
2.1 Microstructure .....	3
2.2 Grey Cast Iron .....	5
2.3 Spheroidal Graphite Iron- SGI .....	7
2.4 Alloying elements .....	8
2.4.1 Alloying Cast Iron .....	8
2.4.2 Cast Iron alloyed with Molybdenum and Chromium.....	10
2.5 Residual stresses during casting .....	10
2.6 The stress lattice .....	11
2.7 The heat treatment .....	12
2.7.1 Principle of the heat treatment.....	12
2.7.2 Skövde's heat treatment .....	12
2.8 Measure residual stresses with sectioning method.....	13
2.9 Thermocouple.....	15
3 INVESTIGATED MATERIALS .....	17
3.1 Grey iron, VIG 275/190 .....	17
3.2 Grey iron, GJL-250 .....	18
3.3 Ductile iron EN-GJS-500-7 .....	19
4. METHOD .....	21
4.1 Simulations.....	21
4.2 The stress relieving heat treatment .....	21
4.2.1 The heat treatment according to Volvo drawing recommendations .....	21
4.2.2 Skövde heat treatment .....	22
4.2.3 Limitations .....	22
4.3 Residual stress measurement by sectioning method .....	24
4.4 Potential bending load case of the stress lattice .....	25
5. EXPERIMENTS .....	27
5.1 Simulations.....	28
5.2 Design of the practical heat treatment.....	30
5.2.1 Design of the cooling rates.....	30
5.3 The practical heat treatments.....	32
5.3.1 Grey Iron, VIG 275/190 .....	32
5.3.2 Grey Iron, GJL-250 .....	33
5.3.3 Ductile Iron, GJS 500-7 .....	34

6. RESULTS.....	35
6.1 Simulation .....	35
6.1.1 Simulations of GJL 275/190 and GJL-250 .....	37
6.1.2 Skövde foundry heat treatment .....	38
6.1.3 Simulating ductile iron GJS-500-7.....	43
6.1.4 Verification of Simulation Model .....	43
6.2 Residual Stress Measurement.....	45
6.2.1 3D scanning the component .....	46
6.2.2 Cast iron VIG 275/190 .....	46
6.2.2 Cast iron GJL-250 .....	50
6.2.3 Cast iron GJS-500-7 .....	52
6.2.4 Comparison of the materials .....	53
6.3 Experimental verification of materials .....	54
6.3.1 Grey iron, VIG-275/190 .....	54
6.3.2 Grey iron, GJL-250 .....	57
6.3.3 Ductile Iron GJS-500-7 .....	59
7. DISCUSSION .....	61
7.1 Simulation compared to the practical testing .....	61
7.2 The reliability of strain gauges .....	64
7.3 Material properties effect on residual stresses .....	64
8. CONCLUSION .....	67
8.1 Simulation by Magma 5 .....	67
8.2 Practical testing .....	68
9. REOCMMENDATIONS .....	69
9.1 Recommendations to Skövde foundry .....	69
10. FUTURE WORK .....	71
References .....	73
APPENDIX A .....	74
APPENDIX B Heat treatments .....	76
Heat treatments of VIG-275/190 .....	77
Heat treatments of GJL-250 .....	82
Heat treatments of GJS-500-7 .....	86
APENDIX D Apply the strain gauge .....	90
APENDIX E Hardness vs. temperature .....	91

# 1 INTRODUCTION

This chapter will present the purpose and the restrictions of the thesis as well as to provide a background to why the study is performed.

## 1.1 Background

When the melted metal in a casting process cools down and solidifies, residual stresses arise from the strain caused by viscoplastic flow and temperature gradients. This is because the thermal energy dissipates faster in the thinner sections compared to the thicker sections and causes a temperature gradient in the material leading to residual stresses. While the thinner part is contracting due to the thermal contraction the core is still hot and maintains its larger volume. When the material is further cooled to room temperature the differences in thermal contractions cause residual stresses. In order to get rid of these stresses heat treatment is required. Residual stresses have a significant effect on the materials mechanical properties and the overall performance. High residual stresses can lead to early fatigue, increased crack propagation and potentially fracture the component.

After the solidification process, cast iron components are heat treated to reduce the residual stresses. This will improve the mechanical properties and avoid undesired stress concentrations in the material. As an example a cylinder head has a complex geometry and residual stresses are unwanted and difficult to predict. The assumption is that these stresses can be counteracted and lowered to insignificant levels with a heat treatment. By investigating varying heat treatment parameters and relate them to the relieving of residual stresses a process optimization can be done. This could in turn lead to higher quality components and improve the overall manufacturing process.

The materials that will be investigated are shown below, specific material properties are shown in chapter Investigated materials.

- *Grey iron, GJL-250 (Basic grey iron, available in Magma5)*
- *Grey iron, VIG 275/190 (Mo/Cr-alloyed grey iron, used for cylinder heads by Volvo)*
- *Ductile iron EN-GJS-500-7 (Used by SKF and Volvo, available in Magma5)*

The software Magma5 simulates solidification and heat treatment to predict the residual stresses. Simulations save both time and money but have requirements on accuracy and precision to be reliable. Finding discrepancies between practical tests and simulations would bring new aspects to improve the simulations and make them more efficient and precise.

## 1.2 Purpose and goals

The purpose of the thesis work is to investigate how the residual stress arises during the casting process of a component designed for this purpose, called a stress lattice. Three iron alloys will be investigated with their respective stress lattices. Both simulations and practical experiments will investigate the stress relieving heat treatment, and a comparison between the materials can be evaluated.

The cast iron materials will be tested and analyzed for different purposes and application, thus the goals for each material differs. Regarding the VIG-275/190 material and the relevance of testing is done in order to further develop the heat treatment cycle of Skövde foundry and making the process more efficient with the parameters available of their furnace. Today the heat treatment process at Skövde is a bottleneck in their production. A more efficient heat treatment could lead to a faster cycle time and their production cycle will become more efficient. Furthermore, the tests done on the lattices will also be of importance for the Magma5 developers due to the unique material compositions tested.

Regarding the other materials, the purpose is to compare the results between alloys. The analyses are done in order to further develop the understanding of the residual stresses in the materials chosen. A potential heat treatment method will be developed for both the materials and will provide useful information if they ever become relevant for use in applications.

### **1.3 Delimitations**

- The research will be performed on three materials. For each material three different holding times will be combined with three different cooling times amounting to a total of nine different heat treatments per material.
- The residual stress will only be measured on stress lattice geometry by the assumption that same revealing effect will be seen in other geometries.
- The practical heat treatment will be performed only at one furnace at Volvo.
- The measurements will only be performed by means of strain gauges with sectioning method. By using relation between strain and Young's modulus (Hooke's law) the residual stresses can be calculated.
- Simulation data is only valid for the unalloyed grey iron and ductile iron.
- No economic aspects will be investigated in the study.
- The residual stress measurements will only be measured at the longitudinal X-axis, since the Z- and Y-axis have negligible stresses in comparison to X-axis.

## 2 THEORETICAL BACKGROUND

This chapter describes basic knowledge about cast iron materials and how alloying elements affect the properties. The theory and procedures behind a heat treatment is presented as well as the fundamental theory of a stress relieving process. Also, an explanation of the used tools and equipment is presented.

### 2.1 Microstructure

Cast iron materials are defined by having free graphite in the iron matrixes. The free graphite is created with by alloying with carbon above 2.2 wt. % and additional 1-2 wt. % silicon. This creates a material known for its properties such as damping, thermal conductivity and machinability. Cast irons are easily cast, as the name suggest, without forming too many defects. The most common type of cast iron is the grey iron and requires few alloying elements in order to be effective and provide good mechanical properties. Other types of cast irons are the ductile iron, known for its ductility and fatigue resistance. Also, white cast iron can be found, with high hardness and abrasion resistance. There are also a more costly variant of cast iron called compacted graphite iron (CGI). This iron is used in same applications as regular grey cast irons but weigh less. The phase diagram of Iron-Carbon is shown in Figure 2.1 and each phase presented in the figure are in explained in the following sections.

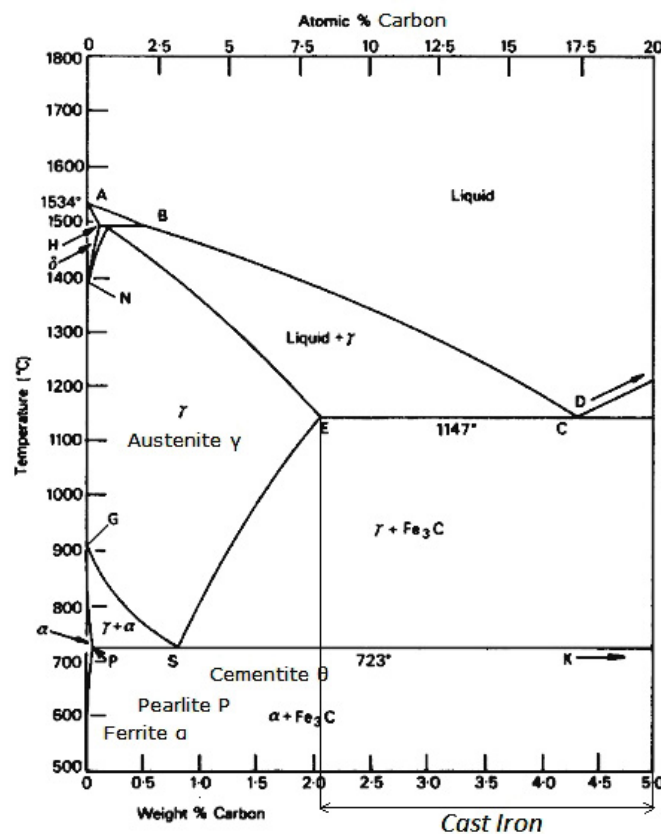


Figure 2.1. The phase diagram of Iron-Carbon. The interval of cast iron is shown in the figure and contains 2 wt. % of carbon or more.

The key to obtain a high quality cast iron is through the austenitic structure. Above the A1 line, at 723 °C austenite is present, shown in the phase diagram in Figure 2.1 The additions of

different alloying elements above A1 (723 °C) affects the amount of carbon the austenite can solve. Increasing carbon content generates a finer austenite structure but compromises other properties in return. Any excess carbon in the austenite is diffused out and forms graphite, a key component in the cast iron and vital for the workability. When the temperature crosses the A1 line the austenite transforms to pearlite. Pearlite is a fine lamellar microstructure consisting of cementite and ferrite. Having chunks of pure ferrite or cementite present in the material is a defect and is caused due to wrong alloying content or cooling rate. Further information of the microstructures of the Iron-Carbon system is described below:

**Austenite** – Is an iron-phase present at an elevated temperature and consists of face centered cubic structure and will solve large amount of carbon due to the structural shape. From 1100 °C to roughly 730 °C some of the austenitic phase decomposes into cementite and later, ferrite + cementite into the so-called pearlite transformation. Assuming only iron and carbon are present in the system.

**Ferrite** – Is a pure iron phase and can only solve small amounts of carbon, it has a body centered cubic structure and occurs most commonly at 730 °C. Ferrite is created from solid state transformation from austenite and with cementite it forms the pearlite structure. Ferrite has soft and ductile mechanical properties.

**Pearlite** – Is a metastable phase consisting of ferrite and cementite. Both phases grow simultaneous with spacing in the micrometer scale. Pearlite is known to be a hard and strong phase. Grey iron consists mostly of this microstructure and ductile iron often has a mix of both pearlite and ferrite.

**Cementite** – Also known as Fe<sub>3</sub>C and together with ferrite forms a lamellar structure known as pearlite. Cementite is an intermediate phase and can solve carbon up to 6.7 wt. %. It is a metastable phase formed through rapid cooling or alloying with elements such as chromium or manganese. At carbon levels above 2.2 wt. % cementite is created in conjunction with austenite when solidifying from liquid iron. Cementite is brittle and worsens workability of cast irons and steel and is due to this unwanted.

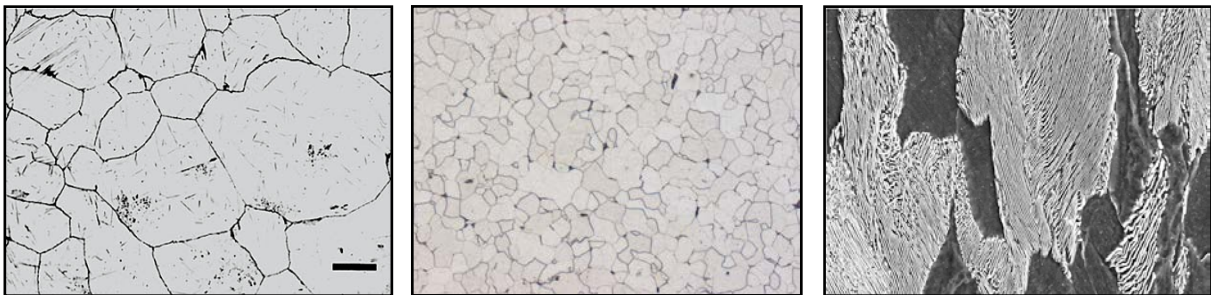


Figure 2.2. The microstructures of Austenite (left), Ferrite (middle) and Pearlite (right).

**Graphite** - Is a crystal formation consisting of only carbon and is the native formation of carbon. In a Fe-C system the graphite forms at the same time as austenite, around the eutectic temperature of 1150 °C. Both phases grow jointly and create a eutectic structure. Graphite is very soft and doesn't provide any strength to the material. Therefore, the shape and quantity of graphite in cast iron affects its mechanical and physical properties. The shape or morphology of the graphite also affects the mechanical properties as well as making machining easier, provide extra ductility to the material or prolong lifetime. The full extension

of the graphite structure is described in the ISO STD-EN ISO 945-1:2008. The standard takes the shape of graphite, distribution and size into account.

In Figure 2.3 six varying and unique shapes of the graphite are presented. A typical grey cast iron would have a graphite flake resembling shape I. This graphite structure provides the best possible mechanical properties to the material. For the case of ductile iron (SGI), would have a graphite shape resembling picture number VI in the figure below. This type of structure creates a more ductile material with higher strength than your usual grey cast iron. In general the shape of the graphite is used to further tailor a cast iron for its application and still provide good casting properties. Take note that not any cast iron have a fully homogenous structure of one of this picture but usually have a combination of two or more. Furthermore, how graphite's cluster, size and frequency affect the material is further discussed in the material section and more general approach is done in the ISO standard 945-1:2008. (Schmidt, 2016), (M. Holtzer, 2015)

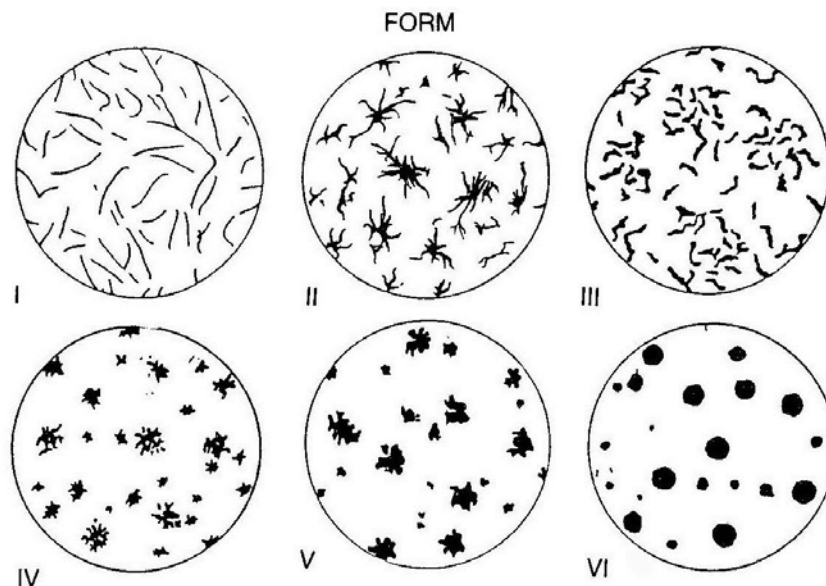


Figure 2.3. The different shape of the graphite according to EN ISO 945-1:2008.

## 2.2 Grey Cast Iron

Grey iron has been used since early 20<sup>th</sup> century for applications within the automotive industry, trains, and heavy-duty equipment. The material has a fully pearlitic matrix with at most 1% ferrite. The amount of graphite in grey cast iron is between 6 and 10% of the total volume. Grey irons are known as cast iron due to their excellent casting properties. The graphite's that are created during the solidification process compensate for the thermal contraction of the iron.

The application of grey iron is broad due to advantages such as good damping capacity, machinability, high wear resistance and self-lubrication effect due to the flake structure of graphite. The graphite structure also provides the material with high compressive strength, three to four times higher compared to the tensile strength. The obtained properties of the material make it suitable for e.g. a cylinder head component. At elevated temperatures exceeding 600 °C the material starts to oxidize and the mechanical properties such as

hardness degrades. This is due to the disintegration of the pearlite structure which transforms to ferrite; grain growth also gives similar effect. Ferrite can only solve small amounts of carbon and the rest decomposes into graphite. Ferrite is in general a soft phase and a larger portion of ferrite and graphite in the material will degrade the mechanical properties further.

Silicon (Si) is used in high amounts to obtain the grey iron, preventing the white cast iron structure to form. White cast iron has a lot of cementite and is created when there is a sufficient amount of carbon. Si locks the carbon and hinders almost all carbides to form, meaning the carbon is mostly all graphite. The graphite has no real strength and can be treated as voids. They do still provide good mechanical properties as stated above.

Additions of Si can provide some support to the thermal degradation of the iron at elevated temperatures. The level of Si provided beneficial effects up to a maximum 5.9% of volume, but the effect is noticeable at levels of 2% of volume. It also has some diminishing effect on grain growth. Additional hardness is susceptible to microstructure changes and is an early sign of decaying/changing microstructure.

The Young's modulus of cast iron is problematic due to the graphite in the material. The graphite pores are treated as voids in tensile load but can provide support in compressive loads, meaning that the material has two different Young's modulus (E) depending on loading case. (Janowak & Gundlach, 2006)

The graphite in the material can also be initiation points for defects and cracks. The lower limit for these defects to appear can be as low as 15 MPa, this number is heavily dependent on alloying elements and can be increased significantly with correct additions. Furthermore, the tensile Young's modulus is not linear for cast irons but is decreasing with increasing loads, following the curve of a decreasing quadratic equation.

From various reports a value between 110 GPa and 135 GPa are suggested for cast iron in room temperature. Due to the relatively small loads expected during the experiment a modulus of 120 GPa is used in tensile mode. In compressive mode the Young's modulus follows a linear curve and is roughly 130-140 GPa regardless of stress. Therefore the E-modulus is chosen to be 130 GPa for the compressive stress.

(Johannesson & Hamberg, 1989) AB Volvo Internal report LM-54159,

(Gjuterihandboken.se, 2015)

Fatigue strength of the grey iron is heavily dependent on the microstructure of the cast iron and a finer cell structure will increase the fatigue strength. A fundamental property attributed grey iron is its heterogeneity which decrease the materials low cycle fatigue and affects the general fatigue properties slightly. The heterogeneity is also creating what is known as heat zones, regions that are susceptible to rapid heating and are more common along the graphite interfaces. When heated the heat zones expand rapidly and can be a source of crack initiation and crack propagations. Even though these flaws exists in the material it is still a cheap material with excellent in thermal cycle load applications.

Improvements to the material are done by additions of Molybdenum (Mo) and Chromium (Cr) and are vital for applications at elevated temperatures. Both additions synergies well with one another and boost the effect of each other. Tin (Sn) is also pearlite stabilizing and can provide the same effect as Cr and Mo but can only be added in small quantities due to the brittleness it causes. (Gundlach, 2005), (Sn-castiron.nl, 2009)

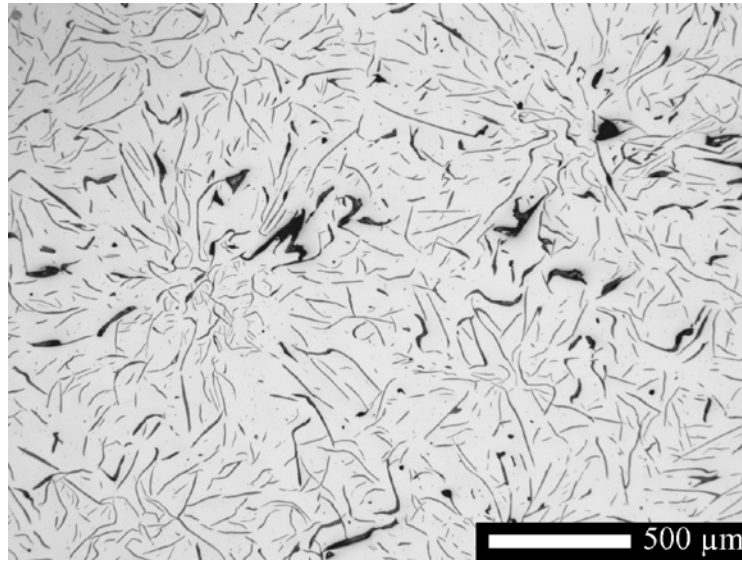


Figure 2.4. Microstructure of grey cast iron. The black parts are the graphite's and the white phase is pearlite (seen as white due to no etching). The microstructure of the grey iron seen in the figure consists of form I graphite. Comparison from ISO 945-1:2008 shown from Figure 2.3.

### 2.3 Spheroidal Graphite Iron- SGI

Ductile iron also named spheroidal graphite iron is a type of cast iron with spherical graphite, rather than the flakey structure most commonly seen in grey cast iron. This type of featured is created when adding a nebulizing element such as Magnesium (Mg). The graphite forms nodules instead of flakes and these changes the mechanical properties of the material. The graphite flakes normally seen in grey iron are the source of stress concentration and by removing these, the toughness of the material can be improved. The spherical graphite's impede the crack growth and reduce the risk of fatigue failure.

The ductile iron has both good mechanical properties and relatively low density for a cast iron material due to the high amount of carbon and silicon. They tend to be cheap and have good properties regarding machinability and ability to be cast. Cooling rates have less impact on the material compared to grey iron. The spherical carbon particles provide lubricant for machining, but can be defined as void due to the low mechanical properties of carbon. The variety of yielding strengths can range up to 900 MPa and 2% elongation (ISO standard 1083-2004). The material is comparable to steels in many aspects while still being cheap and easy to manufacture and machine. Figure 2.5 shows a typical structure of ductile iron. (M. Holtzer, 2015)

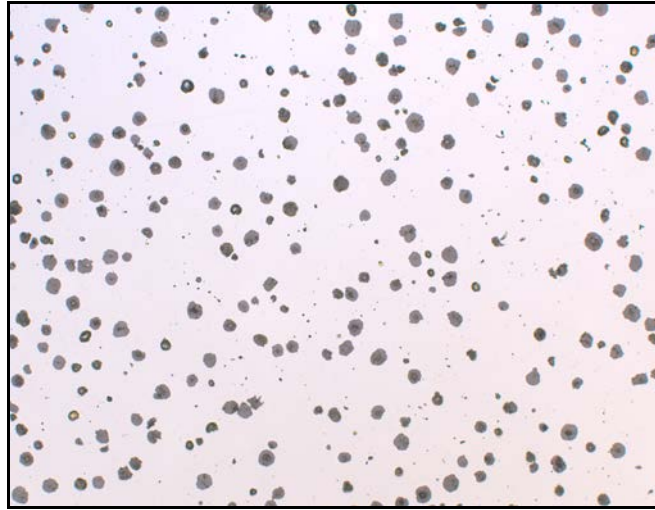


Figure 2.5. Microstructure of ductile iron. The graphite's are spherical due to the additions of magnesium and are seen as black dots and the white phase is the iron (both pearlite and ferrite matrix). A comparison can be made with shape VI in figure 2.3.

## 2.4 Alloying elements

Alloying elements gives a significant effect on the mechanical properties. This chapter will describe the most commonly used alloying elements in cast iron materials.

### 2.4.1 Alloying Cast Iron

Alloying elements in cast iron are used for the purposes of:

- Creating a consistent graphite structure.
- Not creating too much carbides and chills.
- Having no free ferrite in the cast component.
- Creating a uniform and fine pearlite.

These demands are achieved by adding a sufficient amount of graphite promoters and to some degree carbide-formers. Some elements have harmful effects if added in excessive amounts while other elements have synergetic effects and boost each other's presence. Geometries and cooling rates have just as large impact as some alloys which makes it more difficult to find the correct amount of each alloy and the correct solution might vary from case to case.

The austenite and the graphite are the keys to acquire a good cast iron. Graphite and austenite are created simultaneously at the eutectic point at 4.3 wt. % C, point C in the phase diagram, Figure 2.1.

To obtain a cast iron with high strength all the free ferrite is eliminated and the higher amount of austenite present when reaching the eutectic point will lead to an iron with higher mechanical properties and less flaws. The amount of carbon is the principal element determining the proportions of austenite present when eutectic temperature is reached. Instead of carbon, silicon or phosphorous can be used and reduces the amount of carbon required to reach the eutectic carbon content of 4.3 wt. %. The amount of silicon, phosphorus and carbon can all be summarized into what is called the carbon equivalent, CE for short. CE is used to estimate the eutectic composition but cast iron usually has a CE value between 3% and 4%. (\*It should be noted that there is no optimal CE value and it varies with geometries. Thicker sections benefits from a higher CE- value but there are drawbacks such as lower tensile

strength as well). Both silicon and phosphorous together with nickel are all graphite promoters and makes the graphite more easily occurring at higher temperatures.

On the other hand there are carbide promoters, such as vanadium, titanium, tungsten and molybdenum. These alloys pushes the eutectic temperature for graphite downward and pushes the carbide eutectic up. This means that the amount of carbides increases in the cast iron and is unwanted but it is a compromise, while it makes the production more difficult it also increases the mechanical performance of the material.

In general austenite dissolves nickel, silicon and phosphates, meaning that the amount of graphite promoters is reduced when the austenite solidifies and binds promoters. This behavior increases the amount of carbide formers left in the melt, bringing the carbide eutectic point closer to the graphite eutectic. This makes carbides more occurring

Adding more silicon or other graphite stabilizers is not necessarily the best way to reduce the amount of carbides and to acquire a homogenous composition in the last remnant of the liquid phase. Too much of graphite stabilizers leads instead to segregation in the material and lowers the mechanical properties of the material. The solution used today is to limit the amount of elements i.e. chromium and vanadium that raises the carbide eutectic temperatures.

A rapid solidification process beneath the graphite eutectic temperature but above the carbide forming eutectic is also beneficial for the mechanical properties. This is because a rapid cooling process reduces the grain size and allows for a more homogenous composition since the system doesn't have time to achieve equilibrium. This will also lead to a more finely spaced pearlite after the solid-state transformation from austenite to pearlite.

The more common carbide formers used in cast irons are vanadium, titanium, tungsten and molybdenum and all are strong carbide and oxide binders. This property is still helpful during the cooling process of the cast iron. While the iron is still hot and is cooling, dislocation movement occur more easily. When a dislocation moves it will leave a trace of vacancies and voids that are unwanted. By having a sufficient amount of these strong binders they will easily nucleate in these sections and remove the new flaws by creating very strong particles that will instead support the structure. This could potentially lead to lower machinability.

Copper is also a commonly used alloying element in cast iron. It is first and foremost a pearlite stabilizer but it also promotes graphite growths at the pre-eutectic point. Copper also decreases the diffusion of the material and reduces the risk of oxides forming. It is still an expensive alloying agent and is therefore not seen in higher quantities in cast irons.

Alloying elements can also be the cause of defects. Sulphur molding defects causes graphite degeneration at the metal-mold interface; it breaks down the spherical graphite and creates flakes instead. The sulfate enters the molten metal from the sand mold. Due to this there is a requirement to not have too high amounts of SO<sub>2</sub> in the sand mold, usually less than 1%. This is vital if the component has small and sharp edges or needle like features.

Oxygen can potentially be a degrading factor for the graphite in cast irons. The oxygen can create cavities in the mold and bind to Mg to create MgO, a very strong bonded oxide and is unwanted.

Nitrogen is known to have an impact on the formation of flake graphite. In ductile iron this effect is diminished or removed, due to the Mg-treatment that locks up residual nitrogen. The main source of nitrogen is in the binder. The effect of the nitrogen is increased frequency and severity of pinholes, a defect usually occurring a few millimeters beneath the surface.

(Schmidt, 2016), (Gundlach & Arbor, 2005), (Janowak & Gundlach, 2006), (G. I. Sil'man, 2003)

## **2.4.2 Cast Iron alloyed with Molybdenum and Chromium**

By alloying cast iron with Mo or Cr the mechanical properties will improve. Both additions add to strength and heat resistance, making cast iron more viable for high temperature applications. Mo provides strength and reduces the amount of creep at elevated temperature while Cr complements the material at lower temperatures. Both of them have harmonizing effect and boost each other. The downside of adding both of these elements is that it makes heat treatments not as effective and residual stresses are more difficult to relieve.

These changes occur due to the change of the microstructure Mo and Cr provide. The pearlitic microstructure changes towards finer grains and lower internal spacing of the lamellar. This structure creates difficulties for creep to occur but both hardness and strength increases due to the smaller size of the grains. With these two alloys, accompanied with nickel, makes cast iron more suitable for usage in motors and trucks in general.

The upper temperature limit for a cast iron is 650 °C as both oxidation and grain growth starts to occur above this temperature. Diffusion along the graphite grain boundaries increases as well and will result in rapid increase of volume and will result in failure. (Gundlach, 2005), (Janowak & Gundlach, 2006)

## **2.5 Residual stresses during casting**

Residual stresses have impact on the mechanical and thermal properties. It is a result of interactions of temperature changes, deformations and grain structure. The residual stresses can be the cause of decreased strength, distortion and result in cracking; therefore, it is unwished in many applications, especially the tensile portion of the residual stresses.

Residual stresses emerge when thermal expansion and contraction is generated uneven during the solidification. The thermal expansion creates spatial variations in the material and gives rise to strain energy due to the volumetric increase. Materials with high Young's modulus and yield strength tends to deform elastically when the thermal contraction occurs and the residuals stresses doesn't dissipate when the material is later cooled. Thermal conductivity can combat this behavior somewhat by creating a lower temperature gradient in the material but usually that is not sufficient. The compressive load created at the edges is rapidly cooled while the core is still molten. The difference in temperature creates a middle section that is pushed outward by the core and pushed inwards due to the shells contraction. The stresses that occur from this can amount to more than 50% of the tensile strength of the material and is a potential cause of failure.

The residual stresses can have impact on the microstructure and suppress grain growth and even create stress induced phase transformation. Even if residual stresses seem as a severe defect it is usually easy to handle and the stresses can be reduced to insignificant levels by a correctly performed heat treatment process. Residual stresses can never be fully removed due to an uneven cooling and stresses can be created due to the mould prohibiting some volumetric changes in the component.

The strain generated during cooling is generated from a difference in temperature. From this different stress levels can arise and cause problem. Residual stresses are generated regardless of geometry and size of the component and are a fundamental defect of every component that is heated and cooled. Residual stresses can be accurately predicted using simulations given that the material data exists. It is therefore vital to obtain the material parameters in order to predict the stress occurring during the heating and cooling phases. (G. Totten, 2002)

## 2.6 The stress lattice

The stress lattice is a component engineered to create residual stresses during the solidification process and during rapid cooling. The stress lattice geometry will form tensile stresses in the middle section of the lattice while in the outer sections (called legs) a compressive stress will be formed. The outer legs are thinner than the middle section and are cooled down more rapidly and create compressive stresses due to the contraction of the material. Since the middle section has a larger volume the thermal energy is high in this section of the lattice. The high temperature makes it possible for the material to diffuse easier and allow more deformation. The compressive forces in the thinner sections are created from the thermal contraction and pull the middle section thus creating tensile stress in the middle. The stress case that occurs in the lattice can be analyzed and measured by different types of testing methods, e.g. hole drilling and sectioning. The sectioning method is described later in this chapter and is the method that will be used in order to obtain the residual stresses. Figure 2.6 shows the geometry of a stress lattice and location of tensile and compressive stresses.

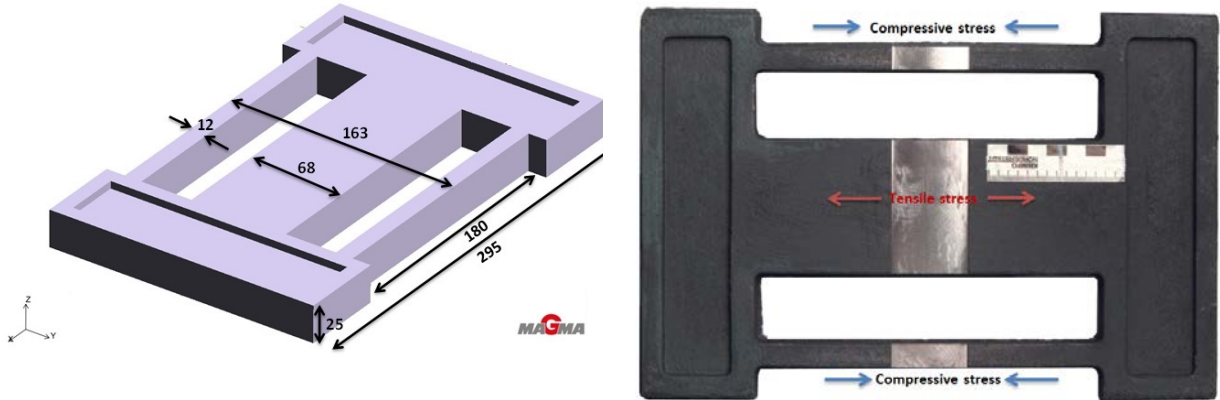


Figure 2.6. The geometry and residual stresses through the lattice component.

## **2.7 The heat treatment**

When a component has been cast and solidifies, heat treatment is performed to relieve the residual stresses. The process is done simply by heating the cast component to levels where the material can diffuse and the possibility for creep to occur which is enough to decrease the inner stress. For cast iron this level is around 600 °C. By increasing the temperature, the activation energy for dislocation and stresses are lowered in the material and diffusion can occur more easily and grain boundaries starts to move, which will relieve the stresses.

For applications such as a cylinder head, stress relieving process is critical to achieve the desired mechanical performance. The heat treatment process can be expensive for the manufactures; therefore, it is vital to reduce the process time. By optimizing the heat treatment and lowering the residual stresses the quality of the component can be improve while both saving time and money, making an efficient heat treatment an investment for foundries.

### **2.7.1 Principle of the heat treatment**

The heat treatment process is divided into four phases. The first phase is the heat up phase, second is the holding time and lastly the cooling phase. The first phase has to be slow enough to not create large temperature gradients between different sections of the geometry. A more advanced and complex geometry requires a slower heat up phase than a simple one. If the rate is too high new stresses arise and could potentially nullify the heat treatment completely. According to the heat treatment recommendations in drawing No.1677285, shown in Appendix B the suggested heating rate is 200 °C/h.

The hold time is the second phase of the HT and is the time the goods are kept at a maximum temperature. For cast irons a temperature of 600 °C is recommended. During the holding time most of the residual stresses should be released and it is therefore important to keep the holding time long enough in order for this to happen. The holding time varies with different materials and the demands of the component but the holding time is normally set to be 3 to 5 hours.

The third phase is the cooling, this process has to be slow and have a low rate in order to not create new residual stresses. A recommended cooling rate would be 50-100 °C/h for the first 300 °C. With decreasing temperature, the risk for new residual stresses to arise are lowered and below 300 °C there is potentially no risk for cast irons to develop new residual stresses. Thereafter the component can be air cooled, which will often generate a much higher cooling rate.

The stress relieving process can only decrease the residual stresses by a certain amount and the heat-treated component will always have some residual stress remaining. By heat treating the component the mechanical properties are increased and fatigue life will be longer. The heat-treating process can somewhat dissolve hard clusters and increase the homogeneity of the particles.

### **2.7.2 Skövde's heat treatment**

Volvo foundry in Skövde delivers the stress lattices for residual stress testing. The lattices are heat treated in two large furnaces. The ovens heats up the iron components to roughly 610 °C

with the purpose to remove most of the residual stresses that has developed during the casting process. This heat treatment process is the one that is in need of optimization since the process is a limitation in the efficiency and is a bottleneck in production. A more efficient process could potentially be beneficial for profits and high quality production.

The capacities of the ovens are extremely large; the bigger of the two is able to contain 100 metric ton of goods. The oven uses convection to distribute the heated air more evenly yet it takes roughly nine hours to heat the oven up to 610 °C, with a heating rate of 67 °C/h, understandable considering the size. The overall heat treatment process takes about 23 hours to be finished. Regarding changeable parameters, phase 2 (holding time) and phase 3 (cooling rate) can be changed but the initial heating process, phase 1 couldn't be changed due to the oven's maximal heating capacity. More information regarding these phases and plots can be seen in Simulations section 4.1.

## 2.8 Measure residual stresses with sectioning method

The elongation (length difference in %) is measured using a strain gauge. Using only one gauge is not sufficient; several gauges are required in order to accumulate accurate data. The strain gauge is a simple technological tool and yet precise and accurate when measuring resistance.

To measure elongation the strain gauge is fixated into the test pieces surface with a suitable adhesive. The adhesive must cover all of the thin copper wiring to ensure that errors are kept small. The setup of the gauge is simple and uses a Wheatstone bridge to calculate the resistance in the strain gauge. The Wheatstone bridge is the electrical circuit shown in Figure 2.7.  $R_{\text{gauge}}$  has an unknown resistivity and can be calculated by knowing all the other resistances. The unknown resistivity changes depending on strain of the section and can thus be used as a way to measure the strain. Figure 2.7 describes the Wheatstone bridge and shows how the gauge is included.

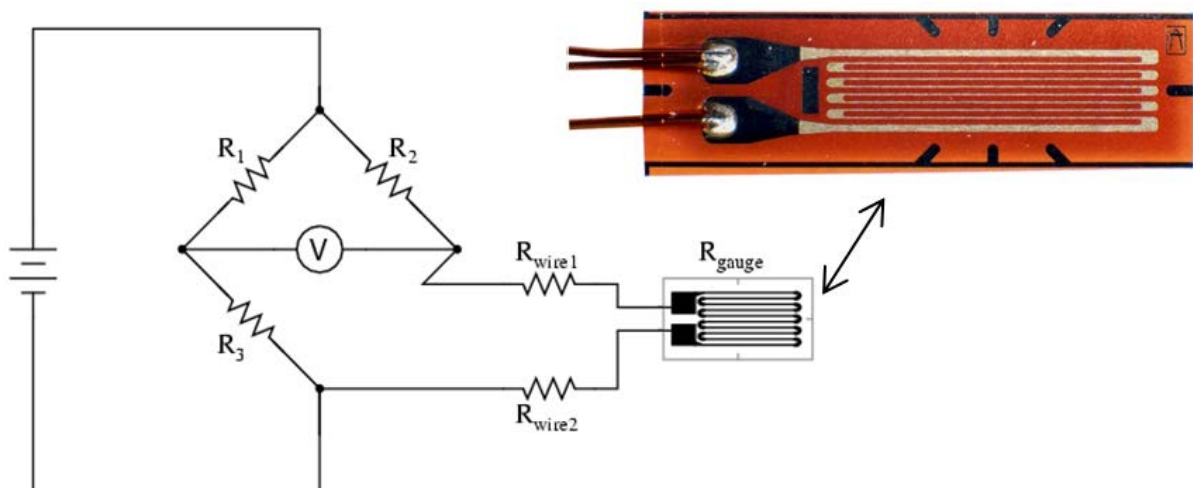


Figure 2.7. The Wheatstone bridge to measure resistance in a strain gauge.

The  $R_{\text{gauge}}$  is what is known as the foil in the strain gauge and does a zigzag thread resemble a spring. This is to ensure that the elongation is completely elastic and makes sure that only

linear elongation occurs, a necessity for precise results. The resistance is very sensitive to changes. Under tension the area of the thread becomes smaller and resistance increases. Under compressive stress the area grows larger and resistance is lowered. From this the load case and stresses can easily be determined using the equations below. From equations Eq.1 and Eq.1 below, GF is Gauge Factor,  $\Delta R$  is the change of resistance,  $R_g$  is resistance before deforming and BV is the bridge excitation voltage.

Equation 1 and equation 2. The relation used to calculate strain from measured resistance.

$$GF = \frac{\Delta R/R_G}{\epsilon} \tag{Equation 1}$$

$$\nu = \frac{BV-GF-\epsilon}{2} \tag{Equation 2}$$

The material used for the strain gauge is specific due to the thermal expansion that occurs during testing. The alloys have been designed so that the thermal expansion of the material cancels out by the resistance decrease due to the extra heating. Figure 2.8 shows the tool used to measure the resistivity from the strain gauge. First the strain is calibrated before the sectioning is performed and will generate the first strain value  $\epsilon_1$ . After sectioning a new strain is measured  $\epsilon_2$  and the difference is calculated as  $\epsilon_1-\epsilon_2$ . The  $\Delta\epsilon$  is used in Hooke’s law and with a Young’s modulus of 130 GPa in compressive and 120 GPa in tensile will give the stress through the lattice.

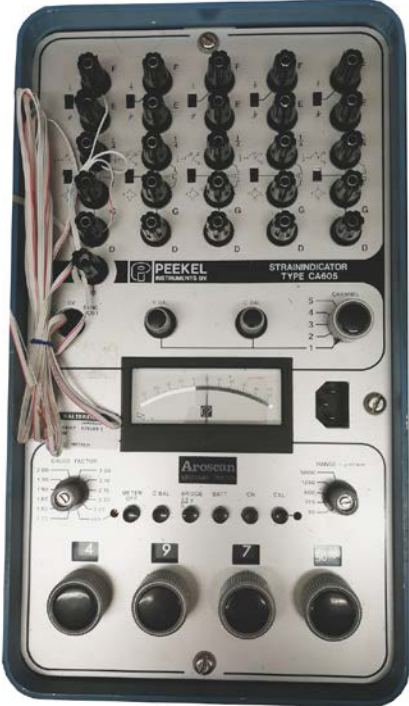


Figure 2.8. The tool used to measure the strain generated from the Wheatstone bridge to measure resistance in a strain gauge.

Following is an example of how the stress is calculated from measurements:

First measure the strain  $\varepsilon_1$  from calibration of the Wheatstone bridge, e.g. 49750. After sectioning, the strain has to be measured once again;  $\varepsilon_2$  is given, e.g. 50000. This gives the total strain of sectioning ( $\varepsilon_1 - \varepsilon_2 = -250$ ), by apply the Hooke's law in compression stress ( $E=130$  GPa) the resulting stress is  $E \cdot \varepsilon = 130 \text{ GPa} \times -250 = -32,5 \text{ MPa}$ .

(National High Magnetic Field Laboratory: Magnet Academy, 2014), (Kyowa, 2017)

## 2.9 Thermocouple

Thermocouples will be used to measure the temperature of the stress lattices in the practical experiments. The principle behind it is simple and it can measure temperature accurately enough to fulfill the demands of the testing. By joining two rods of different alloys with one another through soldering at one end and let the two pieces experience a heat change, a difference in voltage will be generated at the soldered point. The voltage generated from this type of action is called the Seebeck effect. This effect is measured in emk (electro-motive force, in this case it is referred to termo-emk because the difference in voltage is generated due to the temperature difference) and is the sum of change of potential in a circuit.

On the opposite side of the rods, the non-soldered part is then attached to a device measuring the change of voltage over the two metals and display the temperature. The variant used in the experimental part is a type-K thermocouple. The type denotes the alloys used for the thermal coupling. The type-K uses the alloys chromium-nickel and aluminum-nickel. The image below is the specifications of the strain gauges used.

(Kyowa, 2017), (Pentronic, 2017)

KYOWA		MADE IN JAPAN	
Model 型式	KFGS-5-120-C1-11L3M3R	Lot No. Y3745M	Quantity 数量 10
		Batch No. 005A	
Gage Factor (23°C, 50%RH) ゲージ率	2.09 ± 1.0%	Temperature Compensation for 適合材料	STEEL
Gage Length ゲージ長	5 mm	Adoptable Thermal Expansion 適合線膨張係数	11.7 × 10 <sup>-6</sup> /°C
Gage Resistance (23°C, 50%RH) ゲージ抵抗 <small>excluding the leadwires リード線除く</small>	119.6Ω ± 0.4%	Applicable Adhesive 主な適用接着剤	CC-33A, EP-340
Transverse Sensitivity Ratio (23°C, 50%RH) 横感度比	0.1 ± 0.2%	Temperature Coefficient of Gage Factor ゲージ率の温度係数	Refer to Graph グラフ参照
Thermal Output 熱出力	Refer to Graph グラフ参照		共和国-1437
			

Figure 2.9. Package containing the strain gauges and the specifications.



### 3 INVESTIGATED MATERIALS

The experimental part will be performed and compared between three materials; Grey iron GJL-250, Grey iron VIG-275/190 and Ductile iron EN-GJS-500-7. It should be noted that the chemical composition is just for reference. Each foundry adjusts their cast iron composition to achieve the mechanical properties demanded of the iron.

Two foundries produced the stress lattices used for the experimental part, Skövde foundry and SKF's foundry.

#### 3.1 Grey iron, VIG 275/190

The chemical composition of material VIG-275/190 AS/SR (as cast or stress relieved) is according to Table 3.2. A chemical analysis of the cast component has been done by Skövde, the results are corresponding to the specified composition range shown in table 3.2 (lattice).

Chem. Comp.	C	Si	Mn	P	S	Cr	Ni	Mo	Cu	Sn	Ceqvi.
AC/SR	3,05- 3,25	1,7- 2,0	0,5- 0,8	max 0,08	0,08- 0,14	0,1- 0,18	-	0,2- 0,3	0,8-1	0,04- 0,07	3,65- 3,94
Lattice	<b>3,32</b>	1,99	0,56	0,03	0,08	0,11	0,04	0,22	0,91	<b>0,033</b>	3,83

Table 3.1. The specified chemical composition of VIG-275/190 and the measured composition of the lattice. Red text marks out of specification. Note: red text signifies that the value is not within range.

The material matrix consists of pearlite. The material must not contain free ferrite and the maximum amount of carbides must not exceed 1%.

The mechanical requirements are as follow:

- Tensile strength is minimum 275 MPa
- Minimum hardness of 190 HB
- No specification regarding elongation and yield strength

(VISG 275/190 SR, STD 310-0001 [Volvo standard])

### 3.2 Grey iron, GJL-250

The material GJL-250 is a grey cast iron. This material consists of a base of iron, carbon and silicon, i.e. the base elements of cast iron, typically a carbon equivalent of 4.3% or lower. Small amounts of copper, manganese, phosphorous, nickel and molybdenum are added to fulfill the mechanical requirements of the cast iron. These requirements are as follow:

- *Tensile strength is minimum 250 MPa*
- *Hardness is minimum 190 HB*
- *No specification regarding elongation and yield strength*

A chemical analysis was performed on two samples from the cast lattice and the following results are according to the specified composition.

*Table 3.2. Chemical composition of the GJL-250 cast iron. Ti and Sn are trace elements and are not part of the alloy.*

Chemical composition	C	Si	Mn	P	S	Cr	Ni	Mo	Cu	Ti	Sn	Ceqvi.
<b>AC/SR</b>	3,1– 3,4	1,8– 2,3	0,6– 0,8	Max 0,2	0,06– 0,12	-	-	-	-	-	-	3,6– 3,9
<b>Nr. 1</b>	3,41	1,84	0,7	0,021	0,071	0,052	0,041	0,012	0,284	0,007	0,005	3,88
<b>Nr. 2</b>	3,4	1,88	0,74	0,019	0,08	0,045	0,042	0,011	0,299	0,007	0,005	3,88

VIG 250/190 SR STD 310-0001 [Volvo standard]

### 3.3 Ductile iron EN-GJS-500-7

In general a cast iron is named according to its mechanical properties. This is due to the varying conditions and parameters that apply between a large and a small cast component. Meaning composition is less significant in cast irons. Stress concentrations are more severe for smaller components and the size and position of the graphite can be harmful if it is in a critical area. A bigger component is more robust and can therefore withstand the potential flaws of the cast iron. Young's modulus is 169 GPa and the other mechanical properties of EN-GJS-500-7 are:

- *Tensile strength is minimum 500 MPa*
- *Yield strength is minimum 320 MPa*
- *Elongation of minimum 7%*
- *Hardness range of 170-230 HB*

The chemical composition is a comparison between Skövde and SKF lattice. The amount of copper and phosphorus is higher in the Skövde lattice. All elements are in accordance to specification.

*Table 3.3. The specified chemical composition of GJS 500-7*

	<b>C</b>	<b>Si</b>	<b>Mn</b>	<b>P</b>	<b>S</b>	<b>Cu</b>	<b>Mg</b>	<b>Ni</b>	<b>Mo</b>
As cast/SR	3,2-4,0	1,5-2,8	0,05-1,0	0,08	0,02	0-0,5	0,03-0,08	-	-
Lattice Skövde	3,49	2,54	0,3	0,028	0,007	0,33	0,039	0,03	≤0,01
Lattice SKF	3,49	2,32	0,42	0,016	0,009	0,30	0,044	0,02	≤0,01

(VISG 500-7 AC/HT, STD 310-0004 [Volvo standard])



## **4. METHOD**

This chapter describes the theory behind the experimental analysis as well as the collection of useful information to evaluate the results. To see the practical testing plan see chapter 5, Implementation.

### **4.1 Simulations**

Magma5 is a software program used to fully integrate optimization capability for casting simulation processes. The software uses material data combined with a simulation tool (based on Finite Difference Modeling, FDM). The software will be used to simulate the casting process of the lattice and predict the residual stress. The software is also used as a tool to predict the stress relieving effect of a thermal heat treatment. The results from the simulation will be compared with the measured stress results from the experimental testing. The variation and differences between the two methods can show where the simulation varies compared to the experiment.

A CAD-model of the stress lattice geometry is imported to Magma5. The part is split in half to speed up the simulation process; due to a symmetric geometry, this won't affect the results. Virtual measurements are placed in the model to measure tensile and compressive stress. When all the settings and parameters are inserted the simulation of both solidification and heat treatment is started and will take a few hours to finish. To speed up the process time even further the mesh size is decreased from 2 000 000 to 500 000 cells in the following simulations. The use of a bigger mesh size (fewer cells) did not have an effect on the results. (Magmasoft, 2017)

### **4.2 The stress relieving heat treatment**

To get the most out of the practical heat treatments the different treatment profiles were based on recommendations provided from drawings and from Skövde Foundry. For full insight into the heat treatments used see Appendix B.

#### **4.2.1 The heat treatment according to Volvo drawing recommendations**

In Figure 4.1 the maximal recommended heating and cooling rates combined with a decreased hold time is presented. (Volvo drawing No. 1677285); According to the drawings this is the most time efficient heat treatment approved and it will be used as a reference heat treatment. Both the practical and simulated heat treatments will be performed by changing the length and intensity of the different phases and then evaluate the effect on the resulting residual stresses.

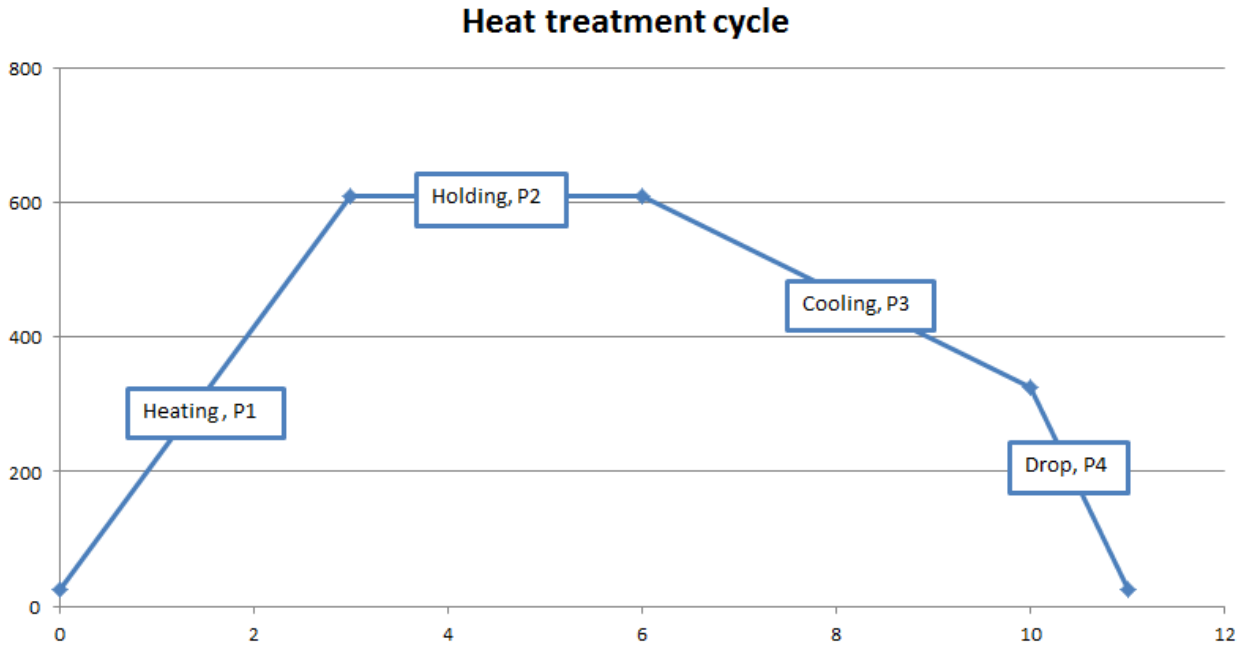


Figure 4.1. The time efficient heat treatment according to recommendations from Volvo drawing No. 1677285.

#### 4.2.2 Skövde heat treatment

The heat treatment oven at Skövde foundry is not built to exceed heating rates over 70 °C/h, which makes the heat treatment presented in the drawings impossible to conduct. The limitations of the oven have to be taken into consideration when testing the different parameters in the heat treatment cycle. With a lower heating rate the time to achieve maximum temperature will increase and result in a higher stress relieving process during this initial phase. By experimental tests a reduction of holding time can potentially be the best way to optimize the heat treatment process. In the experimental part a comparison will be made to see how well the relaxation of residual stresses is performed and how it differentiates from the recommended heat treatment profile.

#### 4.2.3 Limitations

Performing a heat treatment cycle similar to the simulation is difficult to recreate in the practical case. When conducting the HT at Volvo, Lundby the heating rate (phase 1) and hold time (phase 2) is directly controlled by the settings of the oven and therefore not an issue. The oven will guarantee that each run is as similar as possible. The challenge is to get the cooling rate (phase 3) correct. In an attempt to find different heat treatment profiles and templates a thermocouple was used to measure the temperature over time.

*Phase 1 (heating rate, P1)* - The programmed heating rate seems to align with the actual air temperature which can perform both 200- and 67 °C/h options usable as heating rates. Figure 4.2 confirms the programmed heating rate of 200 °C/h and the actual air temperature rate.

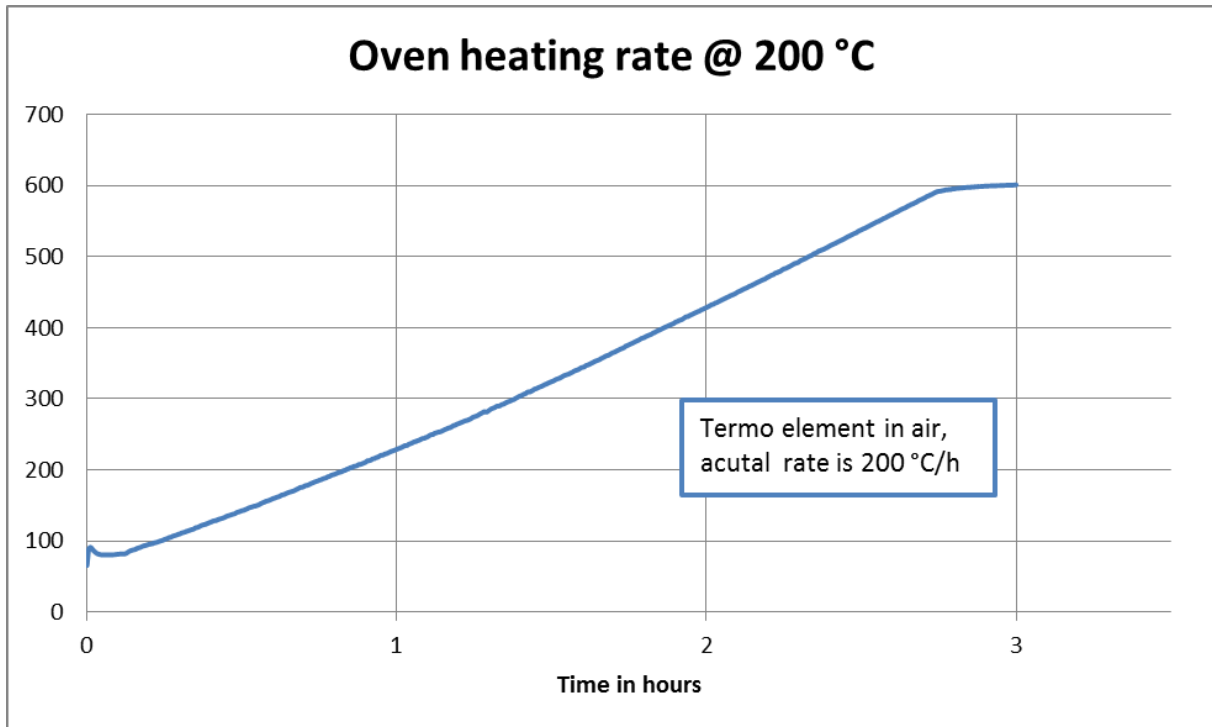


Figure 4.2. Confirms the air temperature follows the controlled heat rate of 200 °C/h.

*Phase 2 (holding time, P2)* - The oven uses the maximal programmed temperature as a hold temperature and the time can be programmed into the heat cycle without interference. The temperature in the lattice gets slightly higher after reaching the maximal air temperature. This can be explained by the way heat can be transferred through conduction, convection and radiation. The heating element will also generate radiation which will be absorbed by a solid metallic material. Some variations are also within the margin of error and the position of the two thermocouples in the oven could potentially affect the variations in temperature registered as well.

*Phase 3 (the cooling rate, P3)* - To control the cooling rate, different materials and tools will be used such as a ceramic blanket and isolating sand. The tests are performed by heating the lattice up to 600 °C and cool it with varying tools in order to evaluate their actual cooling rates. One of the thermocouples are drilled into the lattice and used to measure the temperature inside the component. There is also a discrepancy between the air and lattice temperature. There is a delaying effect on the lattice but it will follow the same trend as the air temperature. The consequence of this is that the lattice might heat up and cool down slower. But as long as the tests are consistent the discrepancy can be ignored and the results can be compared with each other. Figure 4.3 shows the setup of the stress lattice in the oven and how the thermocouple is placed into the lattice.

*Phase 4 (Drop temperature, P4)* – Is when the lattice is taken out of the oven and is left to freely cool down to room temperature. This is the last and final step in the heat treatment and the only requirement is that the drop does not occur at a too high temperature. This is to reduce the risk of introducing new residual stresses in the material and by Volvo standard this temperature is put at 325 °C.



Figure 4.3. Oven 10 is used for the practical heat treatment experiments. The stress lattice is shown in the middle and a thermocouple is put inside the lattice through a drilled hole. Note the shadow of the thermocouple at the back of the oven.

### 4.3 Residual stress measurement by sectioning method

Sectioning is a destructive test method and the purpose is to find the extent of the residual stresses present in the material. The stresses contained in the material will be converted to elongation when the material is sectioned. The way the cuts will be performed is seen in Figure 4.4 marked as 2 red lines. By applying several strain gauges to the piece the elongation can be measured and via Hooke's law the elongation can be translated to a stress value. In the usual components the residual stresses are directed in all three dimensions but the lattice geometry used to conduct the tests creates stresses mainly along the X-axis and only a small portion of the stresses are along the Y and Z-axes. The surface of the lattices where the strain gauges are applied is machined with a milling tool of 40mm diameter as shown in Figure 4.4. The depth of the milling is measured to 1,2mm and will not affect the stress results, according to simulation. It is also shown in Figure 4.4 the positions of strain gauges that have been fixated on the stress lattice.

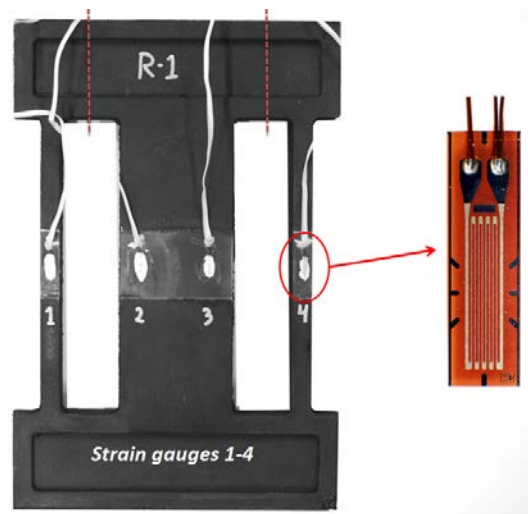


Figure 4.4. The location of strain gauges for the first two measurements. Orientation has been provided in figure 2.6.

### 4.4 Potential bending load case of the stress lattice

Difficulties arise when presumably a bending load case of the lattice is noticed. The strain gauges are easily influenced by different factors and a slight bending of the lattice can potentially skewer the results. Even a small dislocation along wrong axis can have an impact on the results and therefore caution is used when looking at the strain values. When the sectioning is performed an ideal situation would be tensile or compressive stress only in X-direction. In the theory of a bending case, additional stress will be generated by the bending. The combination of the two stress cases are explained in Figure 4.5. The location of strain gauges will therefore be changed to both sides of the cross section. Calculating an average stress value from the strain gauges placed on each side will give the longitudinal stress in X-direction and compensate for the effect of bending stress. This assumes that only the two load cases seen below are present and can only provide an estimation of the real bending and tensile stress.

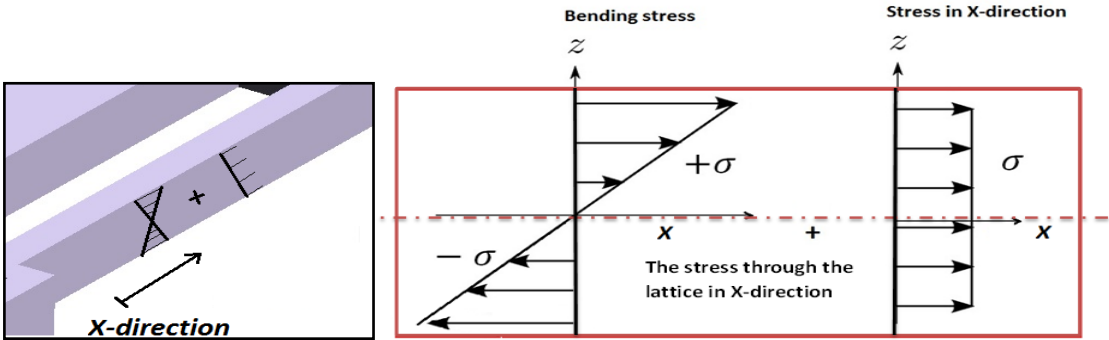


Figure 4.5. The bending case of the stress lattice in X-direction.

Figure 4.6 shows the new location of the strain gauges. Strain gauge 1 and 2 are placed the same positions as previously and measure compressive and tensile stress respectively. Strain gauges 4 and 5 are placed on the other side of the lattice, mirroring the placement of strain gauge 1 and 2. This is to accommodate the small bending case discussed earlier. Strain gauge 3 is placed to confirm the values seen in strain gauge 1 and 4. This is due the scatter seen in previous stress measurement and for added reliability.



Figure 4.6. The location of strain gauges at the heat treated stress lattice. The two gauges to the right have already been coated in order to prevent them being damaged.

The setup seen above worked out well for stress measurements and less scattering was seen in the stress measurements. An evaluation was done regarding the setup of the strain gauges and the conclusion was to skip the third strain gauge since it was found unnecessary. Due to the removal of strain gauge 3, strain gauge 4 and 5 had their number reduced by one, calling them instead strain gauge 3 and 4 respectively. This new positioning is the setup used throughout the measuring phase for both GJL-250 and GJS-500-7 and if any other setup is used it is noted.

## 5. EXPERIMENTS

This chapter describes the practical testing as well as the simulations and how the two parts are performed. Each step of both the practical and simulation experiments is done on all investigated materials, with the exception of simulations of GJL-250. The outline of the chapter is as follows:

- *Simulate solidification process and varying heat treatments to evaluate the residual stresses by changing heat treatment parameters (heating rate, hold time, cooling rate, drop temperature and material).*
- *Measure residual stresses in the as-cast stress lattices. This gives the reference value of the residual stresses before heat treatment.*
- *Try varying techniques to obtain heating and cooling rate profiles and establish suitable heat treatment cycles.*
- *Measure the stress lattices after heat treatment. The remaining residual stress in the lattice will be evaluated and compared to the simulation and reference lattice. From these values further testing will be done to fully grasp the difference between the varying heat treatment parameters.*

## 5.1 Simulations

The simulations are done to examine how the heat treatments affect the stress in the lattice. Both differences and similarities to the practical testing are important to note and can provide insight in how the material handles different parameters. Table 5.1 presents the simulations done. Since the heating rate is restricted at Skövde no changes are done in this phase. Hold time, cooling rate and drop temperature are simulated and evaluated. V2 is the currently used heat treatment at Skövde today and all later simulations have one, two or three changed parameters. The objective of the simulations was to reduce the time of the heat treatment cycle. The following simulations are performed on the alloy GJL-300; this will be used to compare with the VIG material.

Table 5.1 from drawing v7 is the outline of performed simulations directed towards Volvos HT- recommendations (drawing No. 167728). By changing parameters (heating rate, hold time, cooling rate and drop temperature) the effect of each parameter can be found in form of residual stresses. In the last attempt, V22 the combination of high rate and no hold time is investigated.

Table 5.1. Simulations of Skövde foundry. The bold values are the changed parameter from previous version.

Simulation:	Heating rate °C/h	Hold time h	Cooling rate °C/h	Drop temperature °C
Now used parameters (V2)	67	5h	70	110
No hold time (V3)	67	<b>0</b>	70	110
Increased cooling rate (V6)	67	0	<b>110</b>	110
Increased cooling rate (V5)	67	0	<b>150</b>	110
Increased quenching temp. (V8)	67	0	78	<b>200</b>
Increased quenching temp. (V9)	67	0	78	<b>300</b>
Hold time 2.5h (V13)	67	<b>2,5h</b>	78	110
Increased cooling rate and quenching temp. (V14)	67	<b>2,5h</b>	<b>150</b>	<b>300</b>
Extreme values (V15)	67	<b>Removed</b>	<b>300</b>	<b>400</b>
Hold time 1h (V21)	67	<b>1h</b>	78	300
From drawing (V7)	200	2.5	75	300
Low hold time (V16)	200	<b>1.25</b>	75	300
High cooling rate (V17)	200	1.25	<b>150</b>	300
Combination of high rate without hold time (V22)	200	<b>0</b>	<b>150</b>	<b>325</b>

The amount of simulations of the ductile cast iron GJS-500-7 was less, since the aim was just to perform a comparison between the practical testing and the simulations. Only six simulations were run, same as the amount of measured stress lattices. The configuration (heating rate, hold time, cooling rate, and drop temperature) of the simulations are the same as the planned heat treatments.

Table 5.3. The simulation scheme for GJS-500-7. Modifications were done to previous heat treatment profiles and therefore no version numbers are written in the last attempts.

<b>Simulation:</b>	<b>Heat rate °C/h</b>	<b>Hold time h</b>	<b>Cooling rate °C/h</b>	<b>Drop temperature °C</b>
<i>From drawing (V23)</i>	200	2.5	75	300
<i>No hold time (V24)</i>	200	<b>0</b>	75	300
<i>Low heating rate (V25)</i>	<b>67</b>	2,5	75	300
<i>Long hold tim, 5h</i>	200	<b>5</b>	75	300
<i>150 °C/h cooling rate</i>	200	2,5	<b>150</b>	300
<i>High drop temp, 425 °C</i>	200	2,5	75	<b>420</b>

## 5.2 Design of the practical heat treatment

In this section the tailoring of the heat treatments are presented. The parameters that can be changed in the heat treatment cycle are:

- Heating rate (67-200 °C/h)
- Holding time (0-5 hours)
- Cooling rate (75- 150 °C/h)
- Drop temperature (100-420 °C)

The heat treatments are performed in randomized order to avoid uncontrollable influences from equipment and material. Only one parameter should be changed between each trial. The parameter with largest effect on the residual stresses can have an additional heat treatment added in order to do at correct interpolation between the changed parameters.

### 5.2.1 Design of the cooling rates

The oven control settings are programed to control the rates. The results from varying cooling rates are plotted in Figure 5.1. The cooling rates used will be two rates with a large difference, e.g. the maximal cooling rate 150 °C/h and 75 °C/h are chosen to be used in following heat treatments.

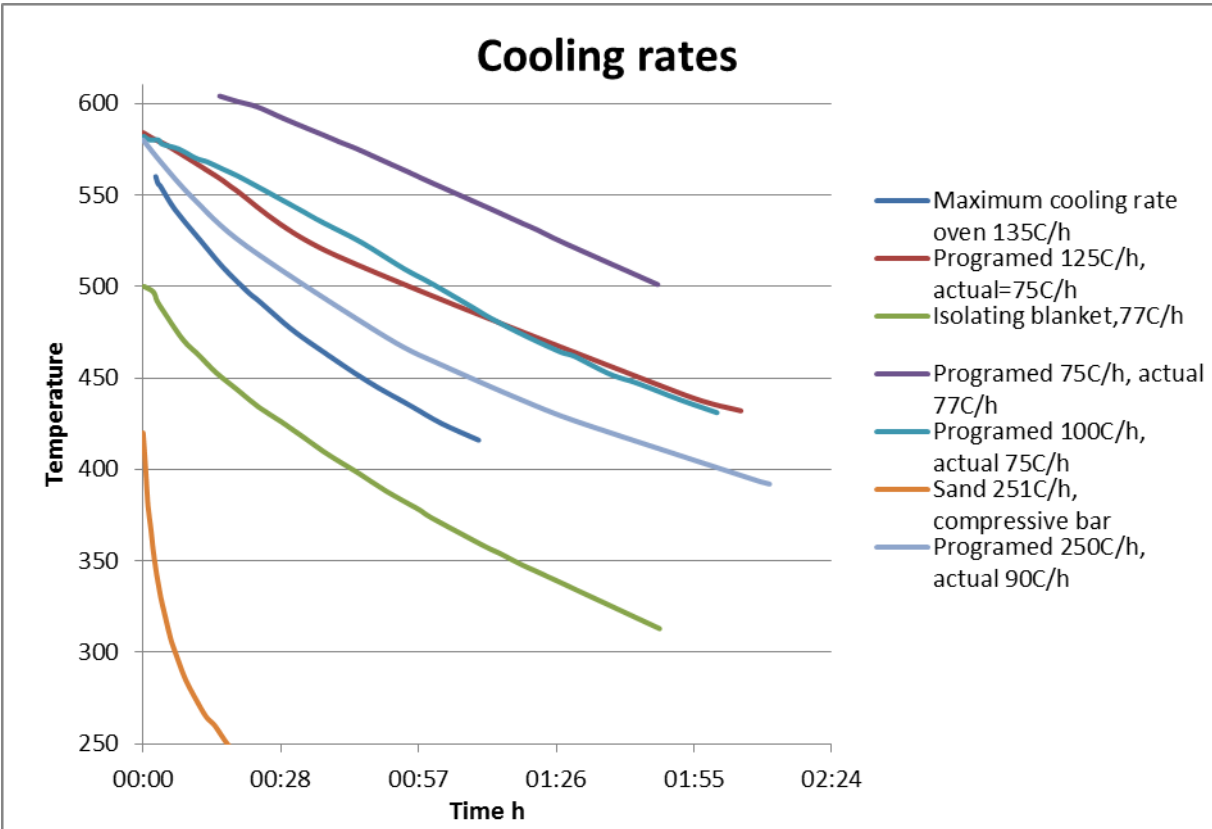


Figure 5.1. The experimental cooling rates of the oven and isolating media.

From the risk of causing too large variances during the cooling phase sand and/or isolating blanket was deemed unreliable and a non-repeatable process. In order to use these methods removing the heated lattice from the oven was required to be able to place it in sand or cover it in the blanket. By removing the lattice from the oven the lattice will be exposed to room temperature leading to rapid cooling of the lattice. In the 600 °C to 500 °C large temperature gradients can easily form, especially during rapid cooling. This in turn leads to increased residual stresses and would reduce the initial stress relieving effect of the heat treatment. Given the fact that the cooling phase is also non-repeatable using these method makes them unsuitable to use. From testing it was shown that the oven is able to cool at a rate of 135 °C/h and this value can be increased further by slightly opening the oven seal. By limiting the option to just using the oven stability and consistency is obtained during the cooling phase, thus making it the ideal choice to use for the experiments.

*Table 5.4. The experimental cooling rates of air, sand and isolating blanket.*

<b>Tool used to isolate the heat</b>	<b>Resulting cooling rate °C/h</b>
<i>Air cooling</i>	~1000
<i>Sand</i>	~250
<i>Isolating blanket</i>	~100

## 5.3 The practical heat treatments

The heat treatments that are performed have the purpose to provide information regarding how each individual parameter affects the residual stresses. Four varying parameters (heating rate, hold time, cooling rate and drop temperature) and one extra attempt at an intermediate holding time requires at least six heat treatments. Using two other lattices as references makes it a total of eight lattices in order to examine in all the variations. With any remaining lattices further testing will be done to complement the results providing better insight in both the effect of the specific parameter tested and also provide information regarding the combining effect if two or more parameters are changed.

### 5.3.1 Grey Iron, VIG 275/190

A total of 16 lattices of VIG 275/190 were delivered, 2 of these were already heat treated at Skövde and would be used as heat treated references. Due to inexperience of working with all the new equipment a few failed attempts were expected. Out of the 16 lattices, 10 went through some kind of heat treatment at the materials lab. The first six treatments were done in the order presented below in table 5.5 while the last remaining four lattices had custom heat treatments in order to further investigate parameters more suited towards Skövde foundry and Magma5.

*Trial 1:* Is done according to the plan, i.e. 2,5 hours holding time and 75 °C/h cooling rate. The changed parameter will be the heating rate which will be the same as Skövdes heating rate (67 °C/h), drop temperature is set to be 200 °C. This change is done in order to create contrast between the attempts where drop temperature is the changed parameter.

*Trial 2:* Is also the heat treatment used as reference; all parameters are according to the drawings shown in Appendix A.1. The only difference is yet again the drop temperature at 200 °C rather than the recommended 300 °C.

*Trial 3 and 4:* The effect of hold time is investigated. Two trials are used for this due to the significant effect the parameter had in the simulations. Trial 3 has no holding time and should create a higher stress than the other five attempts. Trial 4 uses a holding time twice the time of the recommended value 2,5 hours, meaning a 5 hour holding time. If the simulation is correct, this attempt should have the lowest stress of all initial lattices tested and confirms the reference value together with trial 3.

*Trial 5:* Double the cooling rate from 75 °C/h to 150 °C/h. All other parameters remain the same as trial 2. According to the simulation changing the cooling rate shouldn't affect the stresses in the lattice more than a few percent. Confirming this behavior is especially important for VIG-275/190 due to the potential of reducing the heat treatment time at Skövde foundry of same material.

*Trial 6:* Where the drop temp. is increased from 200 to 420 °C. From previous simulation changing the drop temperature from 200 to 300 °C showed no change between the attempts. At 420 °C no major differences were seen in stress levels in the simulation while it also suggests that most of the residual stresses are generated between 600 °C and 400 °C. To confirm this trial 6 is done and hopefully provides valuable information.

Table 5.5. The heat treatment cycles of the first seven heat treatments for VIG- 275/190:

<b>Trial</b>	<b>Heating rate [°C/h]</b>	<b>Hold time [h]</b>	<b>Cooling rate [°C/h]</b>	<b>Drop temperature [°C]</b>
1	67	2,5	75	200
2	<b>200</b>	2,5	75	200
3	200	<b>0</b>	75	200
4	200	<b>5</b>	75	200
5	200	2,5	<b>150</b>	200
6	200	2,5	75	<b>420</b>

*Trial 7:* Performed to create residual stresses with extreme case of a heat treatment and is compare with Magma5 simulations. Seeing previous differences between simulation and practical testing this attempt was done to create contrast between them and analyze why the difference is only seen in one of the tests.

*Trial 8:* Performed due to the assumption that the previous values from trial 2 were wrong and due to it being the reference made it difficult to draw conclusions.

The last two trials 9 and 10 were both directed towards the Skövde cycle. Trial 9 was the new recommended heat treatment for Skövde. The treatment would reduce the time from a total of 23 hours to mere 14 hours, a reduction of 9 hours. The treatment was designed using previous values from attempt 1 to 8. Trial 10 was done in order to compare with trial 9 and was therefore done according to Skövdes used parameters since the two heat treated lattices exhibited unexpected residual stresses. With these tests the last lattices were used and concluded the heat treatments of VIG 275/190.

Table 5.6. The four remaining heat treatments of VIG 275/190:

<b>Trial</b>	<b>Heating rate [°C/h]</b>	<b>Hold time [h]</b>	<b>Cooling rate [°C/h]</b>	<b>Drop temperature [°C]</b>
7	250	0	150	200
8	200	2,5	75	200
9	67	2,5	150	300
10	67	5	75	100

### 5.3.2 Grey Iron, GJL-250

SKF delivered 11 lattices of the unalloyed grey cast iron, GJL 250. The six first lattices were used in the same manner as the previous material; the planned heat treatments are shown in table 5.5. No changes were deemed necessary due to the previous good results and the tests provide contrast between the attempts. If any further testing or certain parameters were required, these could be tested using the last three remaining lattices. The results provided from the initial six lattices were approved and they responded better to the heat treatment than previously expected.

*Trial 7:* The holding time was the single most influencing parameter and in order to fully make out a trend it felt required to do an attempt with a holding time of 1 hour and 15 minutes, half of the recommended holding time of 2 hours and 30 minutes.

*Trial 8:* Directed towards the industry where the cast iron component is shaken out of its mould before it ever has a chance to cool off. In an attempt to re-create this handling of the goods the lattice will be taken out of the oven at a temperature of 600 °C. The assumption is that this will generate high residual stresses due to the rapid cooling.

*Trial 9:* Is done to further investigate the creep in the material. Comparing the values of GJL-250 and VIG275/190 have shown that the unalloyed material responds better to the heat treatments and tend to have lower residual stresses. Looking back at materials presented in the theory chapter this is predicted but how much effect it has in particular is looked more closely at here with this attempt.

Table 5.7. The remaining heat treatments of GJL-250:

<b>Trial</b>	<b>Heating rate [°C/h]</b>	<b>Hold time [h]</b>	<b>Cooling rate [°C/h]</b>	<b>Drop temperature [°C]</b>
7	200	1h 15min	75	200
8	200	2,5	-	600
9	200	2,5	350	200

### 5.3.3 Ductile Iron, GJS 500-7

A total of seven lattices were delivered from SKF foundry. This is less than required to complete the heat treatment used from the previous materials. Because of this limitation, one of the attempts has to be skipped (attempt 1). The conducted heat treatments can be seen in table 5.8. Attempt 7 was done in order to investigate the amount of creep at a lower temperature and look at the possible differences in residual stresses it would cause.

Table 5.8. The reduced heat treatment plan for Ductile Iron GJS 500-7:

<b>Attempt</b>	<b>Heating rate [°C/h]</b>	<b>Hold time [h]</b>	<b>Cooling rate [°C/h]</b>	<b>Drop temperature [°C]</b>
2	200	2,5	75	200
3	200	0	75	200
4	200	5	75	200
5	200	2,5	150	200
6	200	2,5	75	420
7	200	2,5 @ 540 °C	75	200

# 6. RESULTS

The results from simulations and practical experiments are presented and explained in this chapter.

## 6.1 Simulation

The first simulation is performed to calculate the residual stress after the solidification and cooling. Thereafter simulation of heat treatment parameters are performed with varying parameters such as heating rate, hold time and cooling rate. Magma5 simulates residual stresses over time in the casting process and the relieving of heat treatment. The first simulation includes the ingate system; by simulate the solidification process and removing the ingate system the residual stresses gets slightly higher, but no significant difference. The residual stresses after casting will be the output values compared to the stress after heat treatment. Figure 6.1 shows the residual stresses in X-direction after solidification. Three points are chosen to show the local stress values. First point is placed inside the middle section 12.5mm down. Second point is on the surface of the middle section and the last point is placed on the surface of the compressive section.

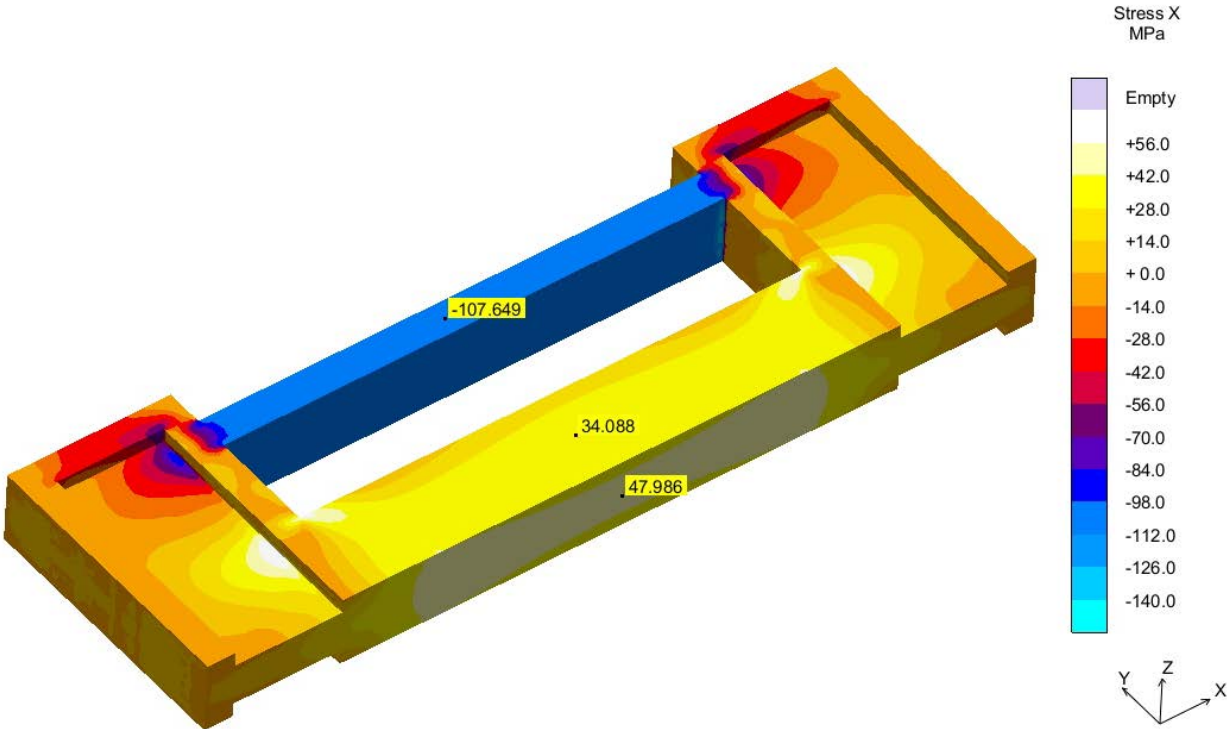


Figure 6.1. Simulated solidification process of stress lattice (simulation v1).

In Figure 6.2 seen below is the lattice after the heat treatment. The simulation shows that the tensile stresses in point 1 and 2 have been reduced by 84% and 77% respectively and compressive stress reduced by approximately 78 %.

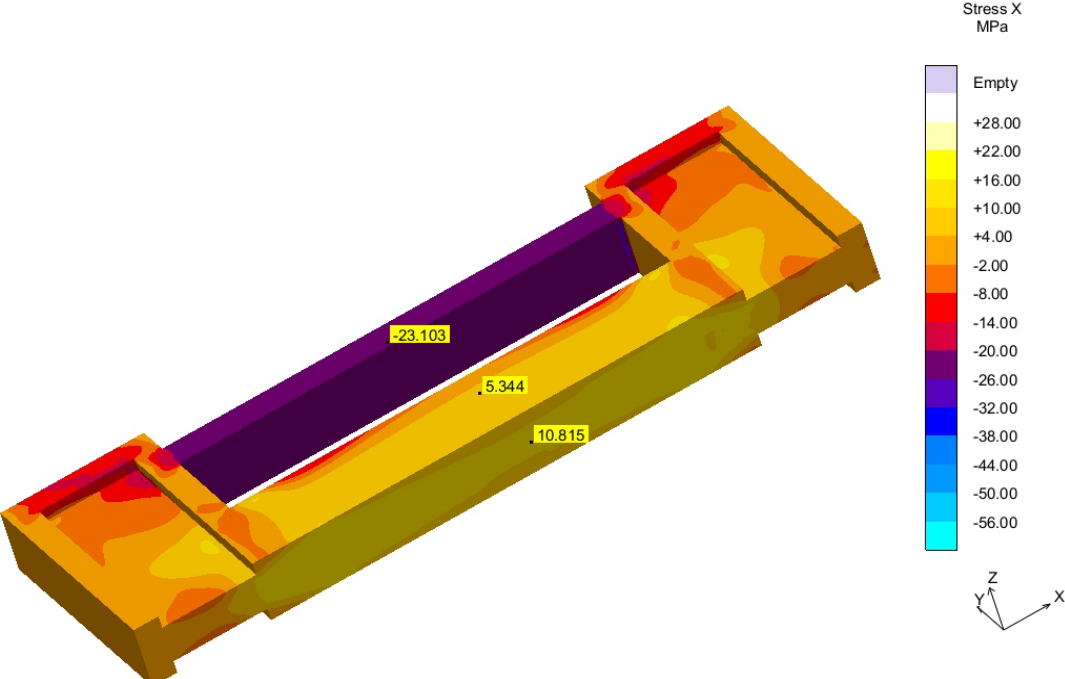


Figure 6.2. Simulation result of the residual stresses after heat treatment (simulation v02).

To confirm the relieving effect of the sectioning method a simulation is performed with the same scenario. The stress relieving section cut can be simulated as a machining operation after heat treatment. Figure 6.3 shows the stress after heat treatment to the left and remaining stress after sectioning to the right. As shown almost all stress is relieved in the compressive section, in the tensile section the residual stress is relieved and causing compressive load due to deformation after cutting. Along the edge of the thick section increased compressive stress are seen.

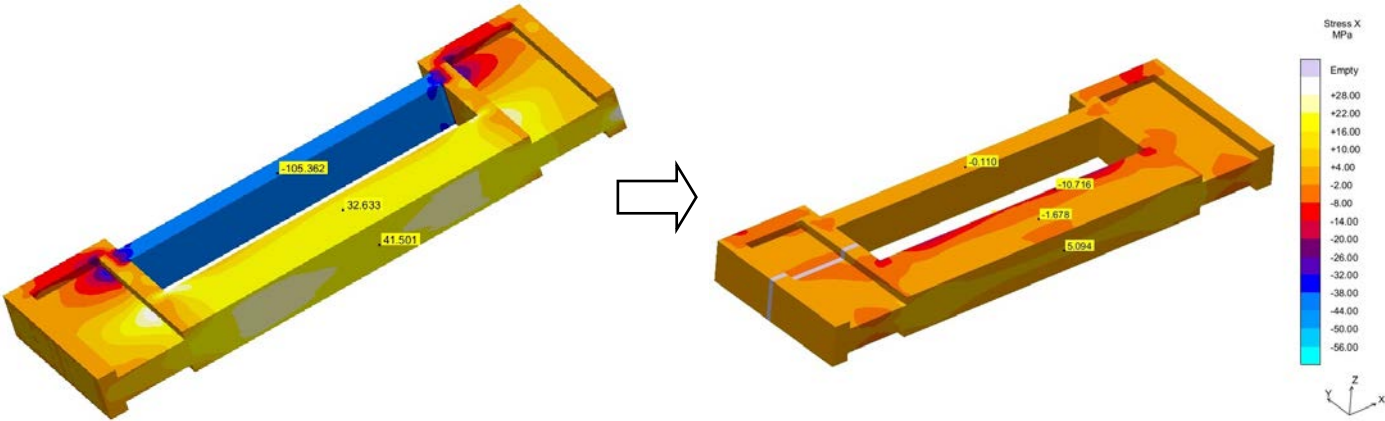


Figure 6.3. Simulation of the stress relieving section cut.

### 6.1.1 Simulations of GJL 275/190 and GJL-250

Simulations of both GJL 275/190 and GJL-250 are the same in Magma5 and there are no differences between the two materials during simulations. Therefore they share the same results and are bundled together. To find when the most stress is relieved the time, stress and temperature is plotted for each run. In figure 6.4 the stress relieving process is showcased and the most stresses have been released by the time the temperature is at its peak. Meaning the majority of the stress relief has already occurred before phase 2 has started.

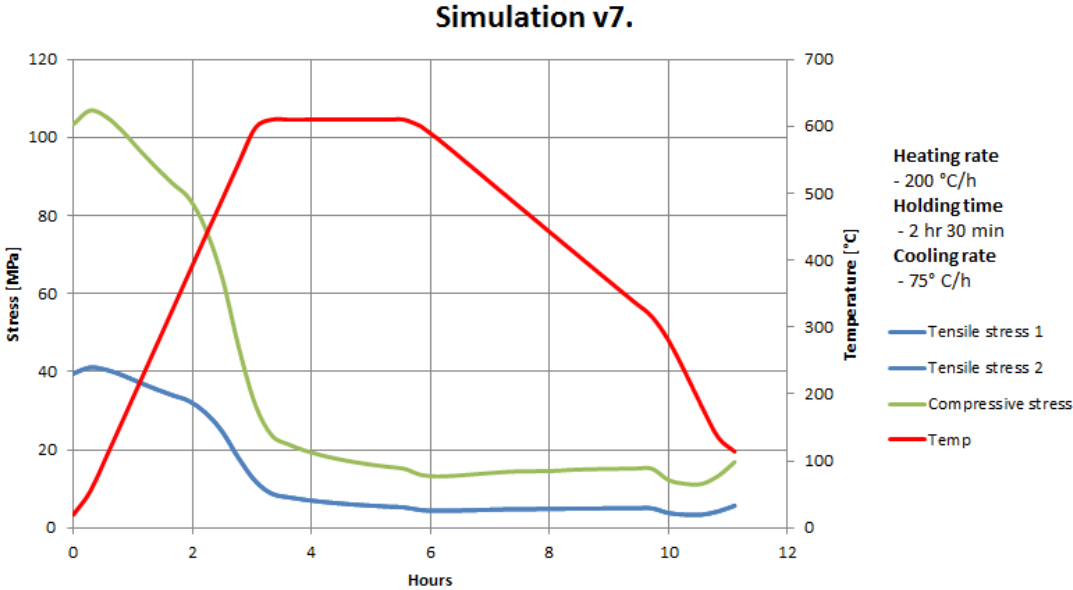


Figure 6.4. Simulation v7 of stress relieving over time. The red curve shows the temperature over time which is followed by the stress relieving effect.

Figure 6.5 shows the stress relieving effect when the hold time is shortened from 2.5 h to 1h 15min. Both the tensile and compressive stresses have changed but only slightly compared to v7 in figure 6.4.

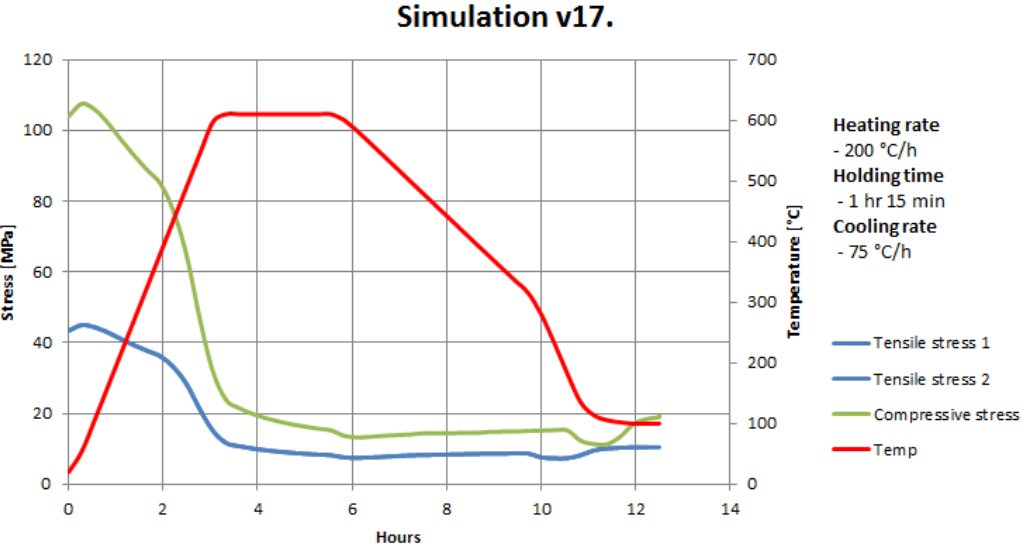


Figure 6.5. Simulation v17, from drawing with 1h 15min h hold time. Tensile stress 1 & 2 are the same.

Figure 6.6 shows the stress relieving when the cooling rate is increased from 75 °C/h to 150 °C/h. No major difference of the residual stresses can be observed by increasing the cooling rate from the simulation program. A concern regarding the later versions of the simulation is the dip in stress at the 8:30 mark. This is thought to be an accumulated error and gets progressively worse. It is possible that the change in cooling rate is the cause of the dip due to different values and more extreme parameters cause a larger change in curve.

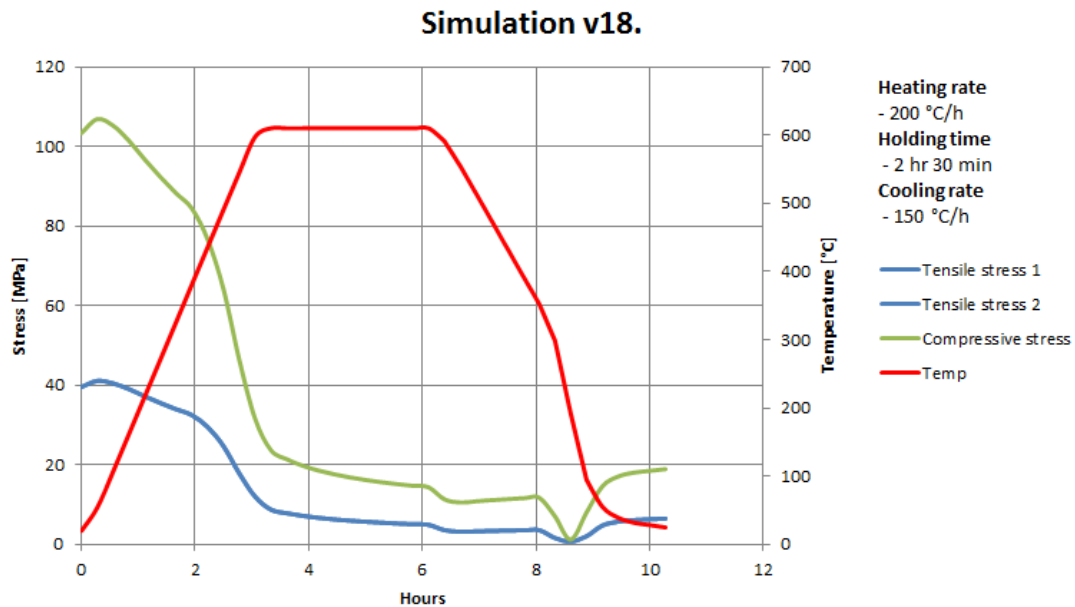


Figure 6.6. Simulation v18, drawing with a faster cooling phase of 150 °C/h.

Table 6.1 shows the remaining residual stresses after the simulated heat treatments, no major effect is obtained by either of the hold time or cooling rate separately. Combining the two parameters seems to have a synergetic effect and increases the residual stresses in both tensile and compression with an estimated 40% compared to each of the parameters alone.

Table 6.1. The simulated residual stresses after heat treatment from drawing.

Simulation:	Tensile stress point 1 [MPa]	Tensile stress point 2 [MPa]	Compressive stress point 3 [MPa]
From drawing (v7)	10,8	5,3	-23,1
Low hold time (v17)	12,6	4,65	-19,9
High cooling rate (v18)	12,3	4,7	-19,3
No hold time + high cooling rate (v22)	18,2	9,7	-33,5

### 6.1.2 Skövde foundry heat treatment

These simulations were based on Skövdes own heat treatment profiles using their heating rate. Parameters such as holding time, cooling rate and drop temperature were changed between each simulation

Seen in figure 6.7 the major effect of relieving residual stresses are found in the heating phase, but also a small portion of the residual stresses are removed during the holding time. an estimated 80 % of the residual stresses are removed before phase two begins.

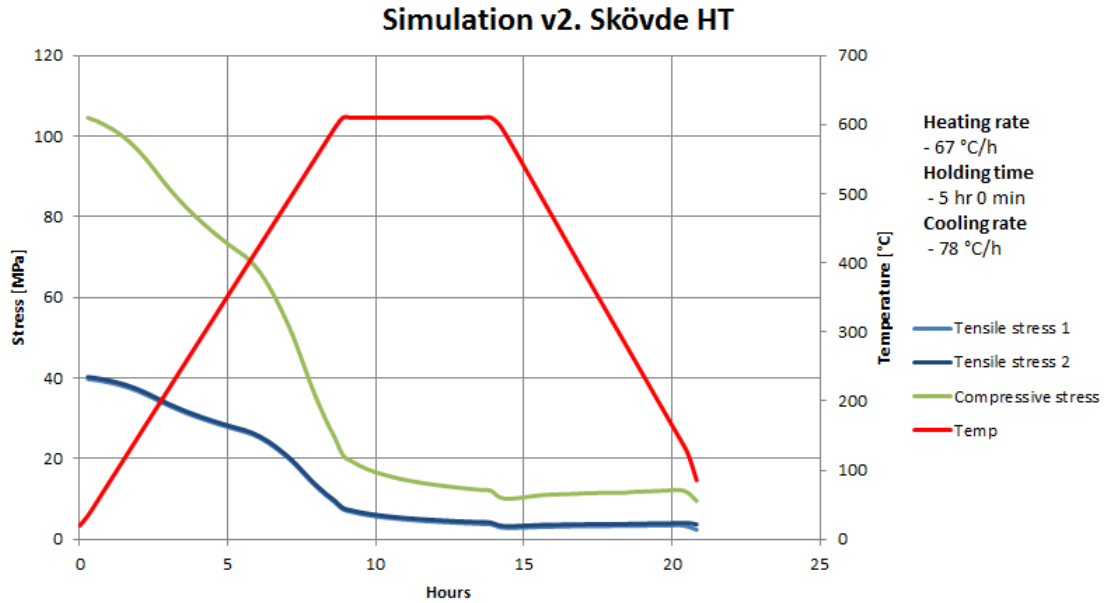


Figure 6.7. Simulation of Skövde foundry parameters (simulation v2).

Next simulations are performed with a heat treatment without phase 2, i.e. no holding time and with cooling rates of 78 °C/h, 110 °C/h and 150 °C/h respectively. The purposes of these simulations are to evaluate what effect phase 3 have on the residual stresses.

From the plot there is a clear indication that the residual stresses are reduced. Taking a look at the last portion of phase 3 in Figure 6.8 a clear hitch is seen and there is a small increase of the stress. This hitch reappears in later simulations and is much more predominant in those cases. Disregarding the hitch the result of the relaxation in the material is good. The stress has been reduced by 75% of the previous stress and the heat treatment seems to be effective. But there is also a small increase of the residual stress during the cooling cycle. The assumption is that this effect is much larger in reality and might be problematic for Magma 5 to simulate.

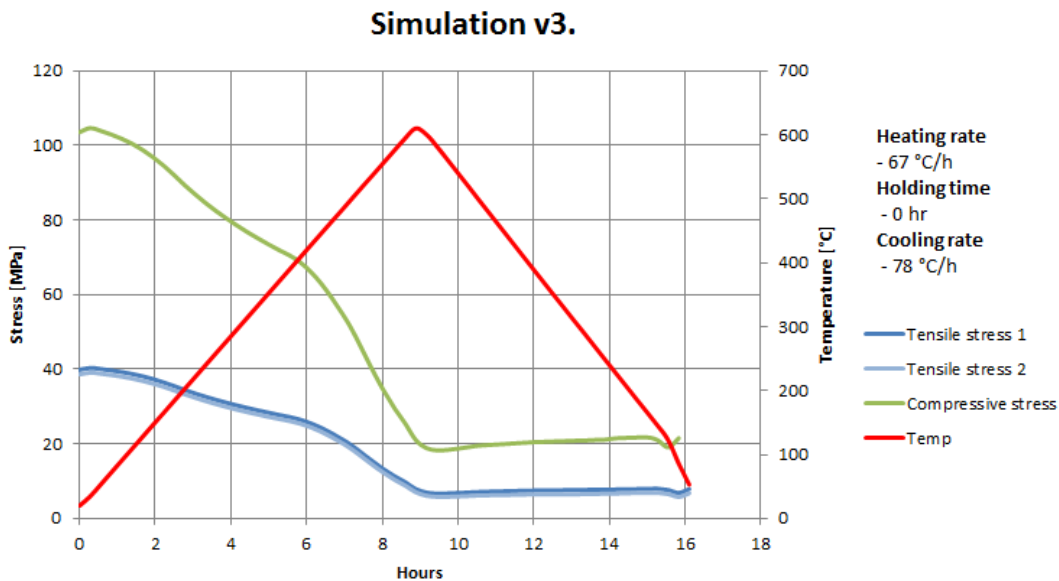


Figure 6.8. Heat treatment without holding time (simulation v3).

The different simulations have been put into separate tables to be more easily observed. The influence of drop temperature presented in Figure 6.9. There is not much difference between

each simulation. All three simulations have a residual stress of 25 MPa in compressive and 15 MPa in tensile stress. The recommendations given by the Skövde drawing seems to be correct.

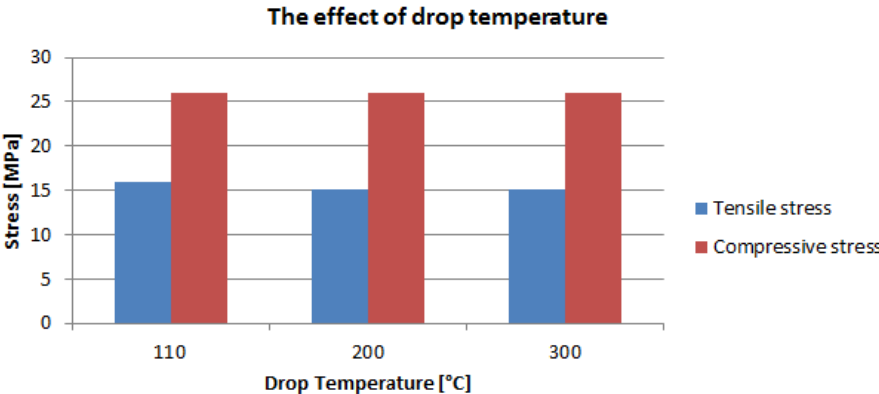


Figure 6.9. The residual stresses with changed drop temperature from simulations.

The significance of holding time is shown in Figure 6.10 and it follows a decreasing exponential curve. The variance between each simulation is large and there is a clear indication that holding time has an effect on the residual stresses. Looking at the curves presented to the right in table 6.3 there is a noticeable difference between the relaxation of compressive and tensile stresses. Compressive stresses are lowered for each run while the tensile stress remains the same in both 2.5h and 5h runs.

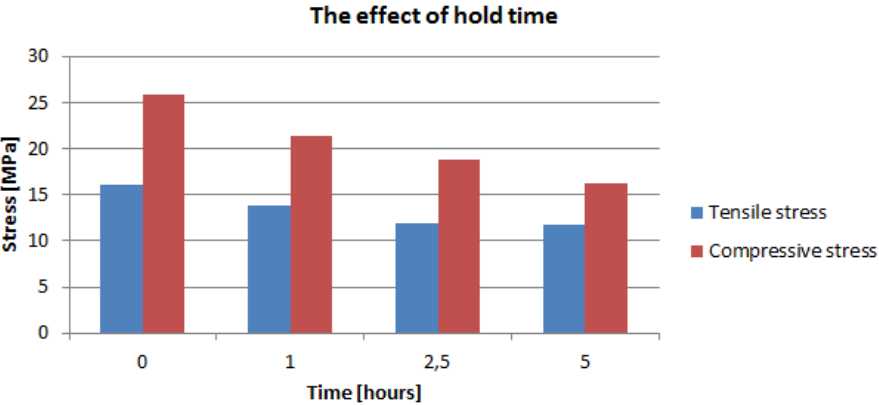


Figure 6.10. The variation of residual stresses due to changed holding time.

Reaching the last parameter that can be changed is the cooling rate. From the Figure 6.11 seen below there is no difference between the different cooling rates. Neither compressive nor tensile stresses changes between the three runs and the resulting residual stresses are kept at the same levels.

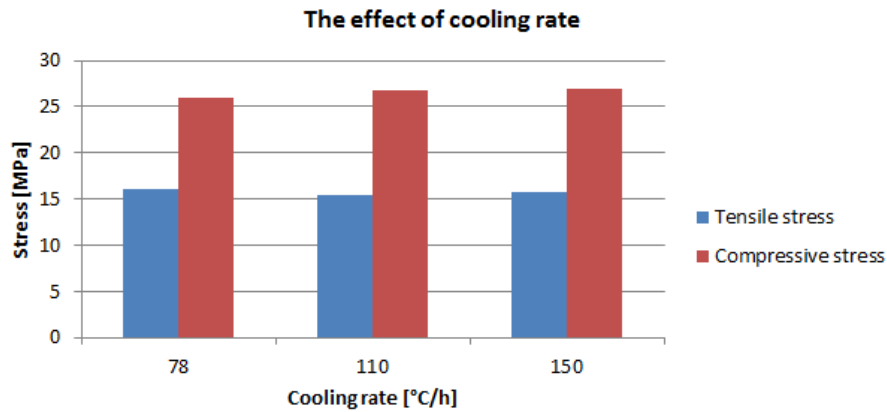


Figure 6.11. The influence of cooling rate on residual stresses.

Based on previous runs an optimal heat treatment curve was created in order to test the combination of all parameters. The optimized curve can be seen in Figure 6.12. A heating rate of 67 °C/h was chosen since no other option was possible. Phase 2 consists of a holding time of 5 hours at 610 °C. Lastly, phase 3 has a rapid cooling of 300 °C/h with a drop temperature at 300 °C. This makes the cooling phase less than 2 hours long. This is impossibility in the practical case and would create new residual stresses.

The optimized heat treatment seems to reduce most residual stresses and neither compressive nor tensile stresses are above 20 MPa. By looking at the curve many bumps can be observed with an especially big one at the end. This bump is visible in other simulations as well but it is very predominant in this version. The irregularities seem to occur when the temperature changes and might be an artifact due to the way Magma handle transitions between different phases.

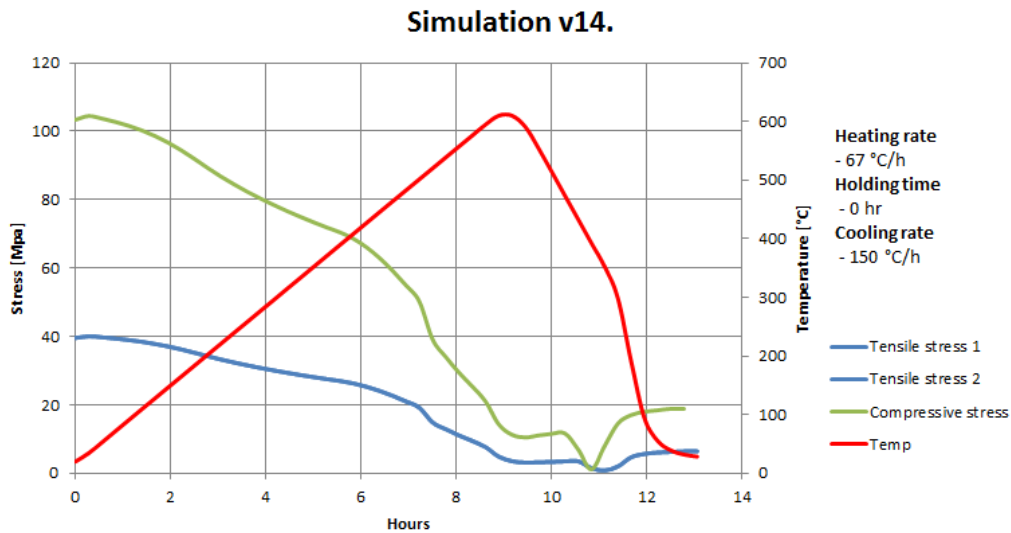


Figure 6.12. Heat treatment parameters based on the optimal result (Simulation v14).

A summarization of all heat treatment simulations is compiled in table 6.2. Each simulation was done in the same way seen in Figure 6.7 but with one parameter changed. This was done to observe and analyze the effect of each parameter. In general Magma 5 seems to have difficulties handling a rapid cooling rate and seem to disregard any extreme parameters; the results seem to be the same regardless. The assumption is that the simulated results are not equal to a physical scenario and therefore the results from the simulation might not correlate with the practical testing.

By comparing the simulations of Skövde foundry HT and the varying parameters the simulation gives a prediction of what will affect the relieving of residual stresses. But the results also indicate that the cooling rate and quenching temperature will not affect the remaining residual stresses. This gives suspicions of what the program can simulate and what the limits are. The cooling rate varies from 78 °C/h to 150 °C/h, and does only have a minimal impact on the residual stresses. Whether or not this is accurate can't be said and practical testing is necessary in order to confirm or disapprove it.

Table 6.2. Remaining residual stresses after simulated heat treatments of Skövde:

Simulation:	Tensile stress point 1 [MPa]	Tensile stress point 2 [MPa]	Compressive stress [MPa]
As cast	46,4	36,8	107,3
In use HT (v2)	12,6	4,9	19,9
No hold time (v3)	16,3	6,7	25,9
Inc. cooling rate (v6) - 110	15,4	7,4	26,8
Inc. cooling rate (v5) - 150	15,7	7,6	27
Increased quenching temp. (v8) - 200	15,1	7,1	26
Increased quenching temp. (v9) - 300	15,2	7	26
Hold time 2.5h (v13)	11,9	4,3	18,9
Increased cooling rate and quenching temp. (v14)	12,3	4,6	19,2
Extreme values (v15)	12,2	4,6	19,2
Hold time 1h (v16)	13,8	5,4	21,3

### 6.1.3 Simulating ductile iron GJS-500-7

The ductile iron is simulated with the same parameters as simulation v7. After the solidification, residual stress is much higher compared to the grey iron and this is due to the higher mechanical properties of the ductile iron. The stress after solidification is shown in Figure 6.10.

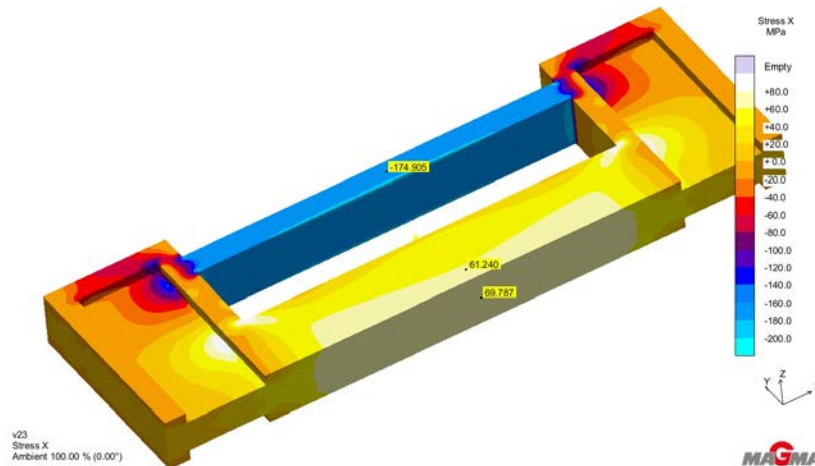


Figure 6.13. The simulated residual stresses after solidification of ductile iron GJS-500-7.

In table 6.3 the stresses of both tensile and compressive points are presented. The table shows that the hold time has a significant effect and that a higher cooling rate will not be affect the stress generated. The stronger ductile iron grade GJS-600-3 was also simulated in order to confirm that a higher tensile strength generate higher residual stresses in Magma5. This would explain why the stress is higher in GJS-500-7 compared to the other two cast irons tested.

Table 6.3. The simulated residual stresses after heat treatment for ductile iron GJS-500-7. \*If no version number is provided a previous version has been modified

Simulation:	Tensile stress point 1 [MPa]	Tensile stress point 2 [MPa]	Compressive stress point 3 [MPa]
After Solidification	69,8	61,2	174,9
From drawing (v23)	20,9	14,6	43,2
No hold time (v24)	31,2	24,2	67,9
Low heating rate (v25)	20,6	14,3	42,4
5h Holding time (v26)	15,7	9,7	30,9
150 °C/h Cooling (v27)	19,9	13,6	40,7
420 °C drop temp.	19,3	13,1	39,3
GJS-600-3	76,2	66,3	191,1

### 6.1.4 Verification of Simulation Model

By comparing the practical testing and simulations it can be seen that the simulations tend to have higher residual stresses compared to the reference lattices tested. In the figure below there is a clear difference in cooling rate between the real material and the simulated one. Another observation is that the phase transformation that occurs at ~720 °C, from austenite to pearlite, is non-existent in the simulation. When this transformation occurs in the physical

material it generates heat and slows down the overall cooling rate of the material. Due to the absence of the transformation in the simulation no such reduction of the cooling rate exists. Therefore the cooling is much more rapid, creating a shift in the plot, generating a bigger discrepancy between the experimental and simulated case, especially after 730 °C. In the simulation this rapid cooling is reflected in the residual stresses, yielding values higher than the physical material, Figure 6.15.

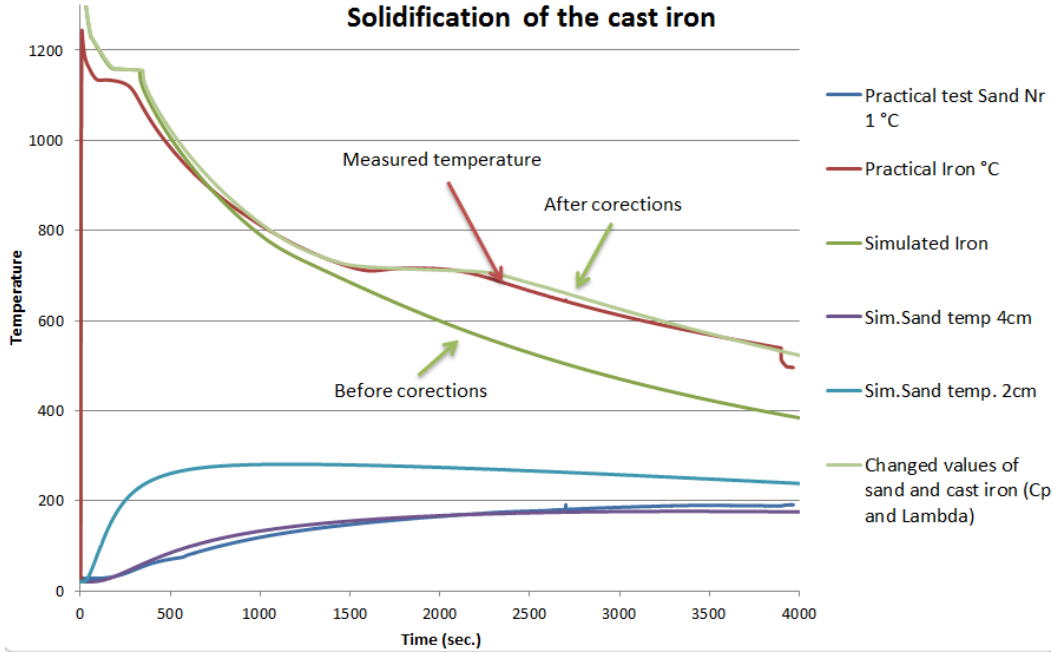


Figure 6.15. Calibration of the simulated solidification process of GJL-250.

In an attempt to make the simulation and the physical solidification process as similar as possible changes were done to material parameters in the Magma database. By changing the heat diffusion and thermal capacity of both the moulding sand and the iron the overall residual stresses were reduced in the simulation. The reduction was small and the improvements didn't make any major changes to the resulting stresses calculated by Magma5. The reduction was a total 9 MPa in compressive lowering the stress to 98 MPa. The stresses in tensile mode did not change more than 2 MPa in the simulation with previous mentioned improvements. All of the values from the simulation before and after can be seen in Figure 6.16 below.

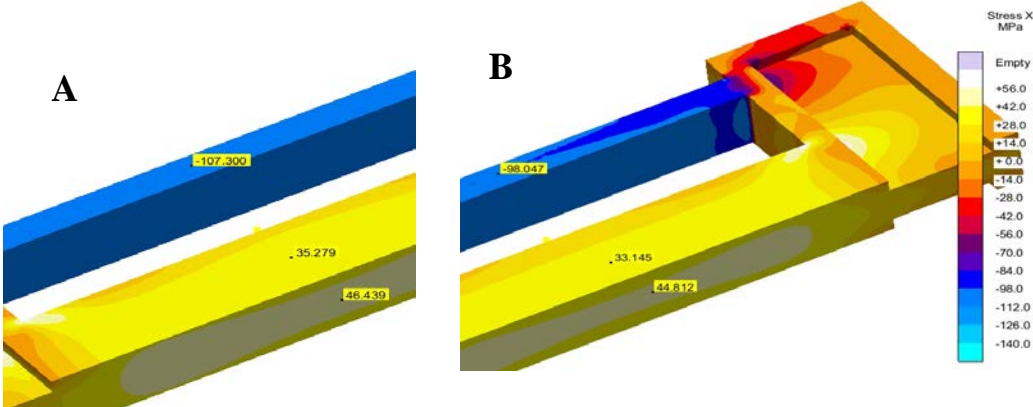


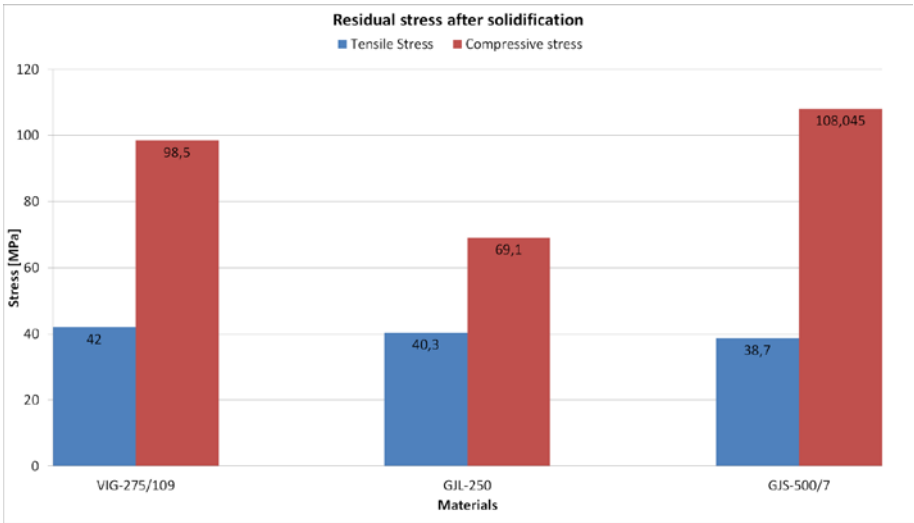
Figure 6.16. In the figure to the left (A) is the simulation before the changes to the material parameters and to the right (B) are the updated parameters with a lower stress.

## 6.2 Residual Stress Measurement

This chapter shows all the resulting measurements of residual stresses. The changed parameters and resulting stress values will be compared to each other to find the most optimal heat treatment and the valuation of each change.

The residual stress is measured after solidification to get the reference stress for each material. These stresses will be used as a baseline before the heat treatments. The Figure 6.17 shows how the measured stress between the materials. It's clear that the residual stress after solidification varies to the materials strength.

Figure 6.17. The reference residual stress as cast for each investigated material.



### 6.2.1 3D scanning the component

To investigate a possible bending load case in the stress lattice the geometry was scanned before and after sectioning to see how the deformation took place. The scanning was performed on stress lattice R3 and R4 (Reference 3 and Reference 4, two as-cast lattices) and resulting strain is shown in Figure 6.18. The significant deformation is along the X-axis, as desired. In R4 this is the case, less than 10% has been deformed along the Z-axis (Bending direction) and is therefore not presented in Figure 6.13. However, in R3 this is not the case; any deformation along the X-axis is less than that of R4's values and there is an equal amount of deformation along the Z-axis in the other half of the lattice. Analyzing both of these cases raise the question if some other lattices have deformed the same way as R3.

Regarding the bending and the presumed effect it might have on the overall stress results some calculations have been made, assuming an exaggerated dislocation along the Z-axis of 0.1mm, ten times the value seen in R3. With this exaggeration a difference of 40% could be created between the top and bottom side of the lattice. From this the conclusion is that these results show that the bending seen in the lattices is not causing the large irregularities of stress values measured. Using strain gauges on both sides and taking the average of the two values eliminates this error as well.

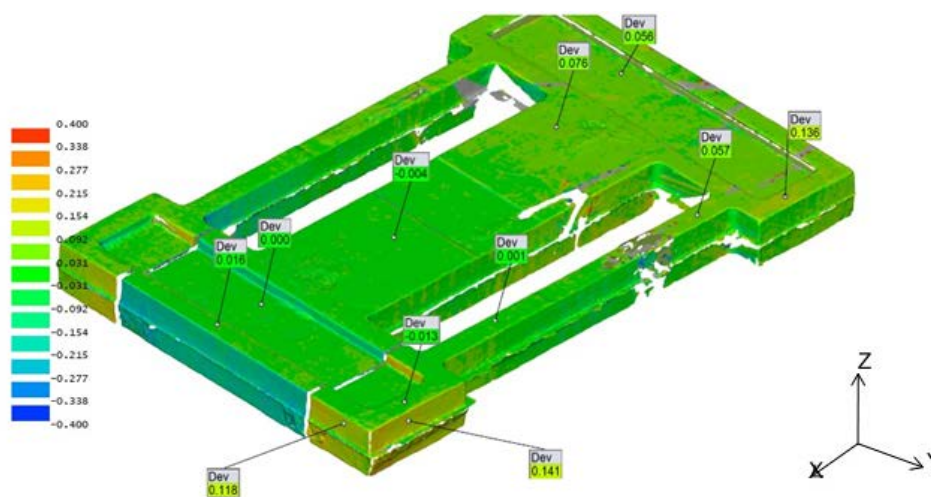


Figure 6.18. Shows the scanning of lattice R3. Deviation after sectioning is measured in mm. The marked points on the surface indicate the deformation. The deviation is significantly larger in x-direction, but the bending case in y-direction can't be ignored.

### 6.2.2 Cast iron VIG 275/190

Find the resulting temperature vs. time plots of each HT trial see appendix (Heat treatments). All parameters for heat treated lattices are introduced in the method chapter. Following will describe the result and variation between the heat treatment runs. Resulting stresses are presented from the experiments in this chapter, both from the sectioning and the result of the different heat treatments performed. The stress results are presented in table 6.4.

Table 6.4. The resulting stress values are calculated to compensate for the bending load case in both compressive and tensile sections. \*Values from HT-SL did not correspond with the stress case and are therefore omitted.

Lattice	Average Compressive MPa	Average Tensile MPa
R1 (No heat treatment)	110	37
R2 (No heat treatment)	90	53
R3 (No heat treatment)	93	37
R4 (No heat treatment)	101	41
Average Reference stress	<b>98,5</b>	<b>42</b>
HT-SL (Skövde heat treatment large oven)	<i>Removed*</i>	<i>Removed*</i>
HT-SS (Skövde heat treatment small oven)	12	14
HT-1 (heating 67 °C/h)	27	9,6
HT-2 (heating 200°C/h)	33,3	3,6
HT-3 (no hold phase)	34	13
HT-4 (5h hold phase)	24	9,3
HT-5 (150 °C/h cooling rate)	29,2	11,9
HT-6 (400 °C drop temperature)	10,9	30,8
HT-7 (no hold time and 150 °C/h cooling rate)	49,7	17,1
HT-8 (redo the HT-2)	31,3	10,9
HT-9 (time efficient HT of Skövde)	31,3	10,9
HT-10 (The HT- of Skövde)	17,6	6,4

The Figure 6.19 shows the remaining residual stress after heat treatment. As shown varying heating rate between 67-200 °C/h has a significant effect on the remaining stress. The hold time at 610 °C also have a significant effect on the residual stress. Cooling rate and drop temperature, however, not showing any larger effect on the stress results. By combining high heating- and cooling rates and no hold time the stresses are much higher which is proven with the last treatment (HT-7).

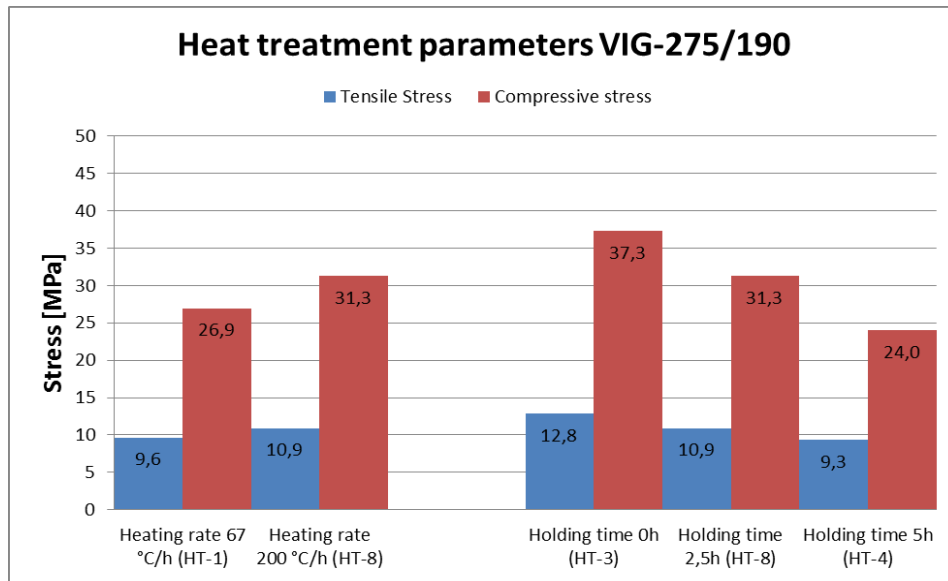


Figure 6.19 Heat treatment parameters effect on residual stresses.

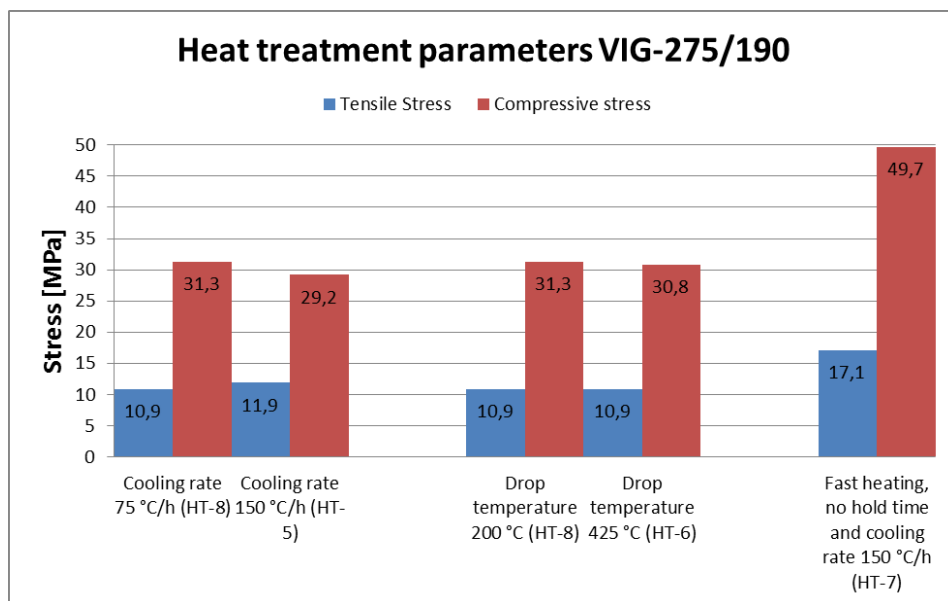


Figure 6.20. The effect of changing cooling rate and drop temperature on VIG-275/190.

At last the current used heat treatment cycle in Skövde is compared to what is evaluated as a time saving heat treatment cycle based on result from previous changed parameters (trial 9). As shown, the heat treatment used today at Skövde foundry obtains much lower residual stress. This is mostly an effect of combination of parameters. The previous heat treatments only change one parameter each run and will therefore not obtain as high relieving effect as Skövde HT, Figure 6.21.

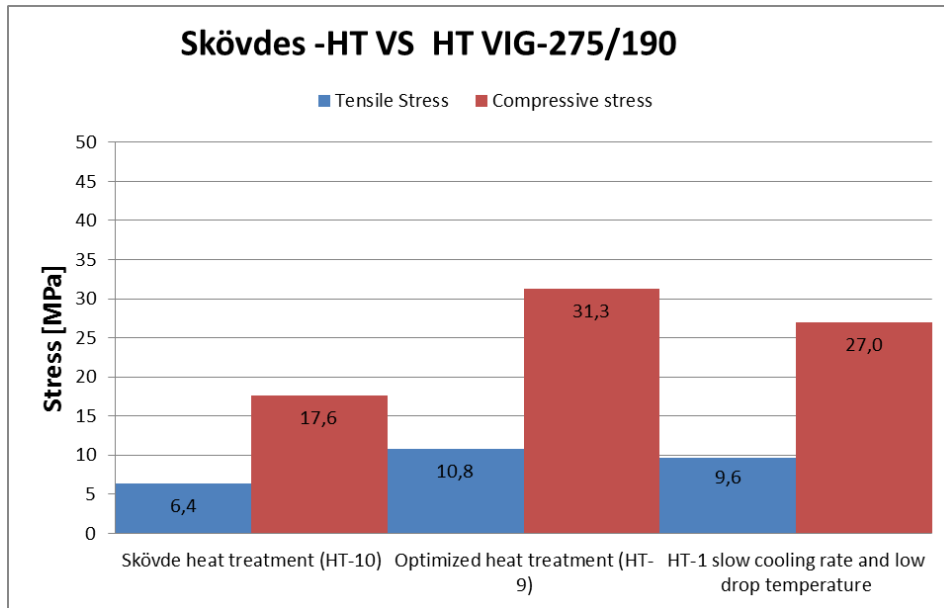


Figure 6.21. Stresses measured from the suggested rapid HT and the current HT in Skövde foundry.

The previous table shows the effect of hold time which highlights the importance for the material to spend time at high temperature. From the HT plots (Appendix B) the time spent above 500 °C is calculated and plotted against the stress relief. The plot only considers the time spent over 500 °C regardless of rapid heating, cooling rate and drop temperature since this indicates to be the most important factor of stress relieving. From the plot a second order relationship exists between relieved stress and time spent above 500 °C. The assumption is that the curve will flatten out close to 10 hours, shown in Figure 6.22.

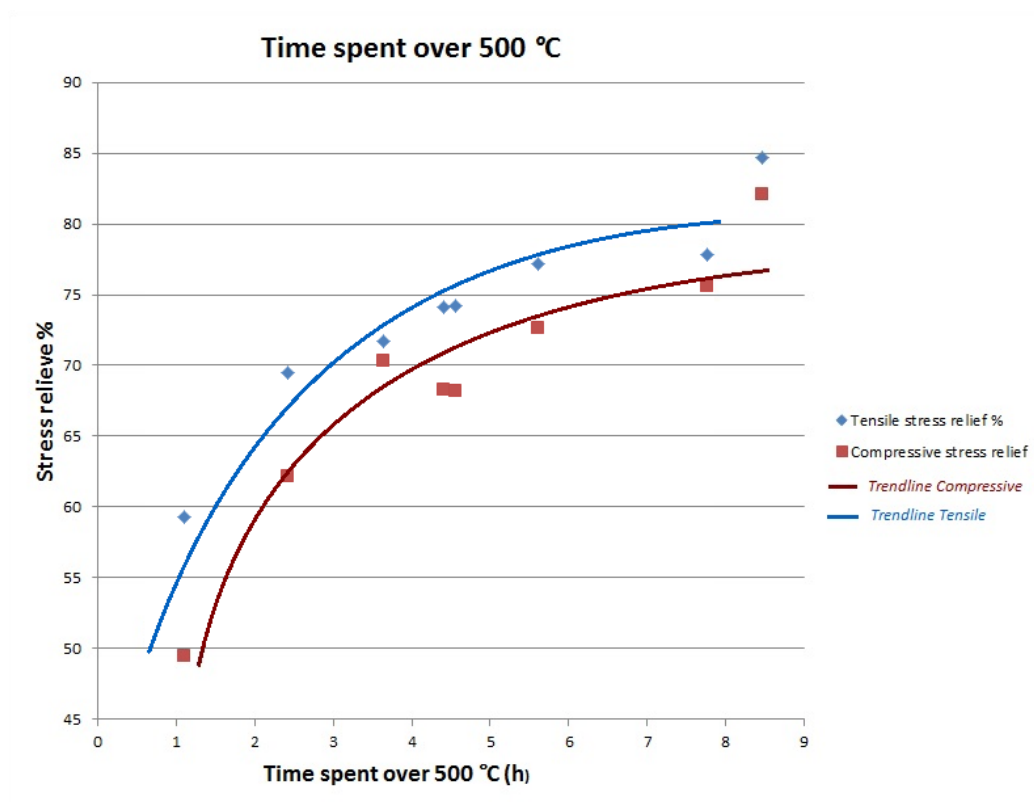


Figure 6.22. Stress relieve in % compared to the time spent over 500 °C.

### **6.2.2 Cast iron GJL-250**

The unalloyed cast iron, GJL-250 responded well to the heat treatment and all tested parameters had an effect on the resulting residual stresses. Holding time was still the most influential parameter in the VIG 275/190. The trend of the holding time is seen clearly in table Figure 6.23. Increased cooling rate and drop temperature seemed to increase the residual stress level, something not observed in VIG 275/190.

Having no hold time with cooling rate and drop temperature according to the test plan provides a significant reduction in residual stresses compared to the reference. With only 75 minutes holding time the residual stresses are halved relative to the heat treatment with no holding time. Compared to the reference lattice with no heat treatment the stresses had been reduced with ~75%. Due to having only 9 lattices to use for the experiments no synergy effects were investigated and all tests have only had one varying parameter.

HT-8 was the last heat treatment performed and was done to investigate the buildup of residual stresses and to provide insight in the casting process. The temperature of the lattice, at 610 °C is close to the same temperature as the cast iron has when the mould is broken up and separated from the goods.

Heating rate was not investigated in GJL-250 due to limited amount of stress lattices. Furthermore, investigating heating rate was only done to VIG-275/190 in order to provide information regarding Skövde Foundry's own heat treatment.

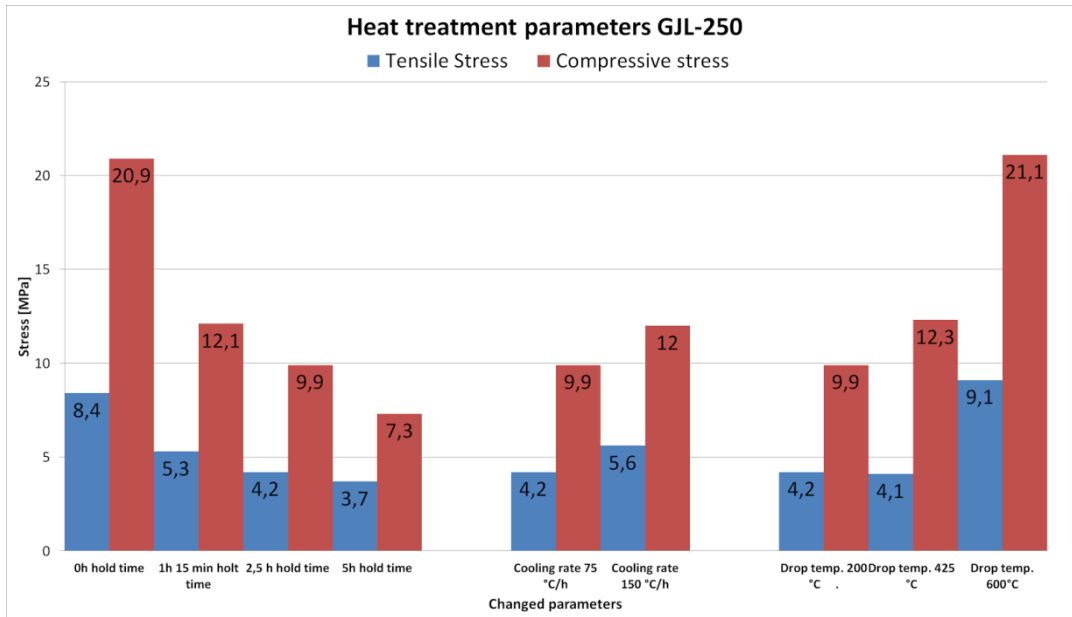


Figure 6.23. The residual stress after HT of GJL-250.

When all HT are performed they are summarized in Figure 6.24 the trend shown by VIG 275/190 is not as clear for GJL-250. Residual stresses are more easily removed in the unalloyed material and parameters such as cooling rate and drop temperature also seems to have affected the resulting stresses. The scatter is more apparent but still a trend shows that the time over 500 °C is important.

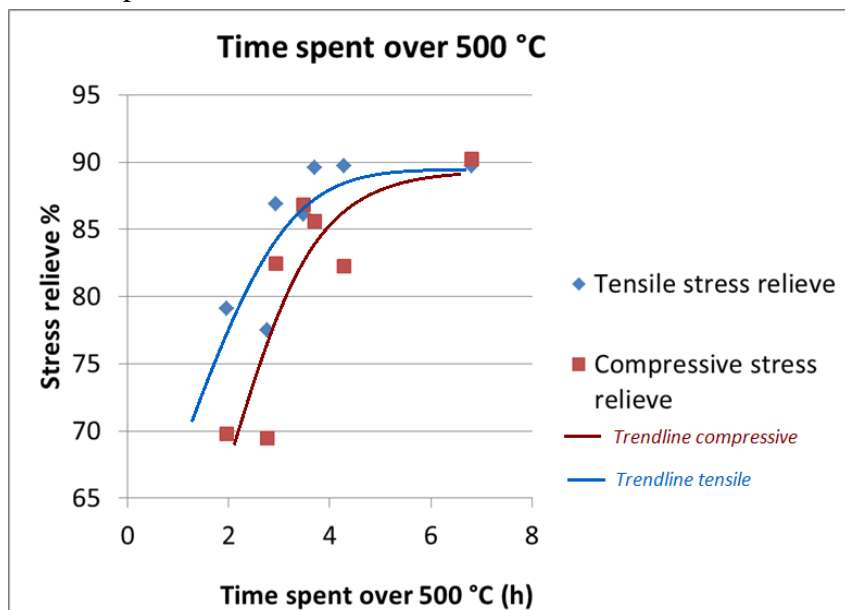


Figure 6.24. The stress relieve vs. time spent over 500 °C, GJL-250.

### 6.2.3 Cast iron GJS-500-7

With four lattices available for heat treatment some adjustments were made in order to fully focus on the most important parameters. HT-2 is the heat treatment described in the plan and will provide a reference value that can be compared with the grey irons. The other heat treatments (HT-4, HT-5, and HT-6) had the same profiles as for the grey irons.

Seen in Figure 6.25 is the stress after each HT. HT-4 seemed to respond well to the increased hold time and showed low stress. Comparing HT-2 with HT-5 and HT-6 shows no remarkable difference of changed parameters in the cooling phase. The differences are roughly within 2 MPa in compressive stress and less than 2 MPa in tensile stress. The increased stress by higher cooling rate indicates to some effect of increasing the cooling rate above 400 °C. In short it looks like the GJS-500-7 has a tendency for faster creeping and responds quickly to the HT.

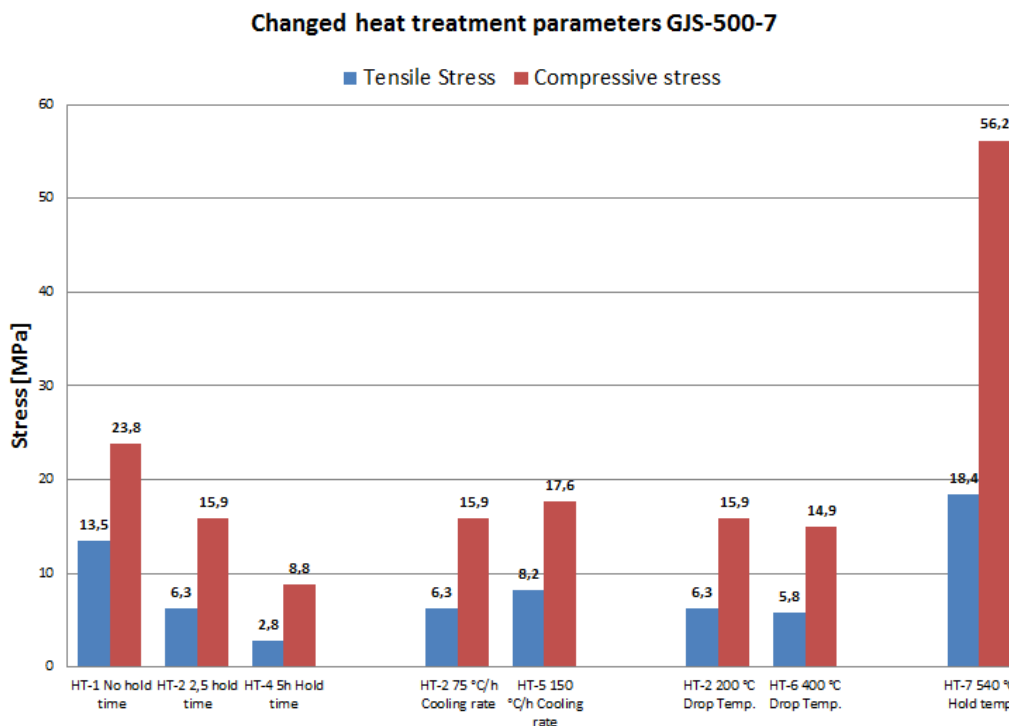


Table 6.25. The residual stress after heat treatments conducted on GJS-500-7

Comparing the results with simulations shows once more that Magma5's model of GJS-500-7 is not fully correct. The values provided from the simulations were far above the actual stress with values more than twice the amount of stress. The stress values from the simulations have been presented in table 6.3. Still the simulations predicted the effect of the different parameters correctly and HT-2, HT-5, and HT-6 had similar values in the simulation, just as the measured values seen in the table above. Yet again do the tests confirm the importance of holding time and the residual stresses are reduced significantly with a longer holding time. From HT-7 where the holding temperature was reduced from 610 °C to 540 °C confirms that that reducing the holding temperature can severely affect the residual stresses. Comparing HT-1 and HT-7 shows the difference between having a higher temperature or longer holding time.

## 6.2.4 Comparison of the materials

In Figure 6.26 all investigated cast iron alloys are presented with the stresses as cast and after HT-2, which is the recommended heat treatment from Volvo. From the table there is a clear difference seen between the alloys not using Mo and Cr. Both the unalloyed cast iron, GJL-250 and the ductile iron GJS-500-7 have roughly 14% of the stress before HT, while in VIG 275/190 the difference is 33/25% in compressive and tensile respectively. The difference seen in relaxation between tensile and compressive in all the alloys is due to the variation in cross section area and volume. This is especially noticeable in the case of VIG 275/190. Another value to note is a low compressive stress in the GJL-250 reference and this low value is assumed to be due to an errant strain gauge, without that value the stress is 76 MPa. This assumption is because the simulation has shown reliable values regarding the GJL-250 cast iron.

Furthermore, the HT-2 has proven to be successful for the two cast irons not containing Mo or Cr and most of the residual stresses has been relieved during the process. With regards to VIG-275/190 a 2 hour and 30 min hold time is not enough to fully reduce the stress.

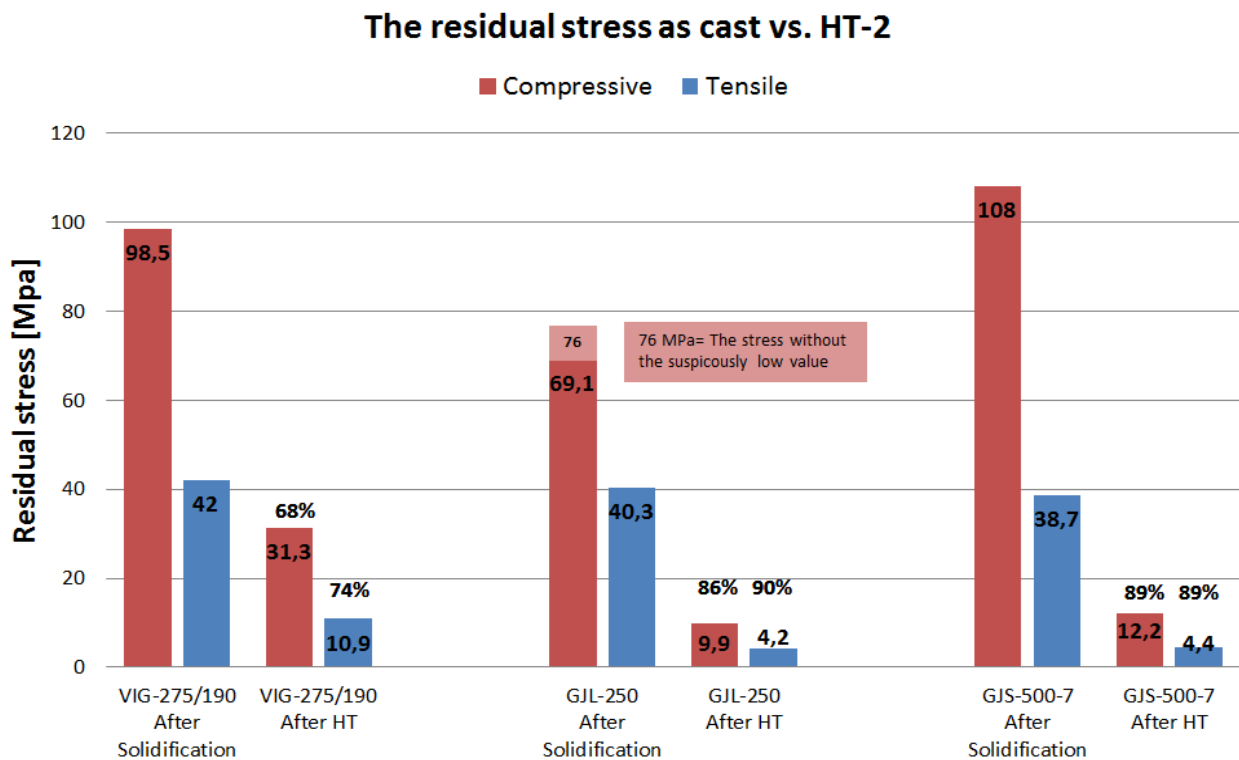


Figure 6.26. A comparison of residual before and after HT-2. The % values show the residual stress reduction during HT.

In Figure 6.27 the simulations of casting process and heat treatment (drawings) are compared to the practical testing. For the VIG-275/190 simulations predict higher stress after solidification and lower stress after heat treatment, i.e. a higher relieving effect. In the ductile iron GJS-500-7 the simulations also predict a higher stress after solidification but also higher stress after heat treatment.

## The residual stress before and after HT

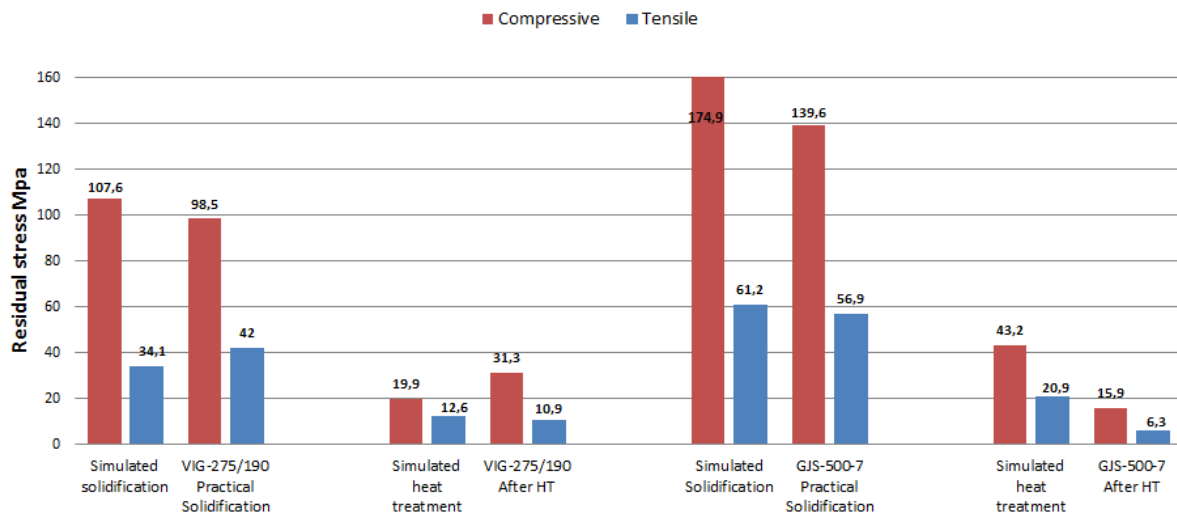


Figure 6.27. Comparison of simulations and experimental test on residual stresses. GJL-250 is not included since it uses the same simulation data as VIG-275/190.

### 6.3 Experimental verification of materials

The verification of the three materials analyzed is done in order to confirm the composition of the material, the microstructure, hardness and the distribution of the ferritic and pearlitic matrixes. Stresses presented previously are valid for the type of materials presented in this chapter.

#### 6.3.1 Grey iron, VIG-275/190

The hardness test shows that the hardness differs between the tensile and compressive sections. The assumption is that the cooling in these sections is different, with a higher cooling rate in the compressive section increasing the hardness. The increased cooling rate changes the microstructure towards smaller graphite and finer pearlite that will provide a higher hardness. The conclusions of hardness tests are the values are within expectations and exceed the specified minimum requirement, table 6.12. In the compressive section of the GJL-250 the hardness differentiates a lot from the tensile section. Regarding the ductile iron, GJS-500-7 the hardness value is high and some values are above the specification. The same hardness values were seen in both SKF and Skövdes lattices and hardness values this high indicates incorrect distribution of pearlite and ferrite, caused by larger undercooling.

Table 6.5, Hardness measurement (Brinell 2,5mm with 187,5kg). Each value is a mean value of three indentations.

Hardness	VIG-275/190	Grey iron, GJL-250	GJS-500-7 SKF (R2)	GJS-500-7 Skövde (R1)
Compressive section	258	228	240	247
Tensile section	231	185	231	218
STD	min 190	190-240	170-230	170-230

The amount of graphite in VIG-275/190 is varying between the tensile and compressive section. The tensile section obtains a graphite amount of 11,4% and the compressive is 8,8% the differences in amount of graphite is influenced by the polishing of the micro samples. Graphites loosely fixated and are very easily removed during the grinding process, thus potentially creating this error. The tests were performed on the reference lattice, R1. No visible difference can be seen between the two samples; the graphite structure looks similar for both images and has a formation of the graphite is in accordance to *EN ISO 945-1:2008*. The type of flakes is the most similar to A + E structure.

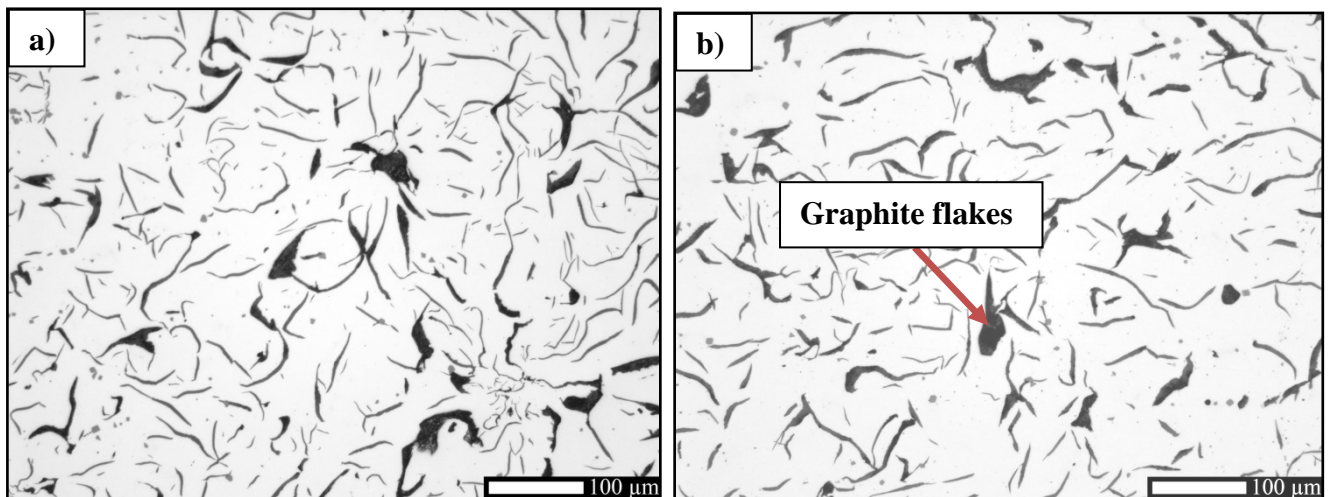


Figure 6.28. The microstructure of graphite VIG-275/190. a) The compressive section b) The tensile section.

When the samples have been etched the lamellar structure of perlite becomes visible, easier to see around the lighter sections. This pearlite structure is also obtained in darker sections; it depends on from which angle the sample is cut. Along the graphite edges there can be small amounts of ferrite, often seen as white sections along the graphite flakes. There is also a slight discoloration in the tensile section, seen as yellow-blue color. Lastly there is a small scatter of grey circular sections (easiest seen in the lower left corner in the compressive section). This is presumed to be Manganese-sulfides (MnS). These particles provide a lubricating effect during cutting and are desirable in small quantities, Figure 6.29.

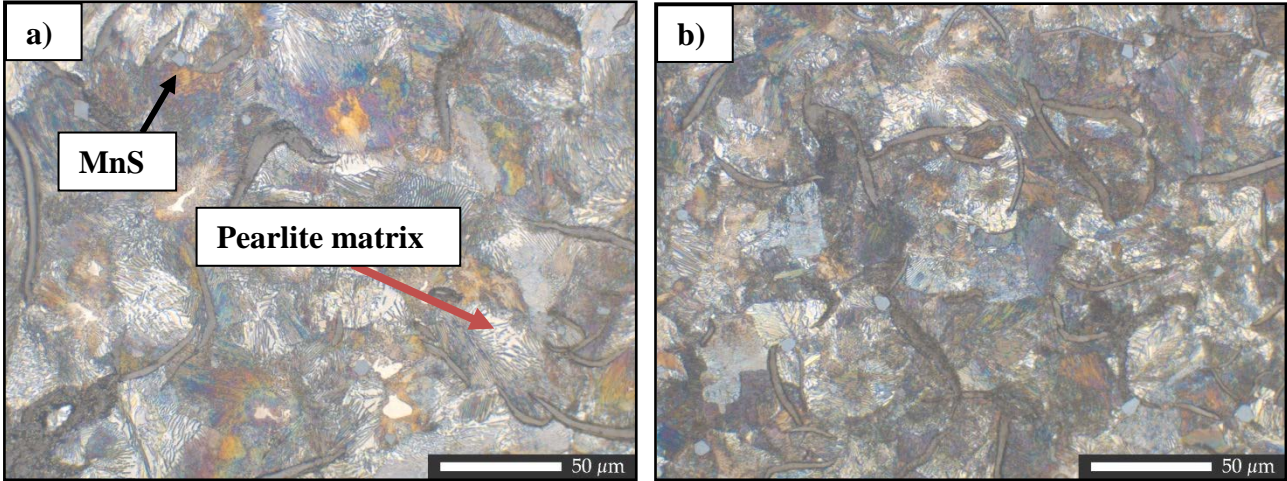


Figure 6.29. a) Tensile section b) Compressive section. The microstructure of VIG-275/190 etched with 1% Nital acid.

Tensile test is performed to confirm that strength is according to specification. As shown in Figure 6.18 the lattice is cut in 6 tensile samples and sent to be manufactured as tensile specimens. Three specimens from the compressive section and three from the tensile section are cut out. The test bars are of type 7C35.

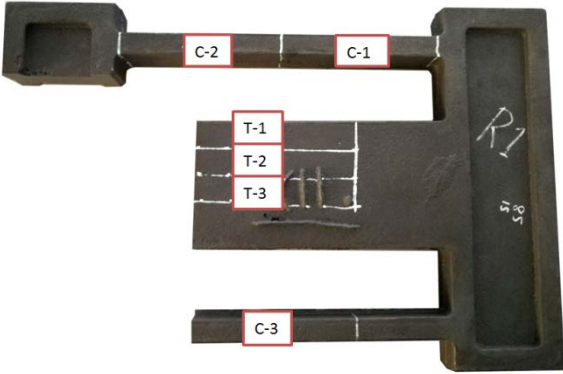


Figure 6.30. The location of where the tensile test specimens are cut out.

All components were not fully functioning in the testing machine when the tensile testing started and therefore C-1 and C-2 are not properly set up (missing values from extensometer). C-3 had its fracture outside of the extensometer gauge and broke very close to its attachment but the result seems to fall within the expected value.

All six tested bars fulfill the requirements of at least 275 MPa (Rm). The compressive bars show a higher tensile strength and this is due to the higher cooling rates in those sections of the lattice. The microstructure is finer and therefore the strength is higher given by the Hall-

Petch relation. T-2 had low values compared to the other tensile bars and a graphite pore is in the crack zone which would explain the low value, shown in Figure 6.19. The testing was conducted by the standard EN ISO 6892-1 A222.

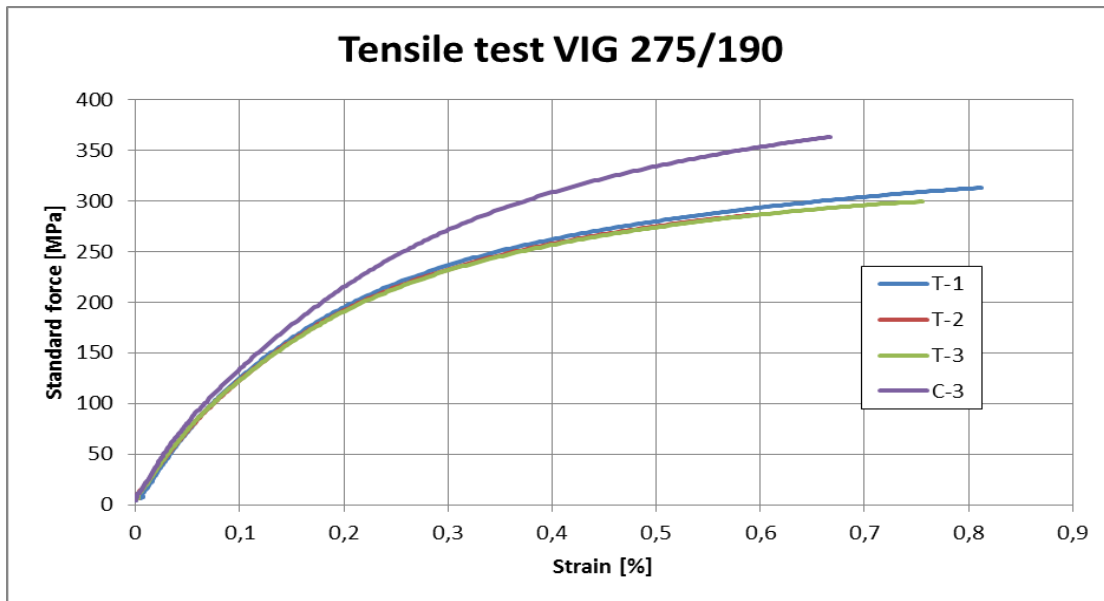


Figure 6.31. Tensile tests C-1 and C-2 were ignored due to invalid values and T-2 is behind T-1 and T-3.

### 6.3.2 Grey iron, GJL-250

In the microstructure samples from GJL-250 the compressive section shows a less distributed graphite structure, 6.20. The graphite in figure (a) is all type-A shaped, the wanted shape in grey cast iron, Figure 6.20 (a) in the thicker section of the lattice. In the thinner part section the graphite shape is changed to B-type graphite due to the undercooling experienced in the section. There is also the transition shape graphite type-D present as well with some smaller portion of type A graphite. It has been stated previously that the hardness of the compressive section is 40 HB higher than the tensile section which would indicate that the microstructure is different and material properties might vary between the thinner and thicker sections.

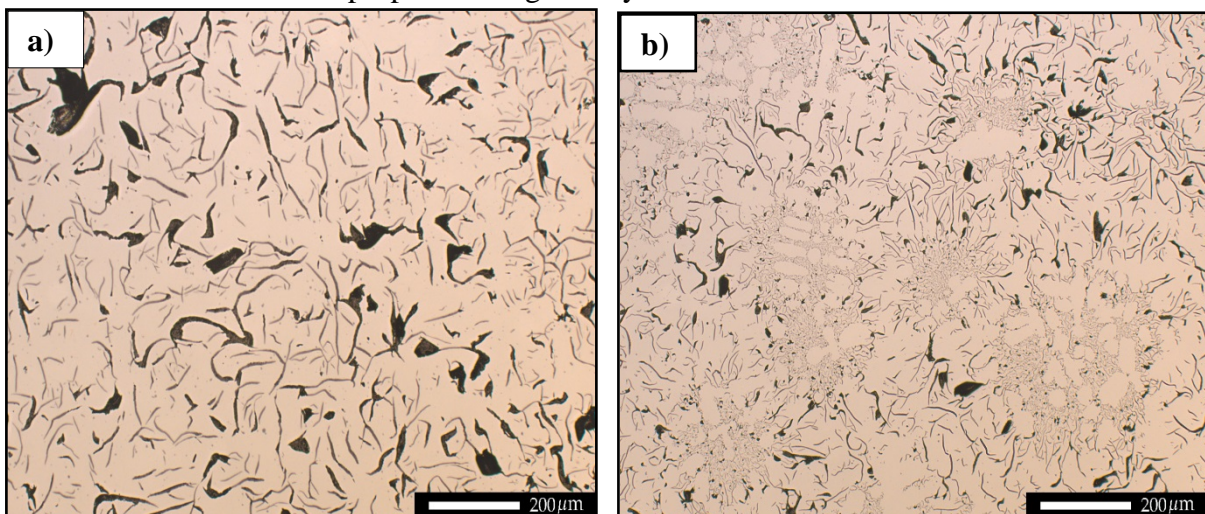


Figure 6.32. a) Tensile section microstructure (thick section), b) microstructure of compressive section (thin section).

Figure 6.21 shows the microstructure after etched with Nital acid 3%. Etching is done to reveal the pearlite structure of the cast iron and it can be clearly seen in both Figures below. Looking at the tensile section (a), there is a lot of ferrite present which is a “defect” due to slow cooling. Requirements for grey cast irons are less than 1% ferrite matrix but the amount of ferrite detected here is above the recommendations.

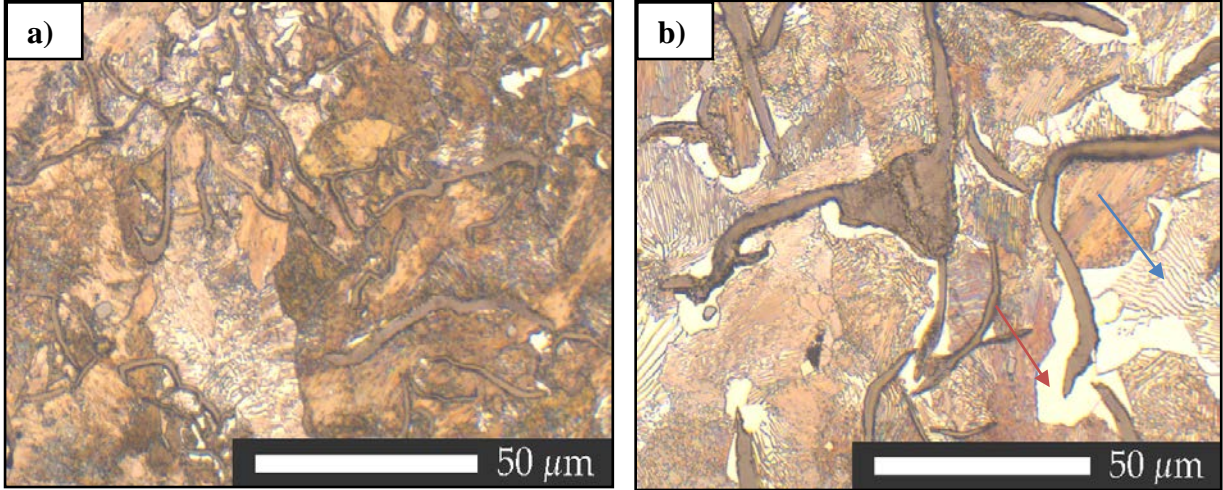


Figure 6.33. a) Tensile section. b) Compressive section. Etched micro-samples shows the microstructure of the pearlite and ferrite around the graphite is clear in sample b. Blue arrow shows a typical pearlite structure and red arrow shows the ferrite (sample b).

A brief overview of GJL-250 is given from the two tensile bars tested. Both tensile bars are within the specifications with T-1 being on the verge of 250 MPa tensile strength.

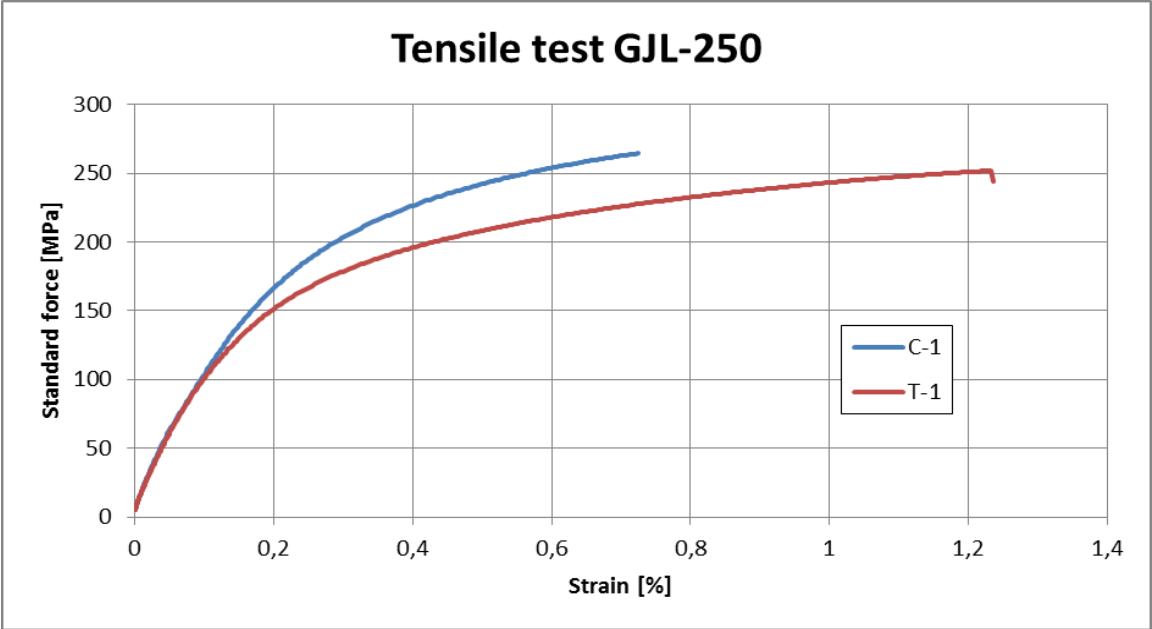


Figure 6.33. Tensile test of GJL-250. Red curve is the tensile and blue is the compressive section.

### 6.3.3 Ductile Iron GJS-500-7

Micro-samples are manufactured to investigate the nodule structure and measure the nodularity and nodule count, shown in Figure 6.34. There are clear differences in nodule sizes and this is due to the cooling rate being higher in the thinner, compressive section.

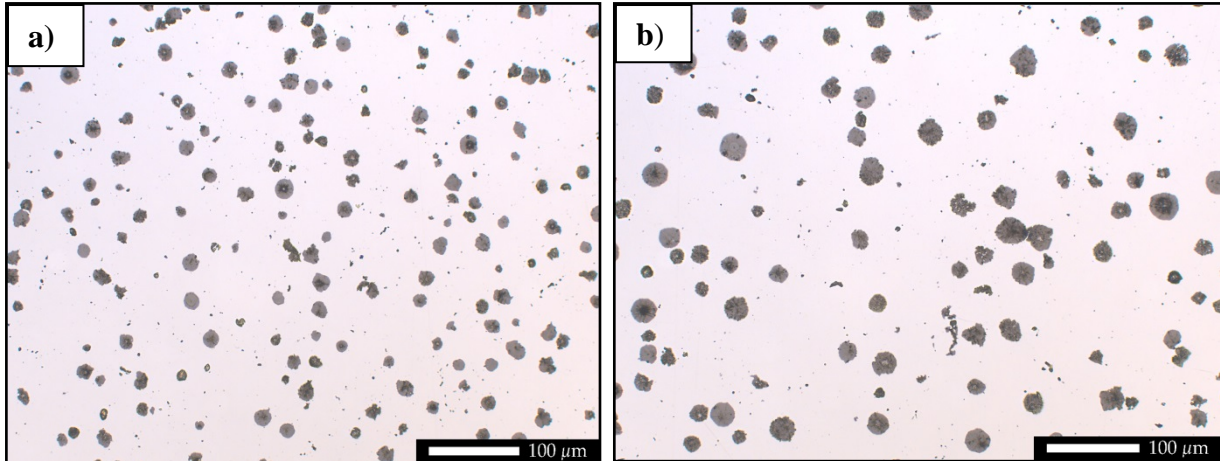


Figure 6.34. a) Compressive section, Skövdes lattice, nodularity 90% b) Tensile section, nodularity 86%.

Etching with 3% Nital acid will show the perlite structure. Shown in Figure 6.35 the bright sections around the graphite is ferrite. The ratio of ferrite/pearlite should be around 50/50 but by analysis the ratio is 30/70. This would also explain the hardness values being on the verge of too high.

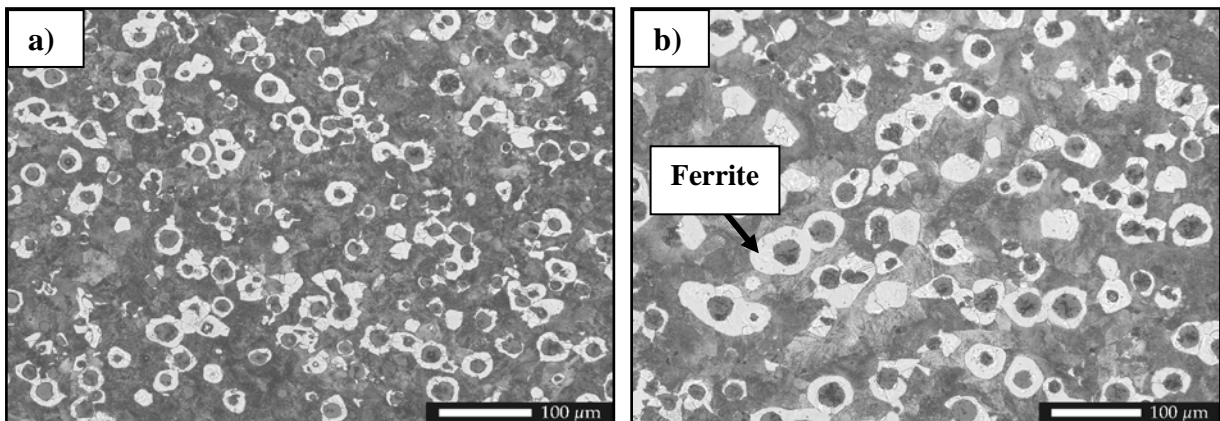


Figure 6.35. a) Compressive section of Skövdes lattice, small graphite due to a rapid solidification b) Tensile section, obtains larger graphite nodules and high amount of surrounding ferrite. High amount of perlite is found in both sections.

The tensile tests of GJS-500-7 show that both bars are outside of the specifications. This is explained by the high amount of pearlite seen in the microstructure. Both the elongation and tensile strength, seen in Figure 6.36 is more similar to GJS-600-5.

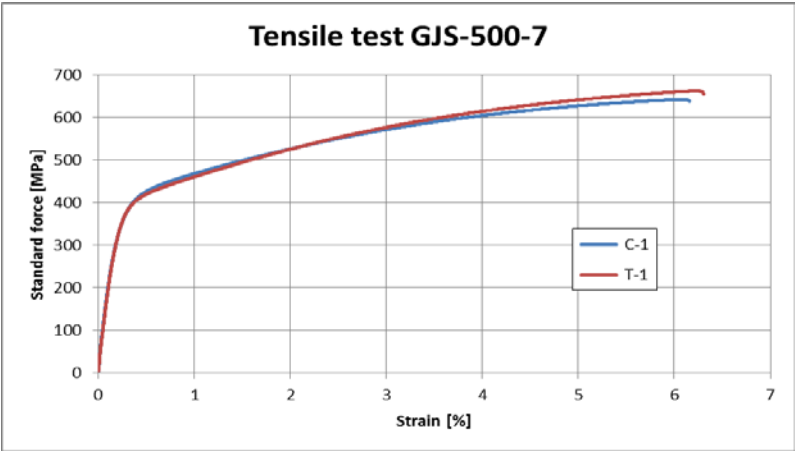


Figure 6.36. Tensile test of GJS-500-7. Both curves are not within the specifications.

## 7. DISCUSSION

Discussion gives a summary of the main results, explaining their meanings and brings perspectives to define possible answers.

### 7.1 Simulation compared to the practical testing

The first material to be tested was the grey iron, VIG 275/190. The material does not exist in Magma5's database; instead the material GJL-300 was selected due to similar mechanical properties. An observation done in the simulation during the solidification was the absence of the phase transformation, from austenite to pearlite. With missing latent heat on transformation the cooling rate is higher and induces more stress into the lattice, generating higher residual stresses in the material compared to the practical testing. From the results, some scattering is seen in practical measurement when comparing them to simulations. The simulated lattices after solidification showed overall too high stresses for all three materials. This difference can be fully explained by the absence of the phase transformation. Regarding the GJL-250, it shows low compressive values which is assumed to be due to one strain gauge showing too low stress. Surprisingly the VIG-275/190 lacked its own material data and yet the simulation is very close to the actual stress values measured in the lattice. The ductile iron, GJS-500-7 shows too high stress in the simulation compared to the practical testing and the difference is large. The missing phase transformation can't fully explain the large differences and further examination is required.

In practical testing the tensile stresses were in general more responsive to the heat treatments and had a higher portion (measured in %) stress relieved at the end of the cycle. This behavior was not observed in the simulations. VIG 275/190 reacted more slowly to any type of heat treatment as well in practical testing. Relaxation in the simulation could occur already at 150 °C and is probably wrong, no relaxation should occur at this temperature and that is a flaw in the simulations. Since GJL-250 uses the same model as GJL-300 the error should exist there as well but the differences in residual stresses should not be as large as those observed in VIG-275/190.

The ductile iron GJS-500-7 had low residual stresses in the physical measurement compared to the simulated material and responded quickly to the heat treatments. Same behavior was seen in the simulations but the residual stresses from the simulations were higher compared to the low values measured from the practical heat treatment. The simulated materials were in general more responsive to the heat treatment at lower temperatures warm-up and most of the residual stresses had already been removed by the time the lattice reached its maximum temperature. The stress curves level out earlier making most of the time spent at max temperature (610 °C) irrelevant which is a non-realistic occurrence since the opposite has been shown in the practical testing.

In general Magma5 correctly predicts the impact of each parameter and it's potential. Cooling rate and drop temperature had less effect on the resulting residual stresses while holding time and heating rate had a larger impact on the stresses. In the extreme parameter heat treatment (HT-7) of VIG 275/190 there was a significant effect from these parameters and there was a

clear difference in stresses when comparing the values with the simulations. The stress in the lattice was twice as high compared to the simulated values.

When the heat treatment was performed the stress of the simulated and practical lattices changes relatively to each other. The values from lattices of VIG-275/190 obtained values above the simulated ones, due to less precise material data existing for this alloy. At the same time the values from the simulation proves that there is a need for a new material profile suited for the VIG-275/190 alloy. GJL-250 shows values similar between the simulation and practical case. Any differences seen between the results could possibly be due to differences when measuring the strain gauges or even temperatures. For GJS-500-7 a heat treatment only increased the error seen from the references. In both cases the residual stresses are reduced, as expected. But the difference in stress relative to each other increases. The heat treated stress values from the simulation were between two and four times larger than the practical values and proves that there are discrepancies in the simulation profile.

A re-occurring problem in Magma5 was the accumulated error seen in the later simulation versions. This was touched upon in the results and the variation between the presented values was similar even if the heat treatments had radical parameter changes. Since no dialogue has been held with MagmaSoft the cause of the issue has not been resolved. Whether the results of our own performed simulations are accurate can't be said and is a source of error. Regardless, the values Magma provide are still several times higher in the case of the ductile iron and would not explain the differences. In the case of the other two materials several Magma5 simulations report relatively good values and the accumulated error is only a minor flaw in the simulation.

Figure 7.1 is a comparison between practical testing and simulations. Some major differences can be shown. The HT- cycle shown by the red line is the same for both simulations and practical testing. The simulations seem to have a higher relieving of the stress at low temperatures. Some peaks in the simulation curve can't be explained. As shown from practical tests the relieving of stress is not significant under 400 °C. The most relieving is shown to be in the heating from 500 to 600 °C, shown by the slope of the green line. The hold time of 5 h is found to have an resulting effect of 17,6 MPa. There are clear differences between the Magma5 and measured values but the different materials has to be taken into account used in Magma5 as well.

## Practical test vs. Simulation

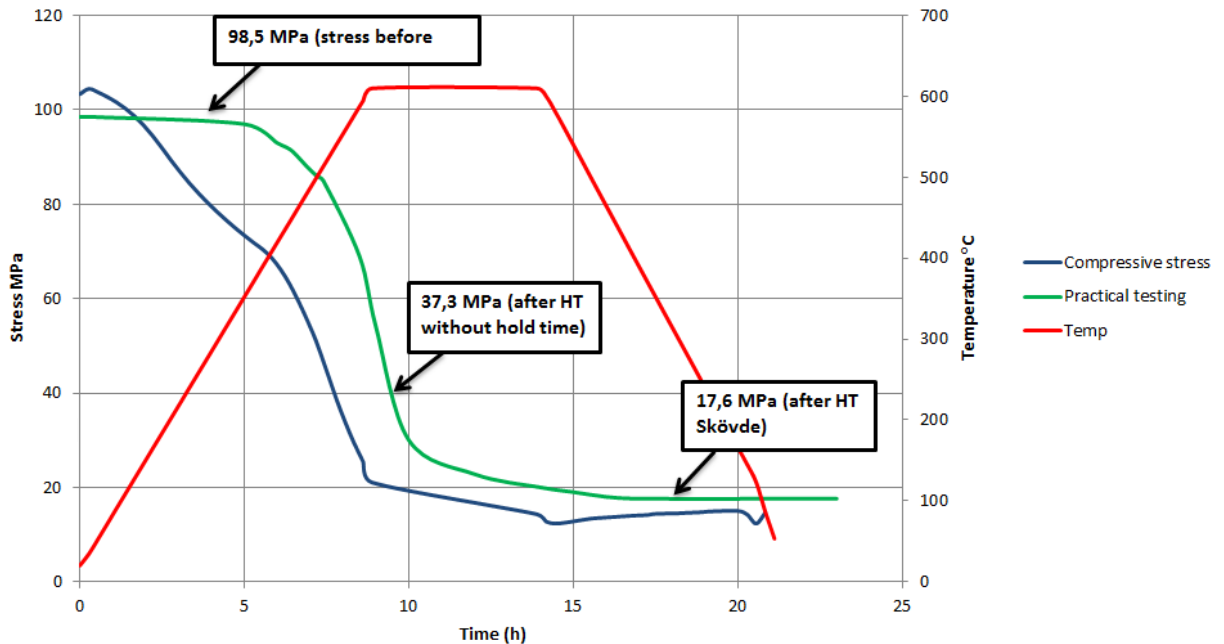


Figure 7.1. The predicted relieving process using accumulated values from testing. The green line is our judgment of how the curve should look like using the experimental results in this work.

As a method to confirm the values measured from the lattices is to use a factor generated from the area of the different sections of the lattice and multiply it with the compressive stress:

$$\frac{A_{Compressive}}{A_{Tensile}} * Compressive Stress \quad \text{Eq. 3}$$

Compressive stress is used in favour of tensile due to homogenous stress gradient in the compressive section, which can be confirmed via simulations. Using this rough calculation the values measured could potentially be sorted and validate to a higher degree making previous knowledge of the material less important. This could also eliminate some error of margin. This type of method of validating was learnt at a later stage of the experimental part and thus was not used.

## **7.2 The reliability of strain gauges**

A frequently occurring problem during the testing was the reliability of the strain gauges. Each gauge was applied in a similar way but the amount of adhesive and temperature changes seemed to affect the measured strain. Most of the time they obtained values within 10% of each other, which is acceptable. But in some cases the strains were far apart and did not make sense and were therefore usually ignored in order to reduce scatter and provide a more reliable mean value. Not being able to fully rely on the measured values makes the method unreliable. The person conducting the test has to be knowledgeable about both the material and what levels of stresses that are expected to be able to discern the wrong ones. There is always a scatter when measuring the strain gauges and differences within 10% can be deemed as potentially the same result.

By simulating the sectioning operation compressive stress are shown in the tensile bar after sectioning. This can cause too high elongation in the gauge and give higher tensile stresses than actually would be existing. The location of the strain gauge has been constant through the testing so it won't affect the comparison between measurements.

From personal experience the strain gauges were difficult to work with and created a lot of discussion due to diverging values and what the potential cause could be. It is still deemed as an accurate method to measure residual stresses with but the requirement to make the testing consistent takes practice. There was also a requirement on the surface roughness not being too coarse and not too polished. Pores could also make it difficult to apply the correct amount of adhesive as well. Even if consistency was achieved the differences persisted between each strain gauge and only when all values were summarized a clear result could be obtained and the trends appeared. By the clear trends of evaluating the results, values from strain gauges seems to be acceptable but not precise.

To note is that the placements of the strain gauges are not the same as the ones in the simulation. Comparing the results might not be fully accurate due to this and the practical testing is potentially showing higher stress values. This is foremost a concern for the tensile bar due to the large area and because the variance in stress varies more in the thicker section. However, the error is presumed to be small and should not have had a big impact on the residual stresses measured.

## **7.3 Material properties effect on residual stresses**

The potential effect cell size and microstructure have on the residual stresses have been assumed being low and the alloying content is what matters the most. This behavior could most easily be seen in GJL-250 where the compressive section had been severely undercooled and had faulty graphite structure, yet the result of the heat treatments were good. Most of the stresses had dissipated regardless of the structure of the material. It was therefore concluded that the elements affect the residual stresses relieving, confirmed by analyzing the trends from VIG-275/190.

*Grey iron, VIG-275/190-* Mo is a potent alloying material which increases both the tensile strength and mechanical properties at elevated temperature. This results in higher residual stress as well as making the heat treatment less effective. (Cr is also increases the tensile strength but not to the same degree as Mo.) Cr also lowers the graphite content in the material and might cause additional shrinkage in the casting process. The time spent above 500 °C shows a clear trend which is important to point out for future work and recommendations.

*Grey iron, GJL-250 -* Comparing the un-alloyed grey iron to VIG-275/190 most results fell within the predictions. The un-alloyed grey iron is responding more easily to the heat treatments, due to a lower tensile strength and no alloying elements that counteract the creep. This is also stated and explained in detail in the theoretical background. The micro-samples of the GJL-250 showed significant variances in hardness and microstructure. Hardness of 40 HB is due to effect of undercooling the material is shown in the thin section. From the tensile test, large differences were seen between the compressive and tensile bars and neither of them are within specifications. However, the chemical analysis showed that the material was within the specifications. Therefore, the assumption is that the stress values measured from the lattices are still valid and the results are valid.

*GJS-500-7-* The ductile iron obtains more residual stress after solidification compared to the grey iron materials, which is related to its higher tensile strength. The heat treatment test confirms that the ductile iron easily relieves residual stress compared to VIG-275/190, most probably due to less alloying elements and no Mo or Cr. The cooling rate seems to have some effect on the residual stress but not to the same degree as hold time. Creep does not occur below 425 °C and was shown by varying the drop temperature. The hold time is the most important parameter, like the grey irons. The hardness of the GJS-500-7 was at the upper limit due to the amount of pearlite being too high. The chemical analysis shows no values outside the specifications. The higher grade ductile iron GJS-600-5 has more in common with the material analyzed and has the same pearlite/ferrite ratio. Even if the material is more similar with GJS-600-5 the results are still valid and the results found can be applied to both materials.

Regarding the stress relieving of HT-2, VIG reduces the stress with about 70%, GJL with 86/90% and GJS with 89/89% (compressive/tensile). This confirms the effect of alloying elements in the VIG-material and shows that GJS-material has easier to reduce residual stress compared to the alloying grey iron.



## 8. CONCLUSION

Conclusions are the summary of the most important findings.

### 8.1 Simulation by Magma 5

- The simulations in all cases show higher residual stresses after solidification compared to the measurement. This can partly be explained by the missing phase transformation at 723 °C from austenite to pearlite. By modification of the specific heat capacity of sand mould and cast iron material the cooling rate can be corrected to match the measured temperature. By making this change the result of the simulation are more in line with the practical measurements.
- In simulation of the HT, stress relieving is observed to be finalized reaching the peak temperature at 600 °C, after this point the stress relieve is no longer significant. The relieving trend is not like what is stated in the theory of stress relieving depending on creep or from what's shown by the practical testing.
- The effects of changed cooling rate and drop temperature are difficult for the software to predict. The simulations do not show any significant effect of a rapid cooling.
- The simulations consecutively show lower stress in comparison to the practical case after the heat treatment (GJL-300 compared to VIG-275/190).
- Simulations of GJS-500-7 are not following the same trends as grey iron. The stress after both solidification and heat treatments shows higher values compared to the measurements. The relieved stress after heat treatment is 89% (both tensile and compressive). The simulation predicted a relieving of 75%/63% (Compressive/Tensile) for the ductile iron which is significantly higher. This indicate that Magma5 has difficulties predicting the effectiveness of the HT and estimates a higher value than the actual case.

## 8.2 Practical testing

Comparing the obtained residual stress of the lattices, the following results can be stated for each material:

*Grey iron, VIG-275/190:*

- In VIG-275/190 the time spent over 500 °C is the most important factor to relieve residual stresses. Alloying elements Mo and Cr lowers the creep and diffusion in the material, especially in the 0-400 °C range and makes the material less responsive to heat treatments. This is stated with HT-7, when the drop temperature was set to 425 °C but the residual stresses remained the same as drop temperature of 200 °C.
- Heating rate and hold time are parameters with most effect on the stress relieving process.
- A low cooling rate from temperatures below 425 °C are not significantly important, due to the creep resistance at lower temperatures.
- Mo and Cr forms a finer cell structure and should by theory increase the potential of stress relieving. But this effect is fully counter-acted by Mo which decrease the effectiveness of creep.

*Grey iron, GJL-250:*

- Responds easy to the HT and obtains higher amount of residual stresses relived compared to VIG-275/190. This is explained by the fact that the material has easier to creep and diffuse.
- Stress relieved mostly by a longer hold time, but also cooling rate and drop temperatures are shown to be of significant importance, due to higher creep at lower temperatures.
- From experimental trials it has been shown that a rapid cooling from 600 °C generates less relieving compared to drop temperature of 200 °C, this observation can be used considering the sand mould opening temperature.

*Ductile iron EN-GJS-500-7:*

- Obtains highest amount of residual stresses as cast compared to the grey iron materials, due to its high strength. This trend is mostly shown by simulations, when measuring the practical lattices the stress after solidification did not have variation as simulations predicted.
- The HT confirms that ductile iron has easy to relieve residual stress compared to grey iron, most probably due to less alloying elements.
- The cooling rate shows to have some effect on residual stresses.
- Increasing drop temperature to 425 °C will not have an effect on residual stresses.

## 9. RECOMMENDATIONS

### 9.1 Recommendations to Skövde foundry

Stated from the conducted heat treatments, heating and cooling rates have less influence on the resulting residual stresses. There are some changes Skövde foundry can do to reduce the time of the heat treatment cycle. Today only hold time and cooling rate can be changed, but Skövde foundry should also consider changes to the heat capacity to increase the heating rate. Doing these changes would reduce hours on the heat treatment and better reproducibility would be obtained.

Today the oven runs sub optimal in the heating process. From previous conclusions, it was shown that more time spent over 500 °C played a significant role. The recommendation is therefore to have a heat treatment with at least 6 hours spent above 500 °C, e.g. a holding time of 4 hours with a rapid cooling rate. The recommendation of hold time would be between 4-5h, due to the significant effect on the result.

HT-9 was supposed to be the recommended heat cycle, but was a mistake since a similar heat treatment was performed on HT-1. The difference is the cooling rate changed from 75 °C/h to 150 °C/h that already been confirmed to not have a significant effect. Whether the residual stress will be as low as Skövdes heat treatment is not stated, it would need another HT test on VIG-275/190 to be confirmed. This study is also based on the lattice component and won't include the effect of components with even thinner sections. To save time a compromise could be necessary.

The following parameters are based on the practical testing and are the final recommendation of heat treatment to reduce time without affecting the stress. By use of the new heat treatment Sköveds HT-cycle can be reduced with approximately 50% and by use of today's heating the reduction would still be approximately 25%.

- Heating rate up to 200 °C/h, maximal used today is 67 °C/h.
- Hold time of 5h, can probably be decreased down to 4h.
- Cooling rate up to 150 °C/h
- Drop temperature of 325 °C/h.



## 10. FUTURE WORK

The practical testing had a limited amount of stress lattices. With a higher amount of test lattices a wider range of parameters and their combinations can be examined. Also, an optimized complete heat treatment cycle could be formed for each specific material.

Further investigation of how high temperatures you can reach (hold temperature) without affecting the microstructure and mechanical properties would be interesting to investigate. To reach as high temperature as possible would make creep higher and accelerate the stress relieving. In the pre-study three hold temperatures have been investigated and their respective hardness have been compared. The results indicate that a hold temperature of 650 ° C is too high and changes the mechanical properties of the material, see Appendix D.

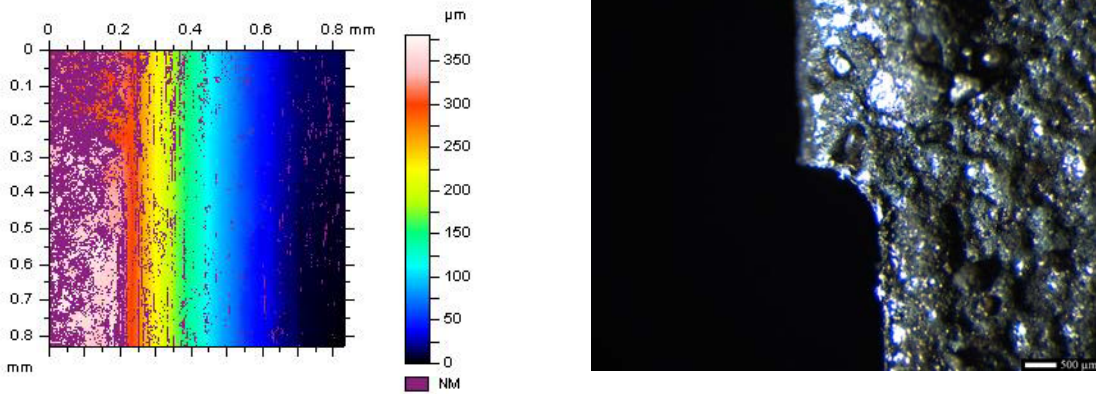
For the material GJS-500-7 it would be interesting to further investigate how low hold temperature you can reach with same relieving effect to save both energy and time.



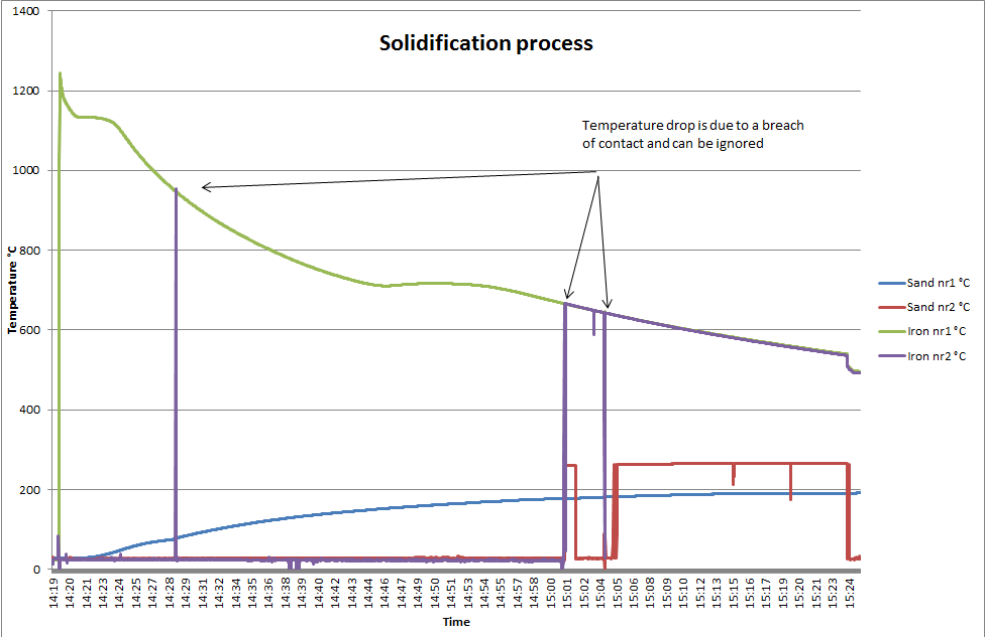
## References

- G. I. Sil'man, V. V. (2003). Effect of Copper on Structure Formation in Cast Iron. In *Metal Science and Heat Treatment* (pp. 254-258).
- G. Totten, M. H. (2002). *Handbook of Residual Stress and Deformation of Steel*. ASM International.
- Gjuterihandboken.se. (2015, 01 01). <http://www.gjuterihandboken.se/handboken/3-gjutna-material/32-graajaern>. Retrieved from Gjuterihandboken: <http://www.gjuterihandboken.se/>
- Gundlach, R. B. (2005). The effects of alloying elements in the elevated temperature properties of Grey irons. Michigan: AMAX material research center.
- Janowak, J. F., & Gundlach, R. B. (2006). *A Modern Approach to Alloying Gray Iron*. American Foundry Society.
- Johannesson, B., & Hamberg, K. (1989, 11 24). *Spännings/töjnings-egenskaper hos gråjärn avsett för cylinderhuvuden [Internal report LM-54159]*. AB Volvo. Technological Development.
- Kyowa. (2017, 03 09). [http://www.kyowa-ei.com/eng/technical/strain\\_gages/index.html](http://www.kyowa-ei.com/eng/technical/strain_gages/index.html). Retrieved from <http://www.kyowa-ei.com>.
- M. Holtzer, M. G. (2015). *Microstructure and Properties of Ductile Iron and Compacted Graphite Iron Castings*. Springer.
- Magmasoft. (2017, 01 23). [www.magmasoft.com](http://www.magmasoft.com). Retrieved from <http://www.magmasoft.com/en/solutions/ironcasting.html>: <http://www.magmasoft.com/en/solutions/ironcasting.html>
- National High Magnetic Field Laboratory: Magnet Academy. (2014, 12 10). Retrieved from Nationalmaglab.org: <https://nationalmaglab.org/education/magnet-academy/watch-play/interactive/wheatstone-bridge>
- Pentronic. (2017, 04 11). <http://www.pentronic.se/>. Retrieved from <http://www.pentronic.se/start/temperaturgivare/teori-om-givare/tabeller-och-polynom.aspx>.
- Schmidt, P. (2016). *Cast Iron*. Volvo Materials Technology.
- Sn-castiron.nl*. (2009). Retrieved from [http://www.sn-castiron.nl/en/castiron/en\\_gjl.html](http://www.sn-castiron.nl/en/castiron/en_gjl.html): [http://www.sn-castiron.nl/en/castiron/en\\_gjl.html](http://www.sn-castiron.nl/en/castiron/en_gjl.html)

# APPENDIX A



The measured thickness that is milled down on each surface of the lattice.



The solidification process of casting the stress lattice, the dips is due to breach of contract.



*Zwick 1486 Machine used for tensile testing. The picture to the right is a close up of the tensile test bar.*



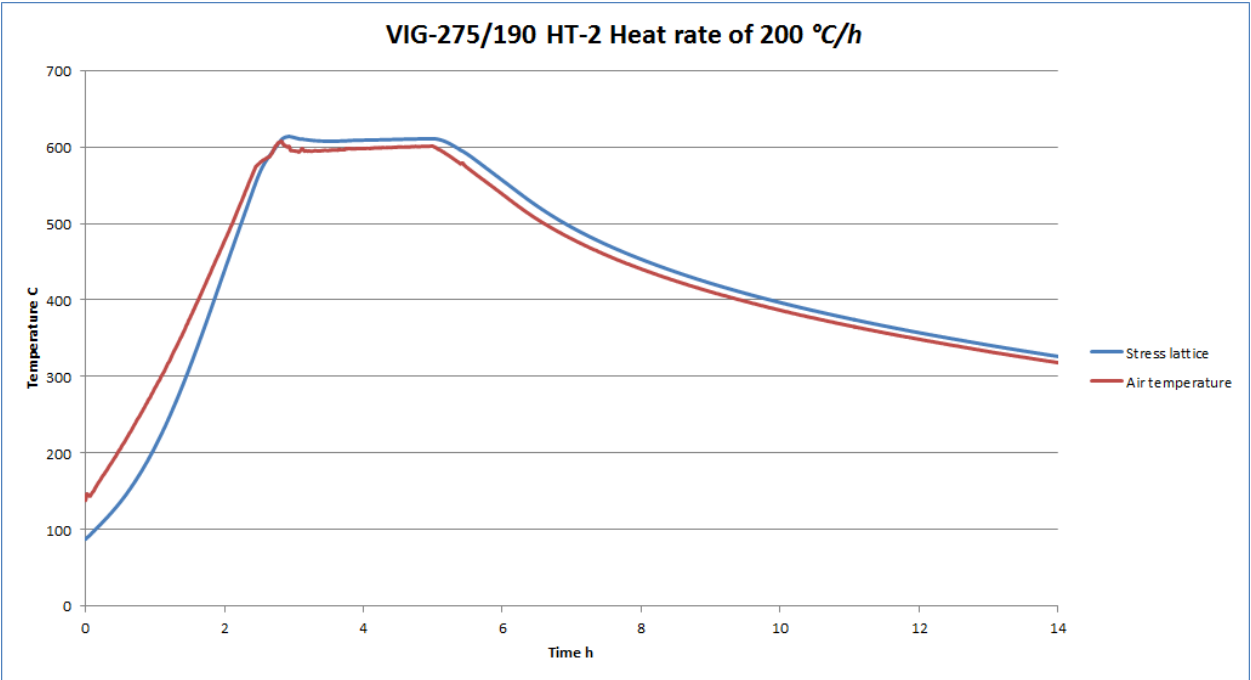
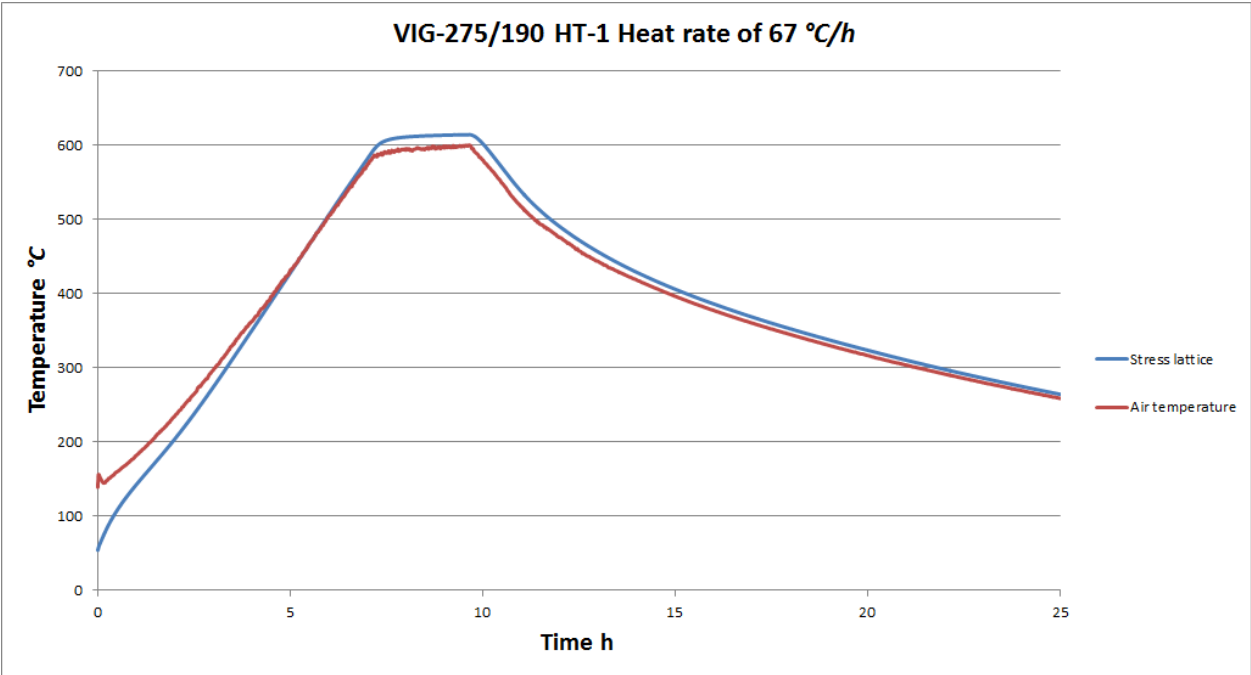
*The heat treatment Oven 10 used for the practical testing and the Brinell hardness machine comp. no. 8900044/0001.*

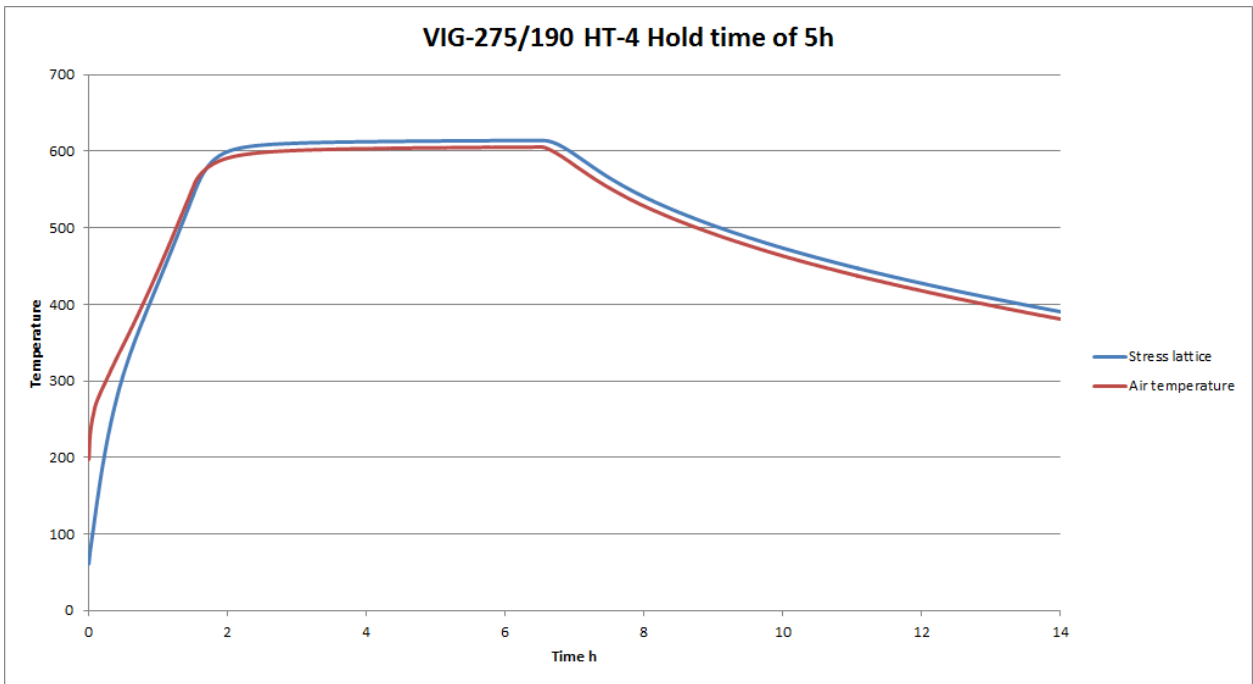
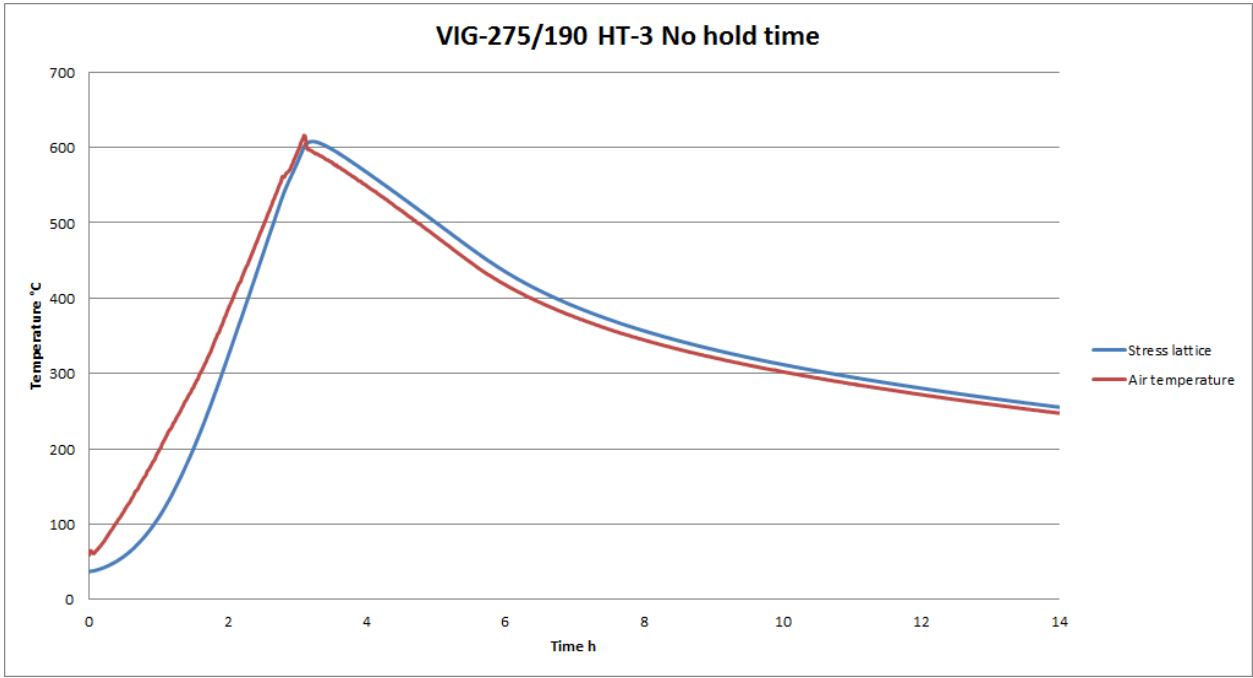
# APPENDIX B Heat treatments

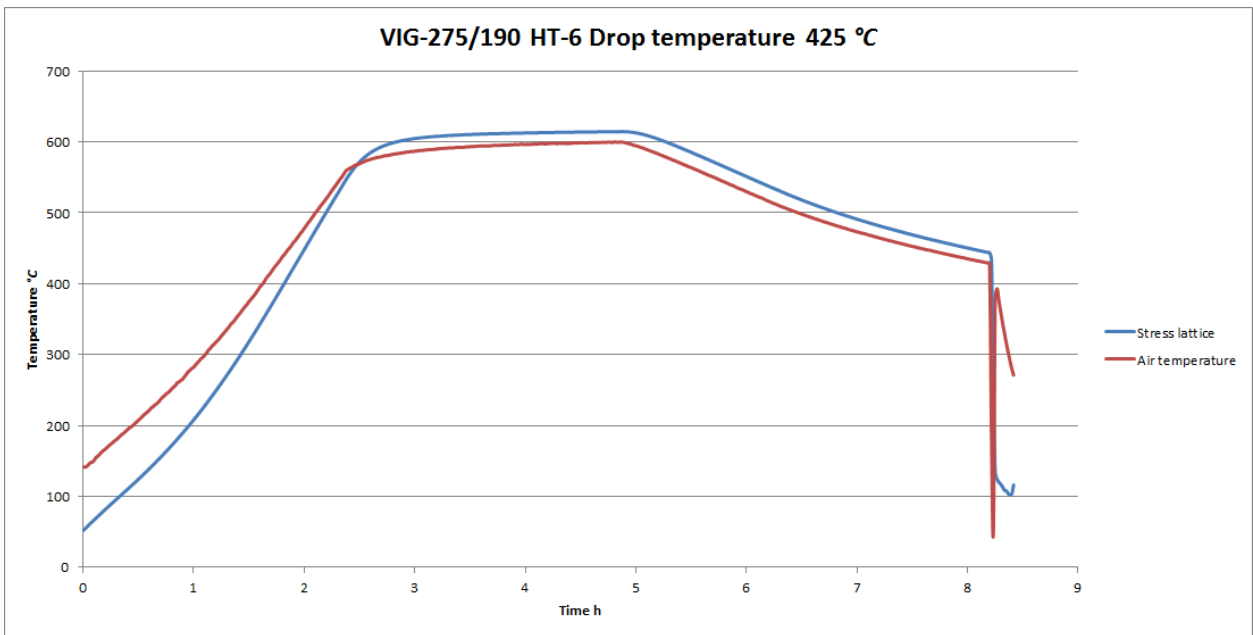
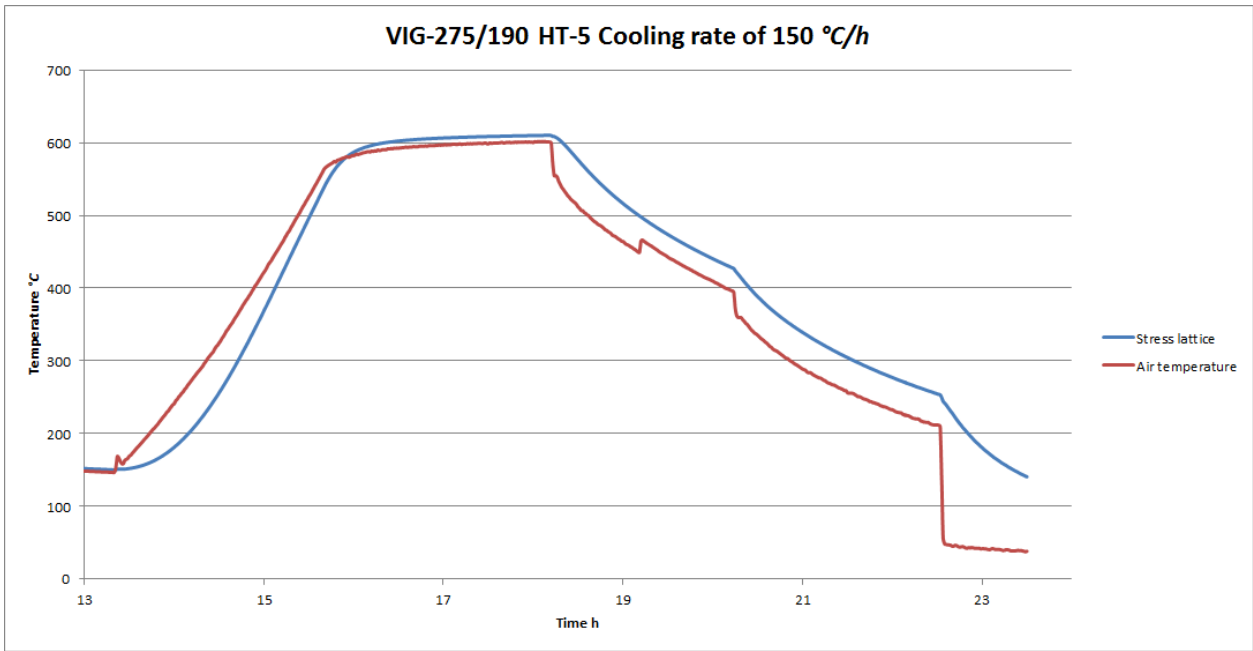
	7	6	5	4	3	2	1	
E	<p>COOLING PROCEDURE AFTER CASTING:</p> <p>ALT. 1 (STRESS RELIEVING ANNEAL):          THE CYLINDER HEAD SHOULD BE HEATED TO 595-650°C AND HELD WITHIN THAT TEMP. INTERVAL FOR 2 HOURS MIN.</p> <p>OVEN TEMP. BEFORE CHARGING: 100°C MAX.          HEATING SPEED: 200°C/HOUR MAX.</p> <p>COOLING SPEED: 75 °C/HOUR MAX TO 325 °C MAX.          THEREAFTER FREE AIR COOLING.</p> <p>DURING COOLING STAGE (MAX 75°C/HOUR), MAX. ALLOWED TEMP. DIFFERENCE WITHIN THE CYLINDER HEAD IS 50 °C.</p> <p>ALT. 2: WHICH IS NOT TO BE USED BEFORE APPROVAL FROM ENGINE DESIGN DEPT. AT VTC, GOTHENBURG:</p> <p>CYLINDER HEAD WHICH HAS COOLED IN HOMOGENOUS SAND FORM TO 425°C MAX DOES NOT HAVE TO BE ANNEALED ACC. TO ALT.1 ABOVE.</p> <p>THE COOLING SPEED IN THE TEMP. INTERVAL 650 °C-425 °C MAY NOT EXCEED 30°C/HOUR.</p> <p>THE TEMP. SHOULD BE MEASURED ON THE INNER WALL OF THE INJECTOR HOLE AT CYL. 3 OR 4.</p>							E
D								D
C								C
B								B
A								A
	7	6	5	4	3	2	1	D3 FORM

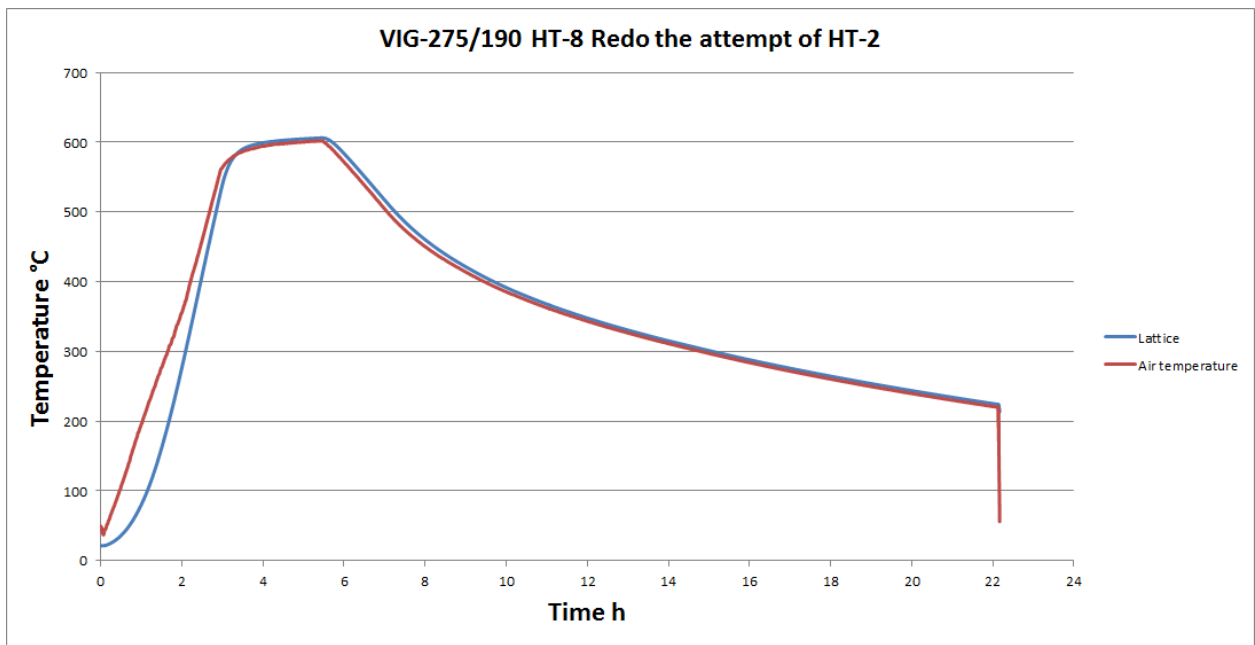
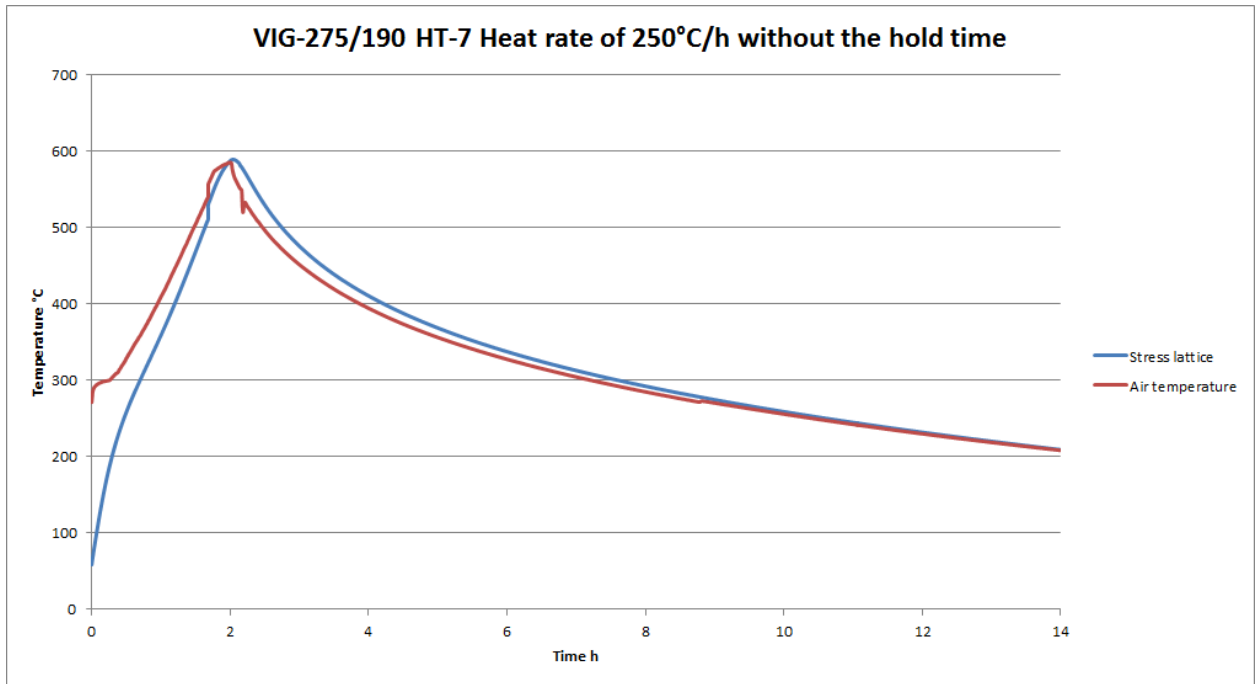
*Heat treatment recommendations of Volvo drawing 1677285*

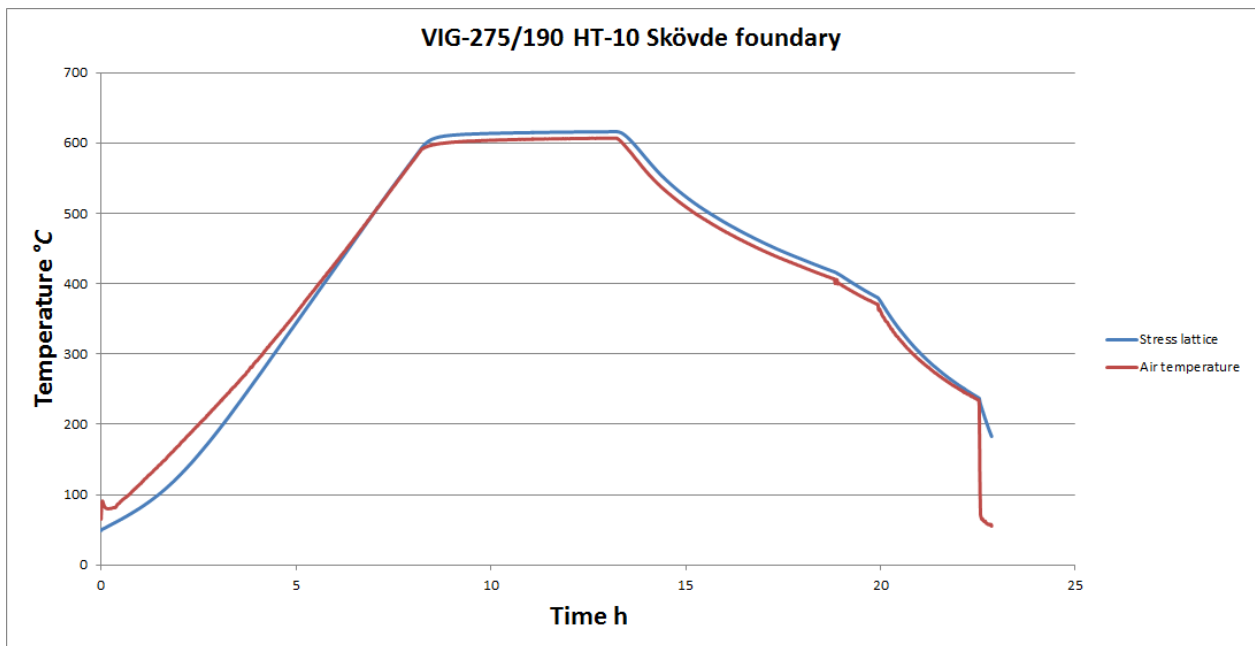
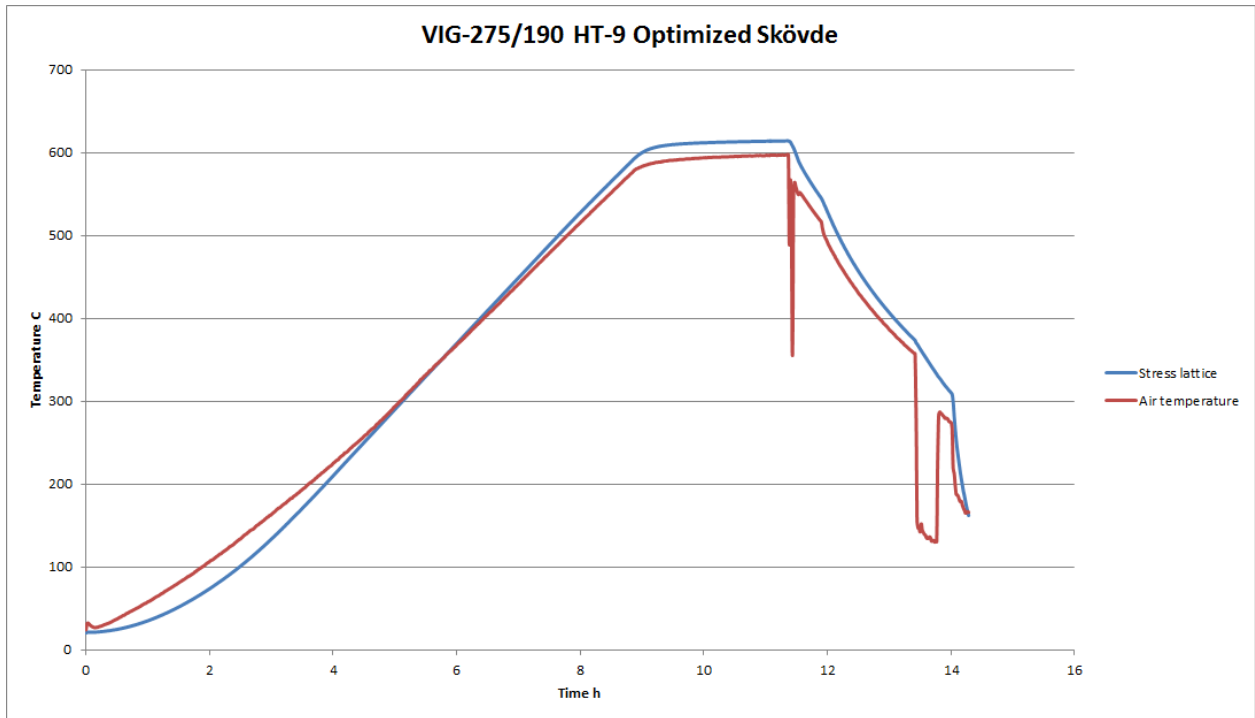
# Heat treatments of VIG-275/190



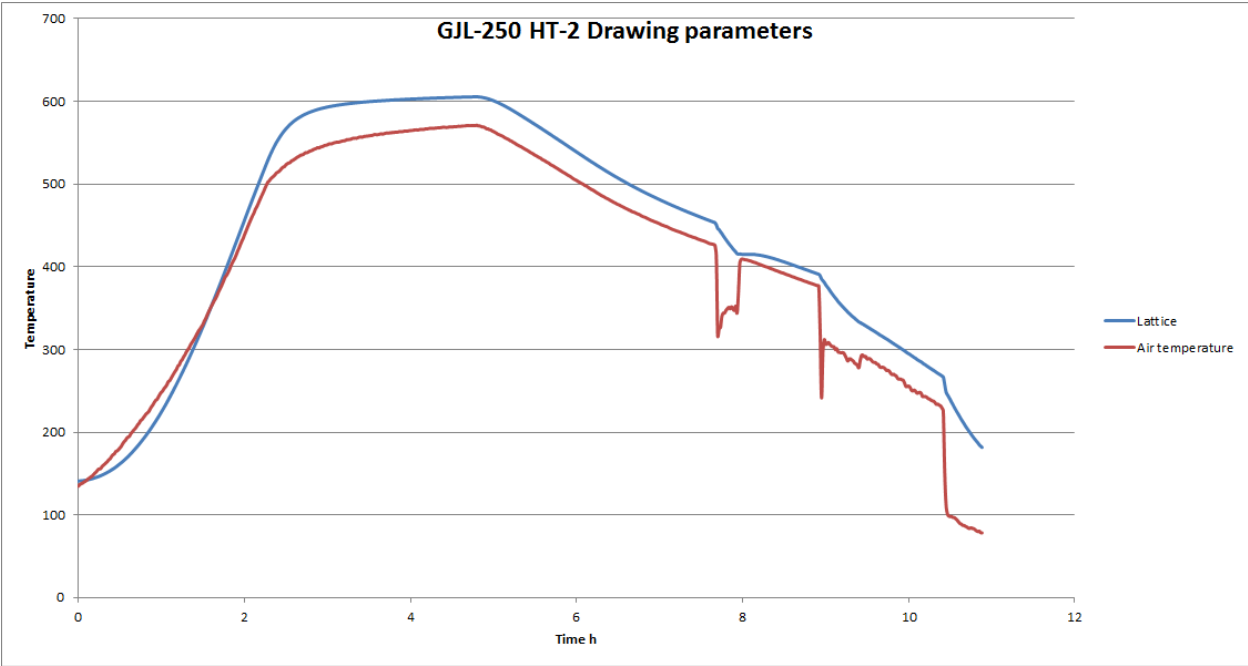
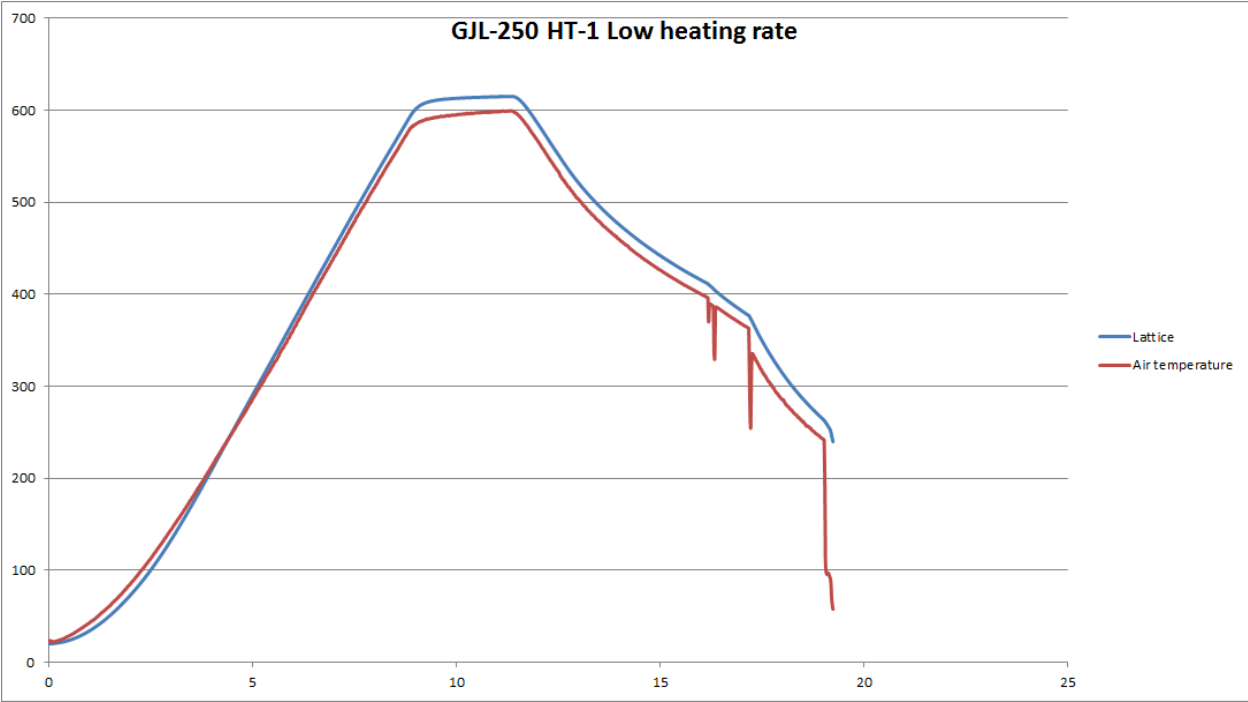


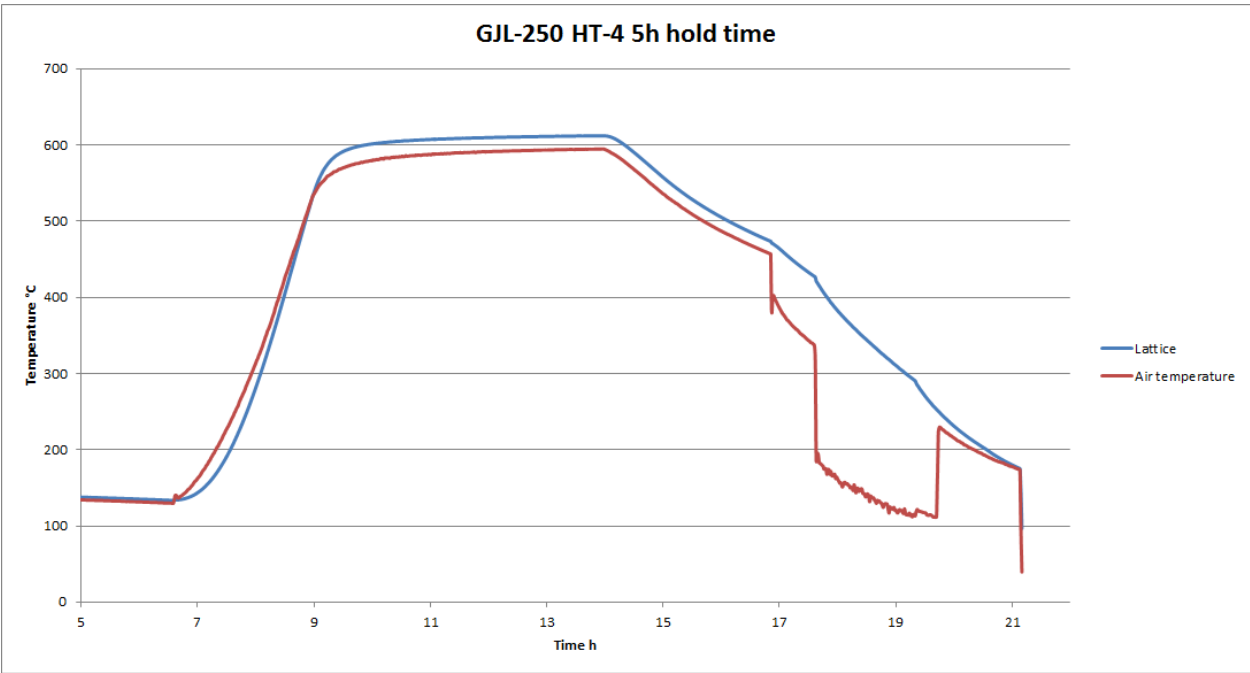
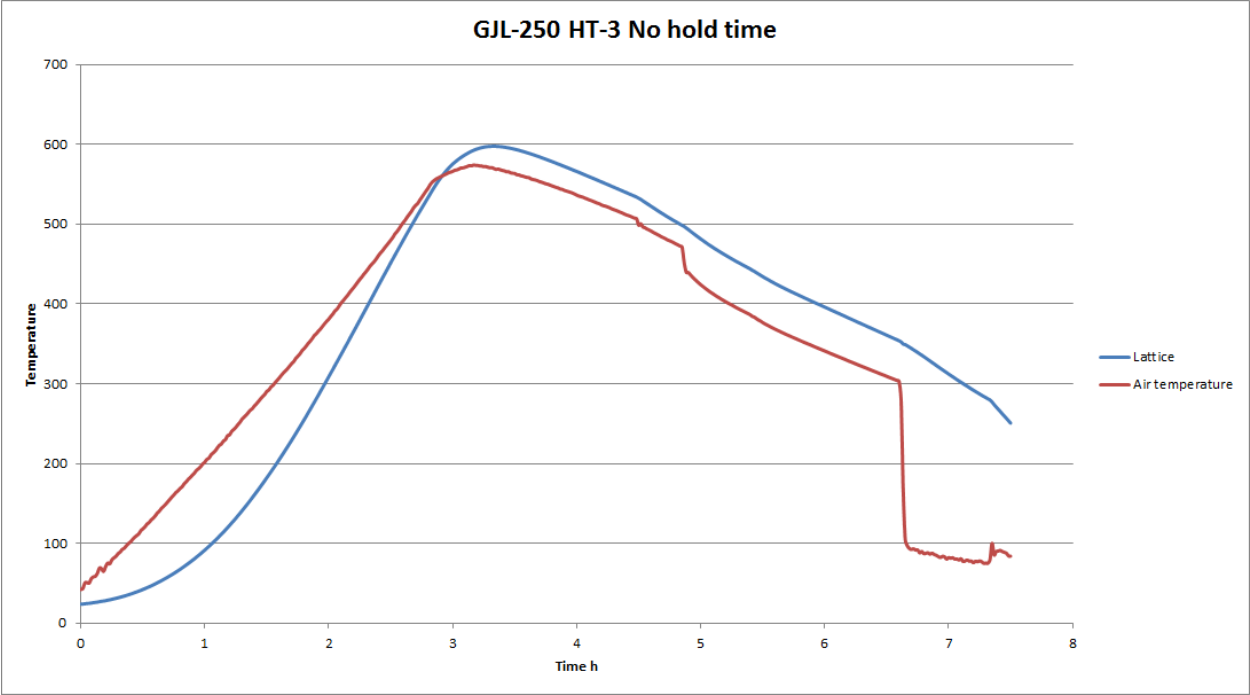


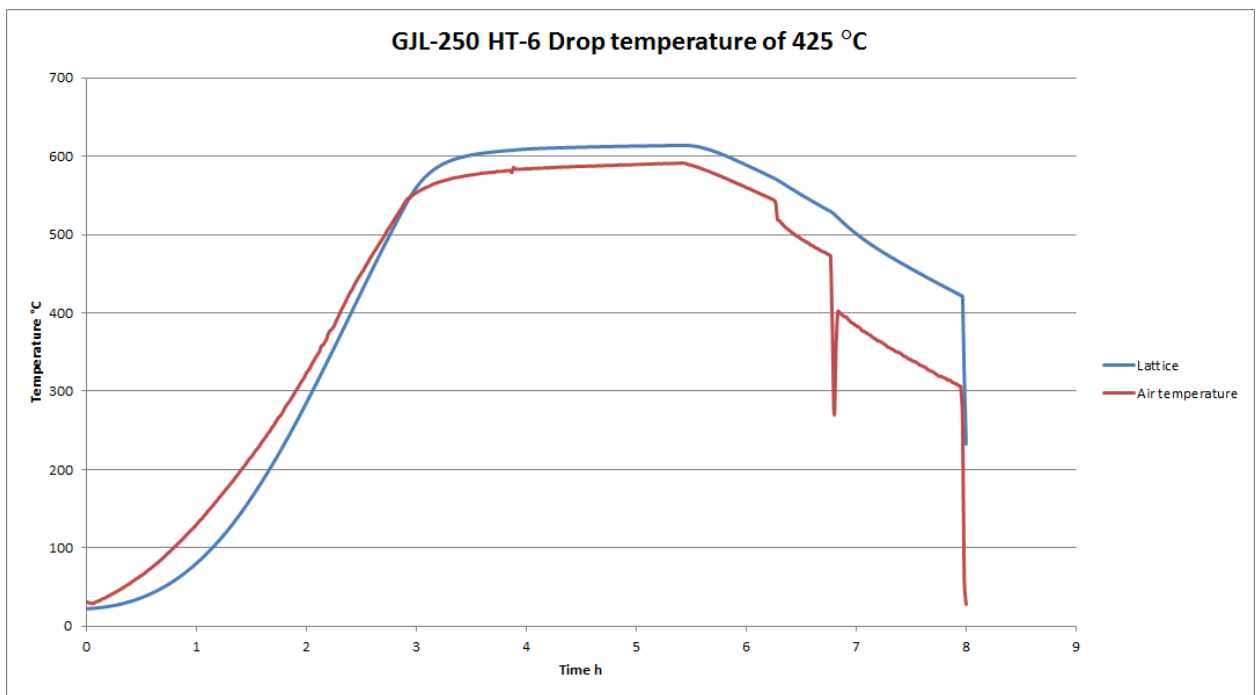
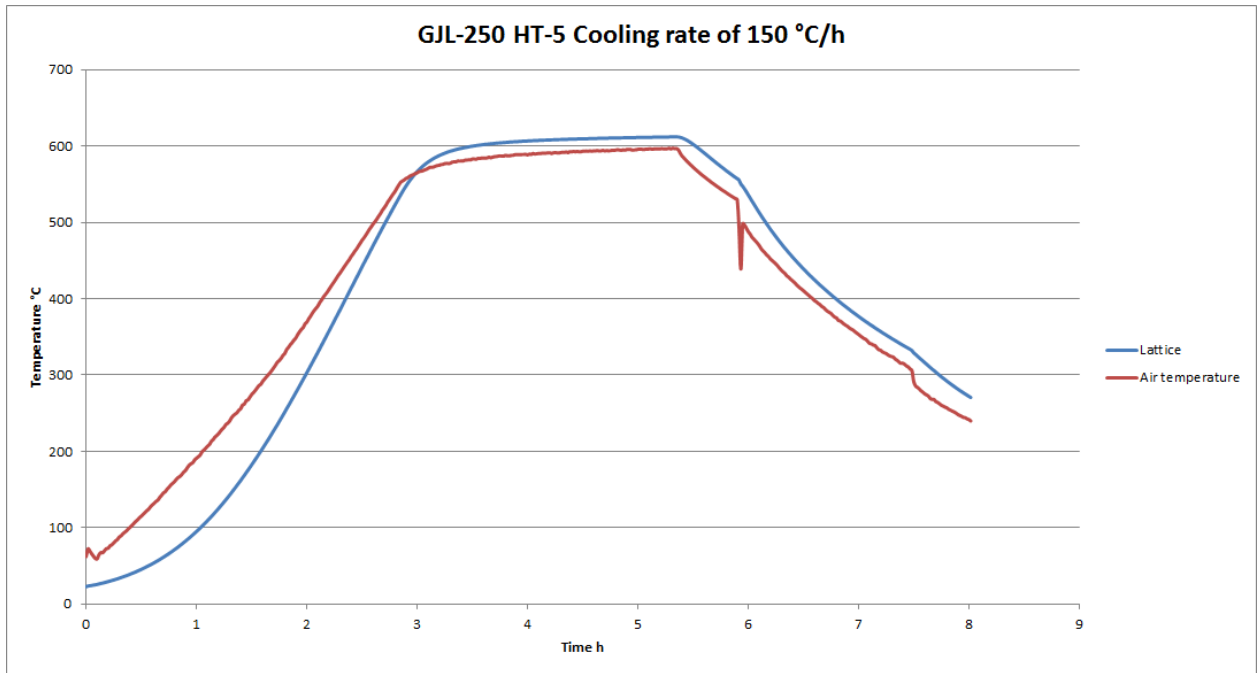


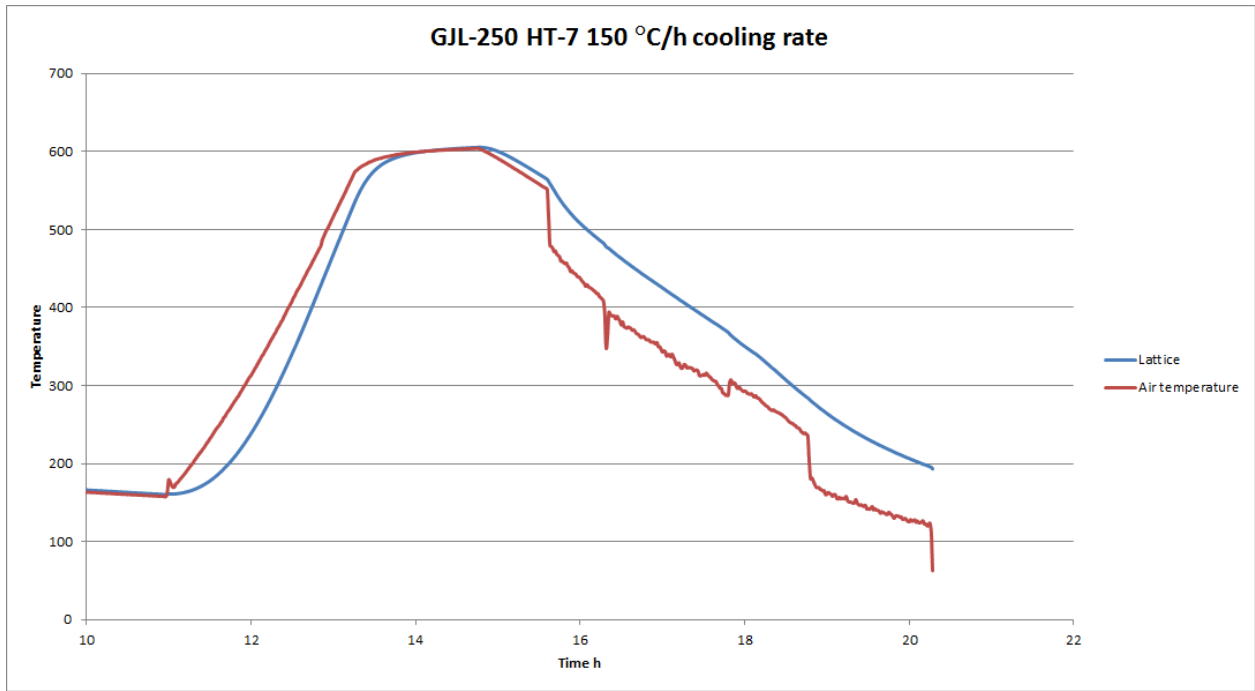


# Heat treatments of GJL-250

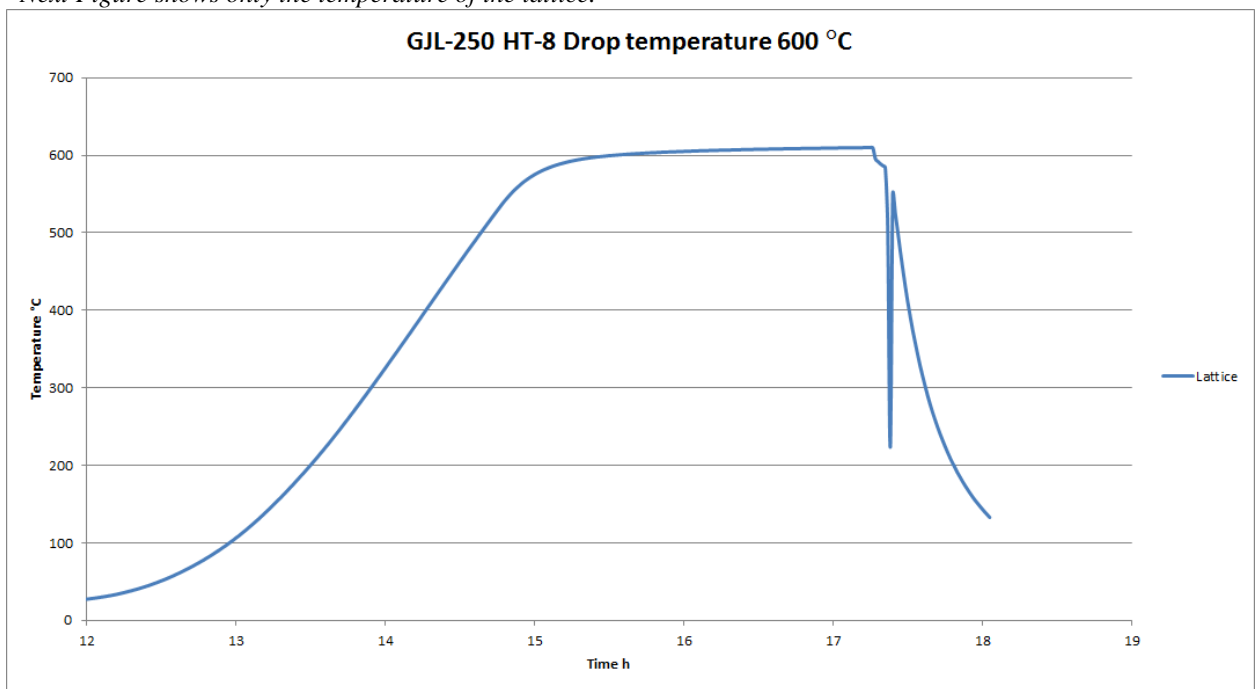




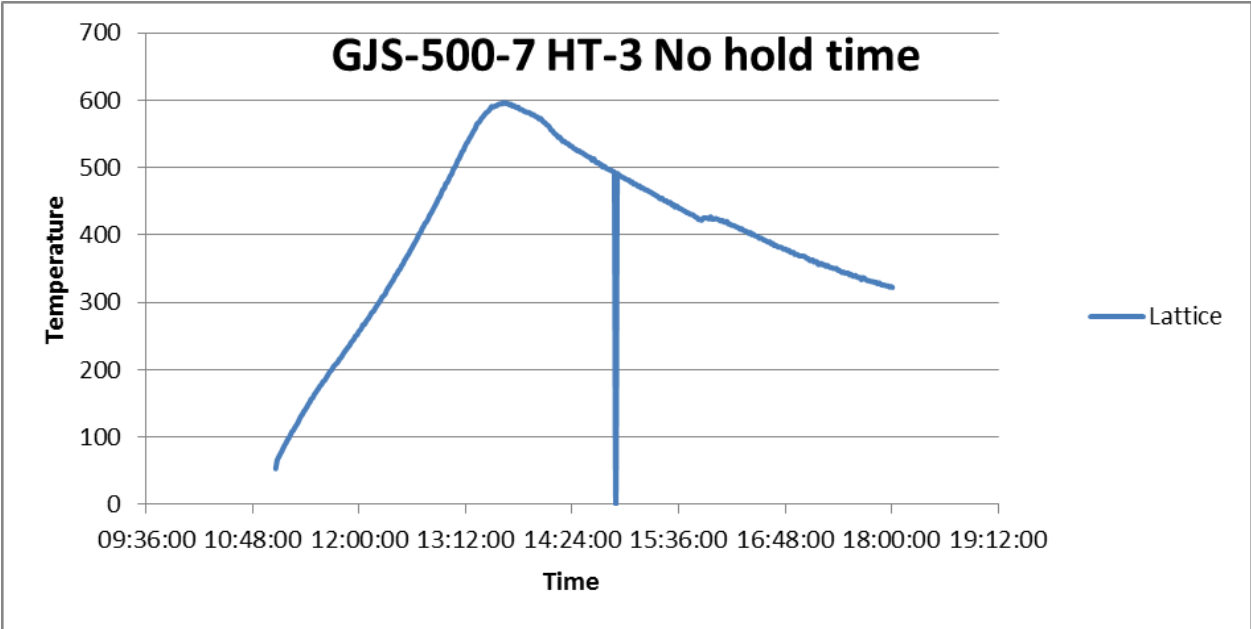
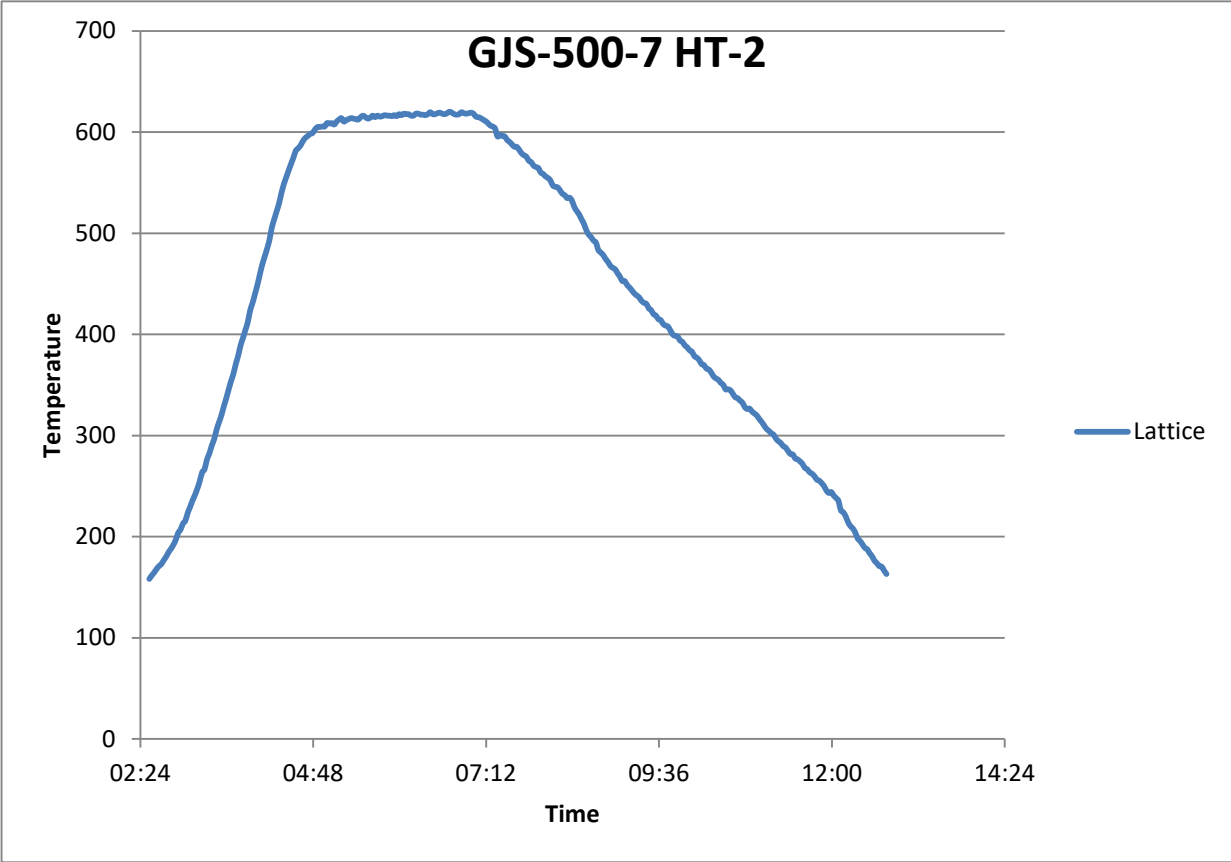


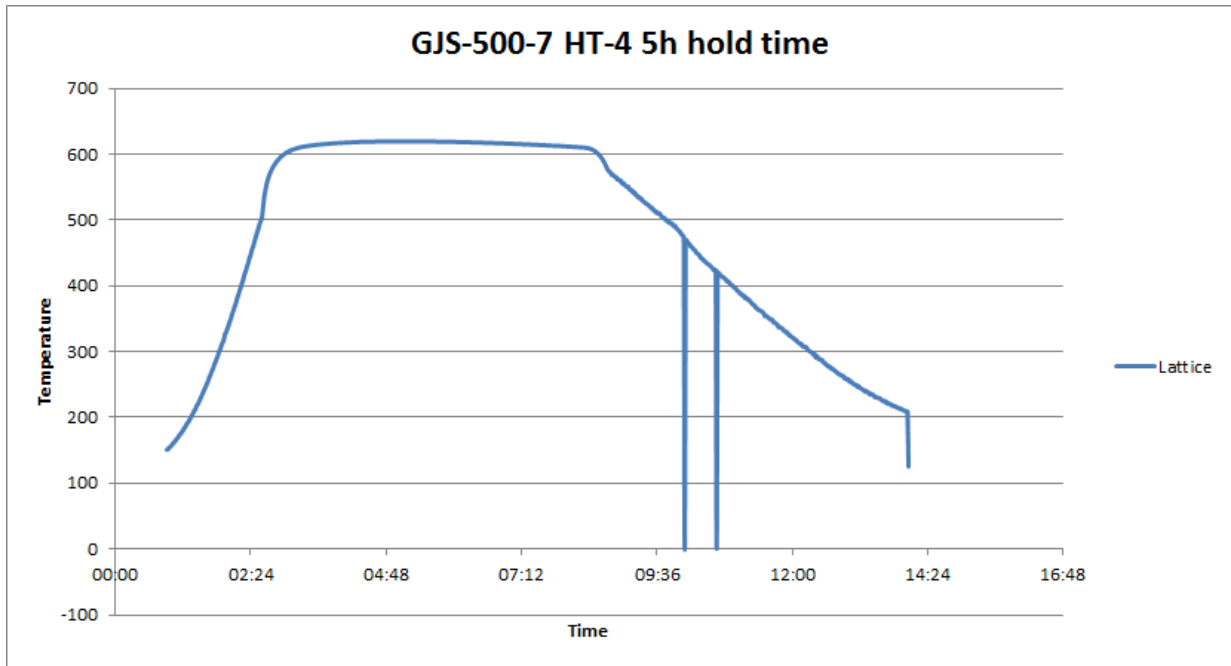


*\*Next Figure shows only the temperature of the lattice.*

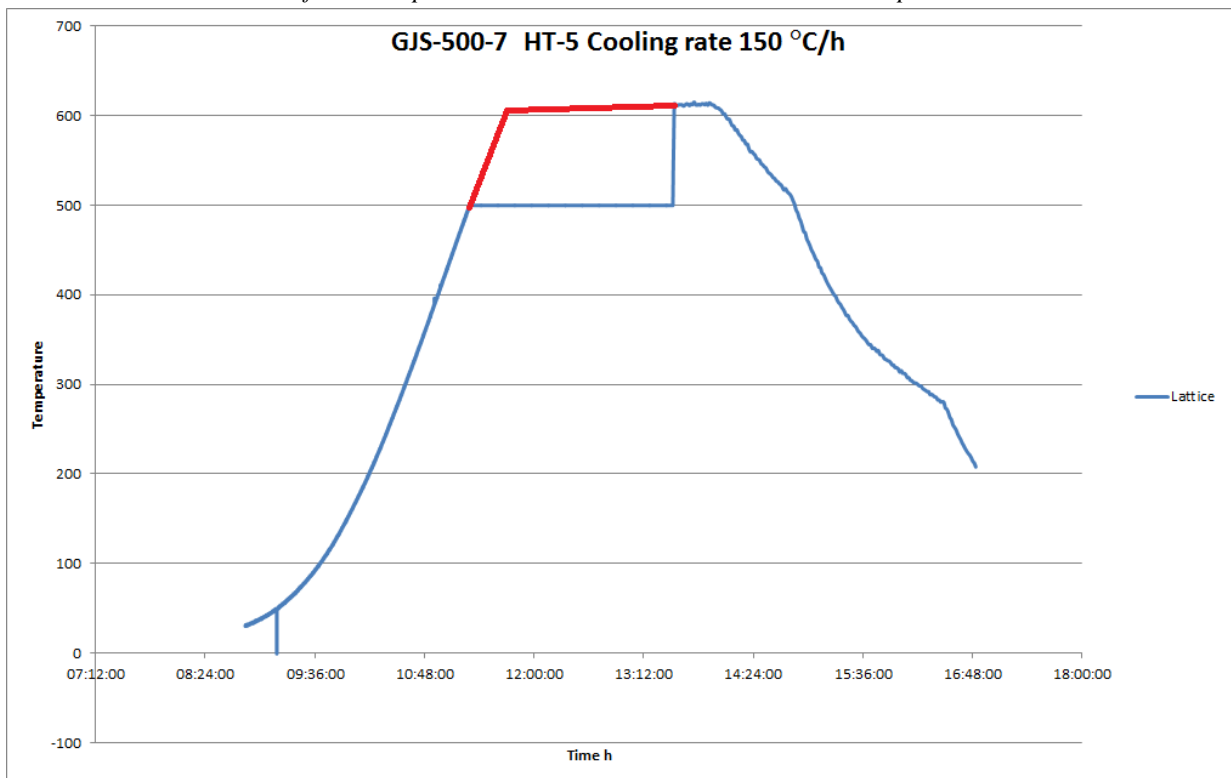


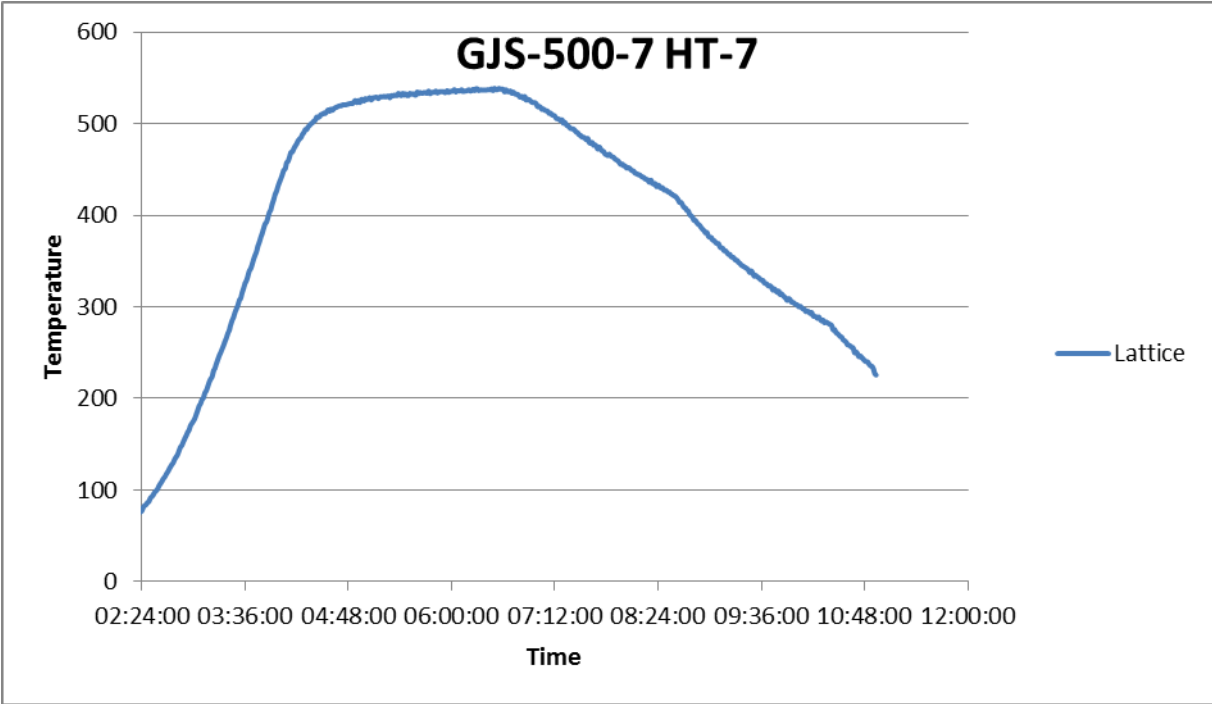
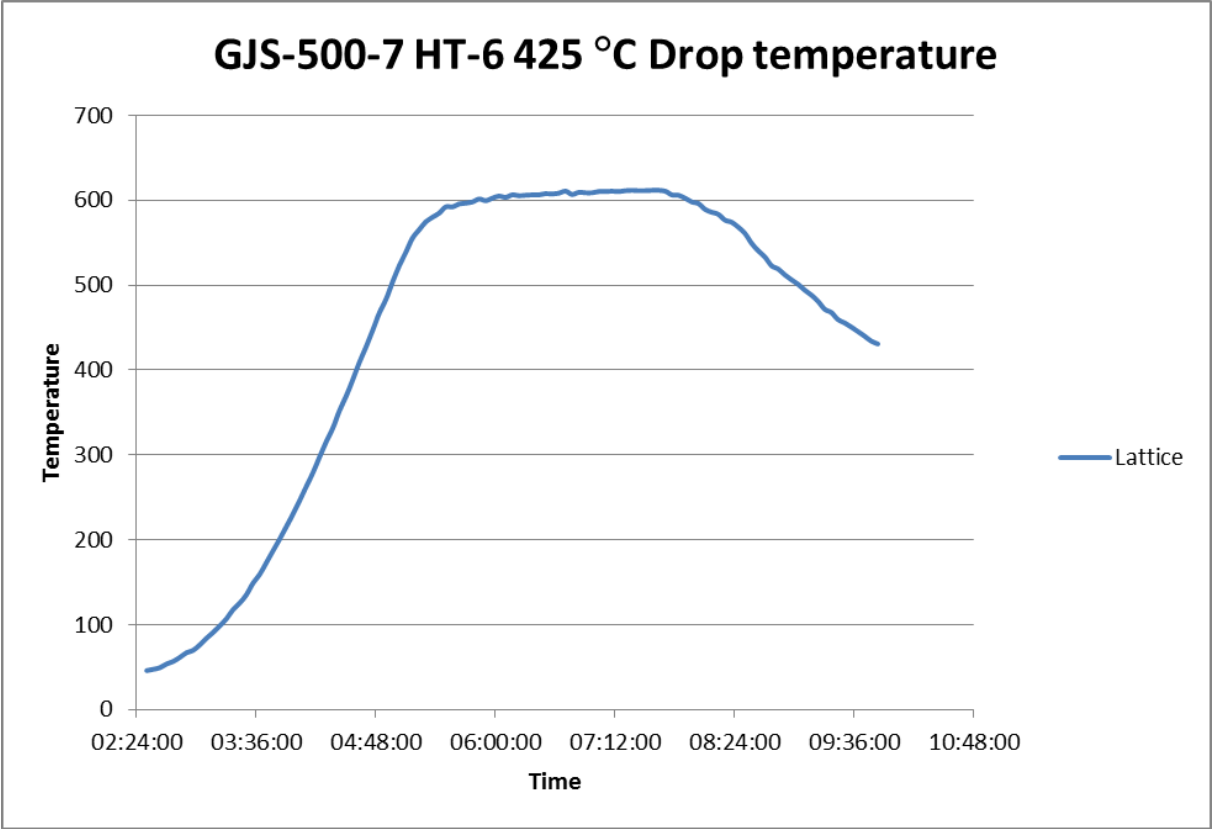
### Heat treatments of GJS-500-7





\*A new thermo log are used to measure the heat treatment curve. The software was set to reach maximal 500 °C but is corrected in the end of the hold phase. The red lines show how the actual temperature is in the lattice.





## APENDIX C User recommendations of oven 10

- *to* = Delay time in (h) before the heat treatment starts
- *rmp1* = Heating rate °C/h to dwell temperature
- *tmp1* = Temperature for 1st dwell temperature
- *t1* = Dwell time at 1st dwell temperature
- *rmp2* = Heating rate °C/h to final temperature
- *tmp2* = Temperature for 2nd dwell temperature
- *rmp3* = cooling rate °C/h

**Heating rate-** The delay time and heating rates works according to what is programed into the oven controller.

**Hold temperature** - Will need to be programed with a slightly higher value in the controller to obtain the requested oven the right temperature. E.g. the requested oven temperature is 600 °C and then the controller needs to be set to 615 °C.

**Cooling rate-** Because of the isolation and no external extraction system, the cooling rates are hard to control. The cooling rates will decrease exponentially over time. By setting the controller to 999 °C/h (maximal cooling rate) the obtained cooling rate is reaching close to 150 °C/h from 600°C. The rate will be decreasing over time and can be compensated by inserting a small object between the hatch and the oven (increasing the diffusion of heat). Cooling rates under the 150 °C/h are more easy to control, but will still as well obtain an exponential decrease. E.g. by set the control on 100 °C/h from 600°C the resulting cooling rate of the oven will be around 75 °C/h. It's also important to keep in mind that the delaying heat distribution of the treated material. In cast iron materials the conductivity is high and will result in a less lag from air temperature. The maximal obtained temperature in the treated material can also be higher than the air temperature. This can be explained by the three ways heat energy is transferred, i.e. conduction, convection and radiation. From the surrounding air the treated material will absorb energy by convection, but also heat from radiation directly from the heating elements. E.g. the maximal obtained air temperature is 600 °C the resulting cast iron material can be closer to 610 °C.

## APENDIX D Apply the strain gauge

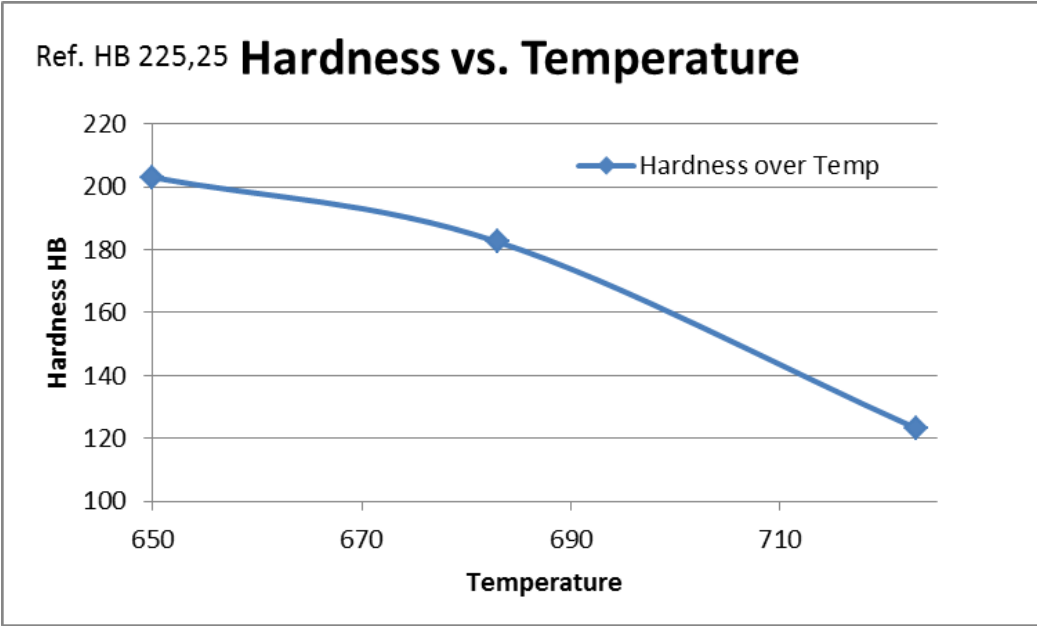
A good adhesion is important for the strain measurement, which entails requirements on the surface finish.

- The surface needs to be machined and then ground with Grit 120/P120 and 200/P240.
- Ground with an acidic and alkaline surface cleaner. To get rid of oil layer acetone can be used.
- The strain gauge is applied with help of a tape. It's important that the strain gauge surface will go directly from the wrapping to the applied surface.
- When the strain gauge is applied the tape is lifted and metallic glue is applied. Press steady on the strain gauge to obtain good adhesion. Wait 10 minutes and then remove the tape fast and steady from the directions of the strain gauge wires to the end.
- Control the adhesion under a microscope by touching the corners with a needle.

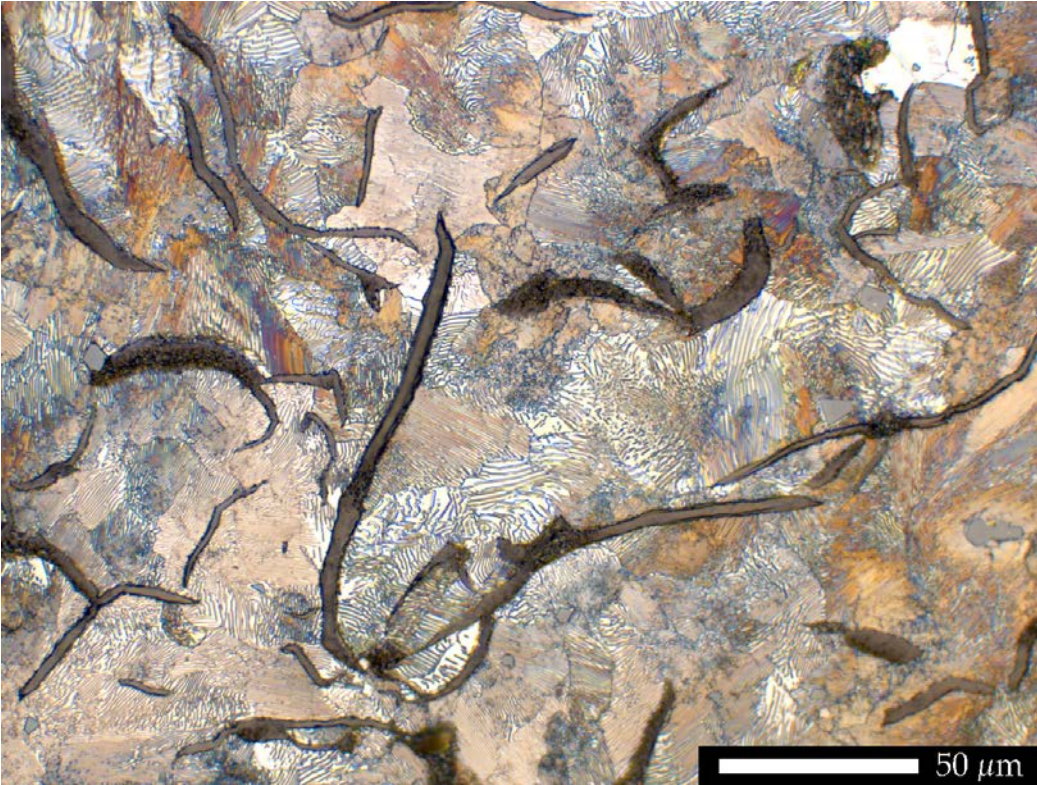
Following link is a recommendation of how to apply a strain gauge correctly:

<https://www.youtube.com/watch?v=SjXpF61HRys>

# APENDIX E Hardness vs. temperature



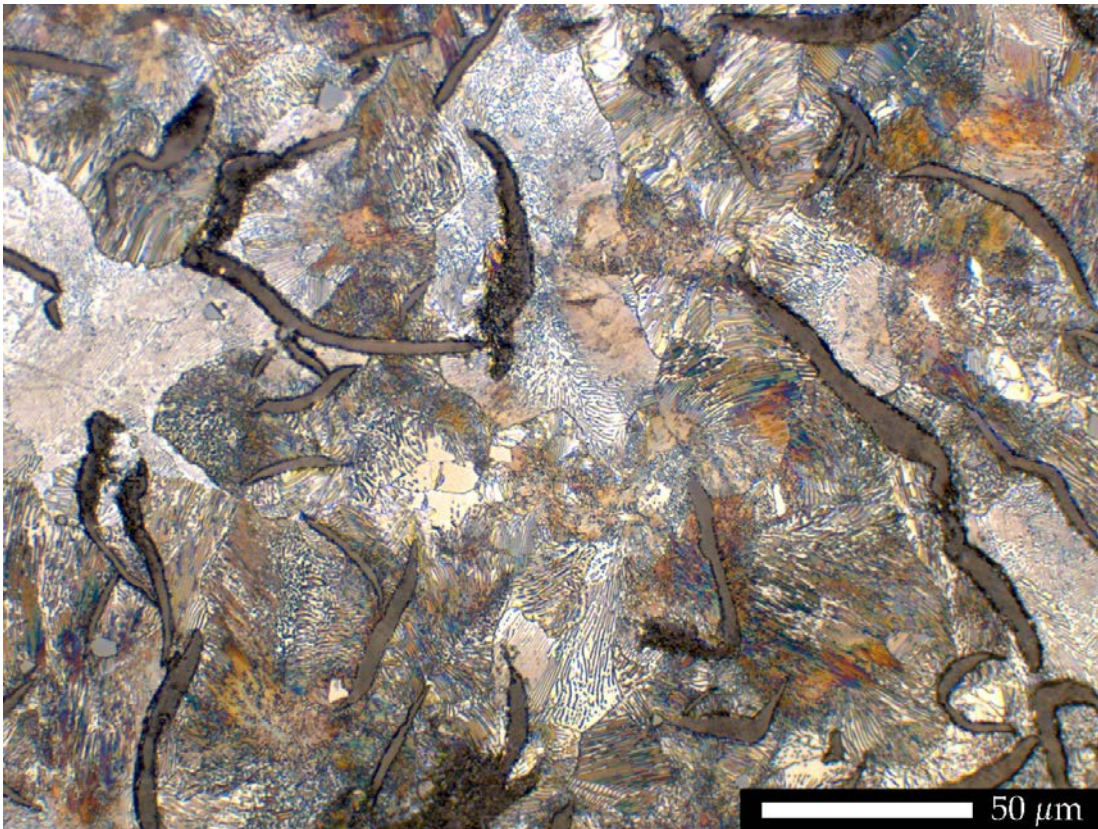
Hardness vs. hold temperature



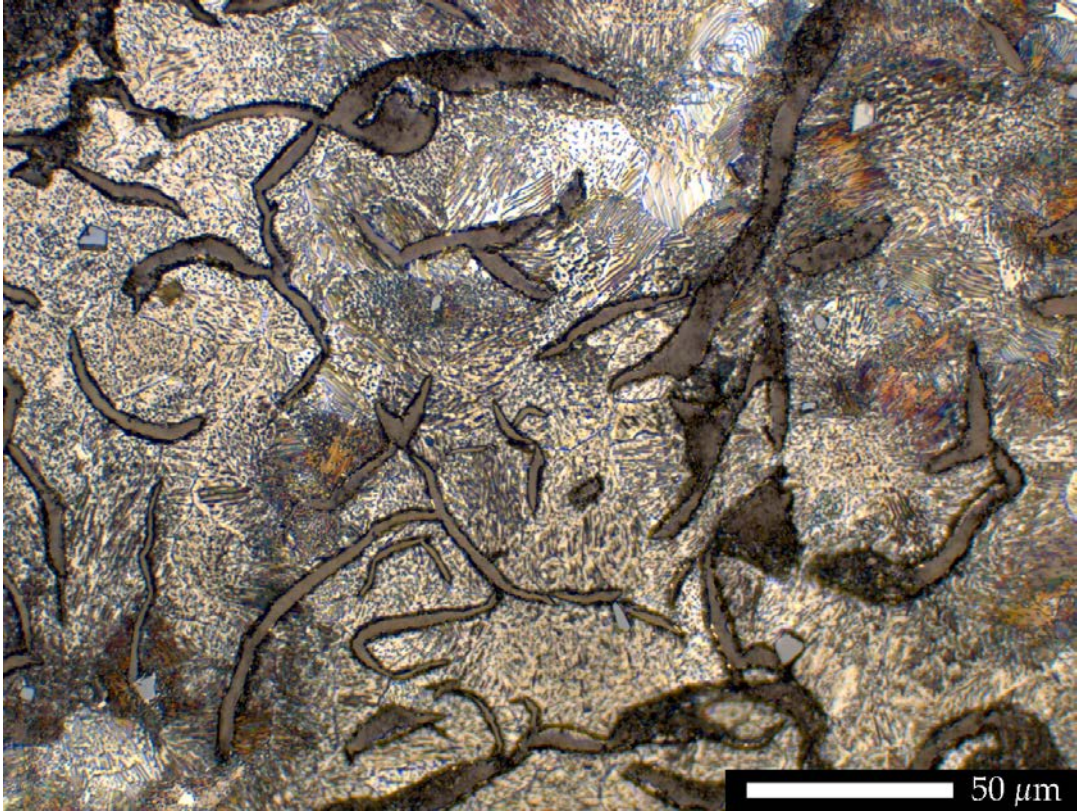
Reference microstructure



*Microstructure after 650 °C, 5h heat treatment*



*Microstructure after 683 °C, 5h heat treatment*



*Microstructure after 723 °C, 5h heat treatment*